Distributed Autonomy Meets Neuromorphic Intelligence

Abderazek Ben Abdallah
School of Computer Science and Engineering
The University of Aizu, Japan
Email: benab@u-aizu.ac.jp

会津大学
THE UNIVERSITY OF AIZ
Advanced Computing Systems Laboratory

Biography

Education

1988.9–1994.6 B.S. in Electrical Engineering, University of Sfax, and Huazhong University of Science and Technology (HUST)
1994.9–1997.7 M.S. in Computer Engineering, Huazhong University of Science and Technology (HUST)
1999.4–2002.3 Ph.D. in Computer Engineering, The University of Electro-Communications (UEC), Tokyo

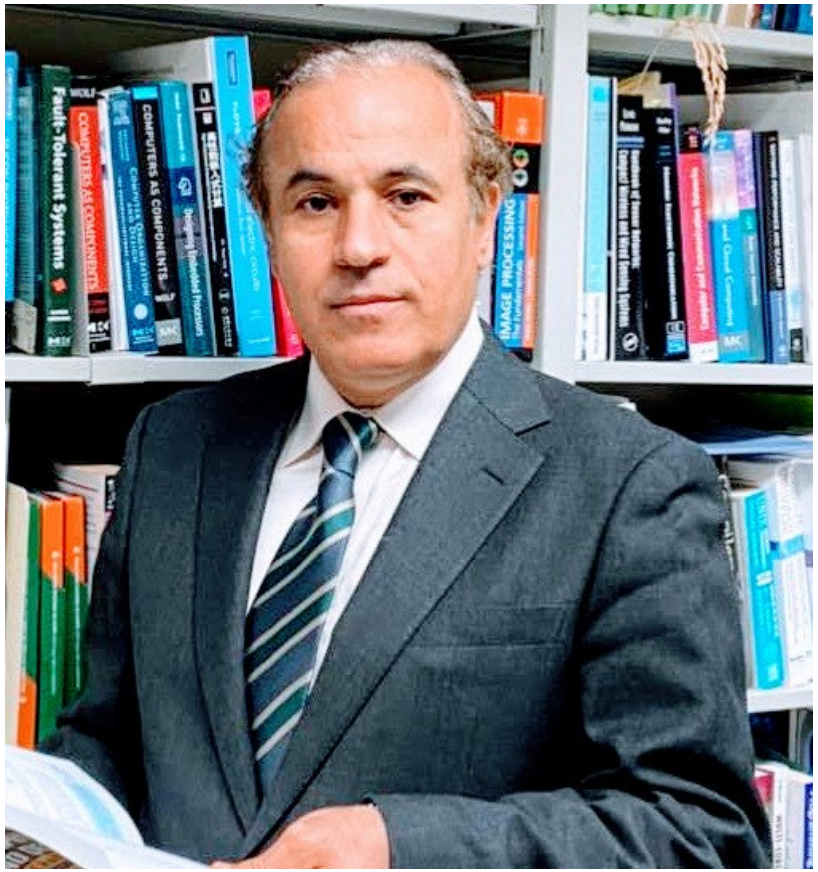

Professional Experience

2002.4–2007.3 Research Associate, UEC, Tokyo
2007.4–2007.9 Assistant Professor, UEC, Tokyo
2007.10–2011.3 Assistant Professor, University of Aizu
2011.4–2012.3 Associate Professor, University of Aizu
2012.4–2014.3 Senior Associate Professor, University of Aizu
2014.4–Present Professor, University of Aizu
2014.4–2022.3 Head, Computer Engineering Division, UoA
2014.4–Present Member, Education & Research Council, UoA
2022.4–Present Chair, Dept. of Computer Science & Engineering, UoA
2022.4–Present Dean, School of Computer Science & Engineering, UoA
2022.4–Present Regent, University of Aizu

Agenda

- The Evolution of Autonomy
- Distributed Autonomous (DA) Systems
- Neuromorphic Computing
- DA + Neuromorphic Intelligence
- Applications and Case Studies
- Research Challenges
- Vision & Outlook

Why is Autonomy Shifting from Centralized to Distributed ?

- Centralized vs. distributed autonomy
- Limitations of cloud-centric AI
- Real-world examples where distributed autonomy is essential
  - Multi-robot systems
  - Smart mobility
  - Environmental sensing networks

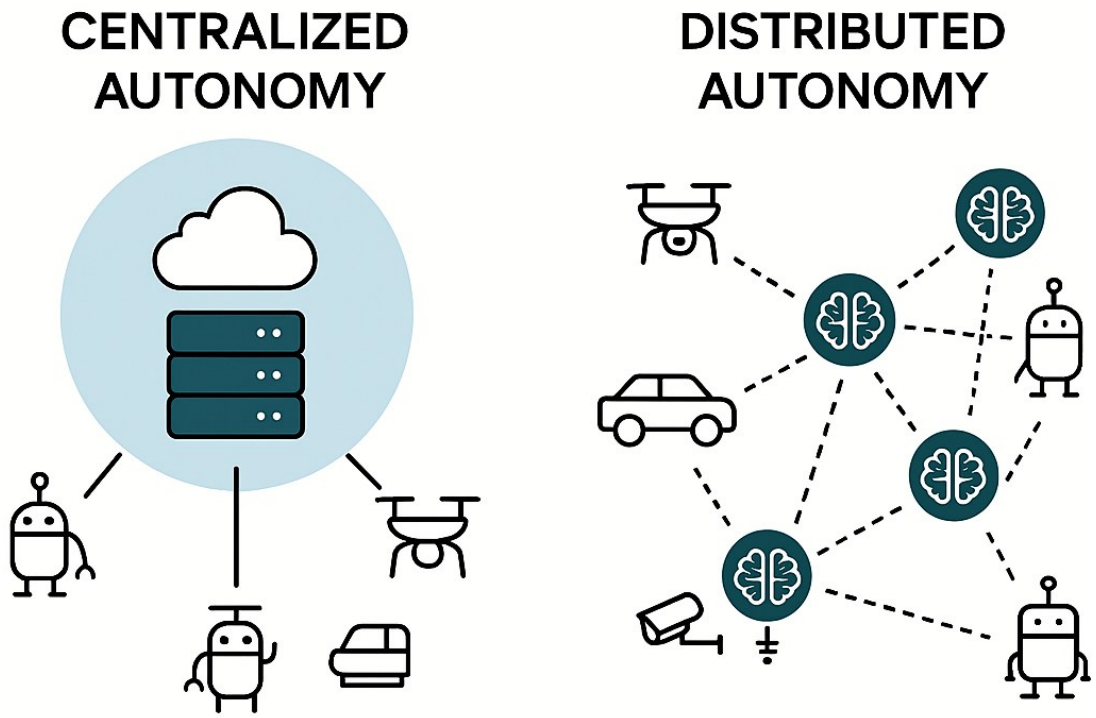

Why autonomy is shifting from centralized to distributed

benab@u-aizu.ac.jp

Architectural Principles of Distributed Autonomous Systems

- Local perception and decision-making
- Peer-to-peer coordination
- Emergent collective behavior
- Robustness and scalability

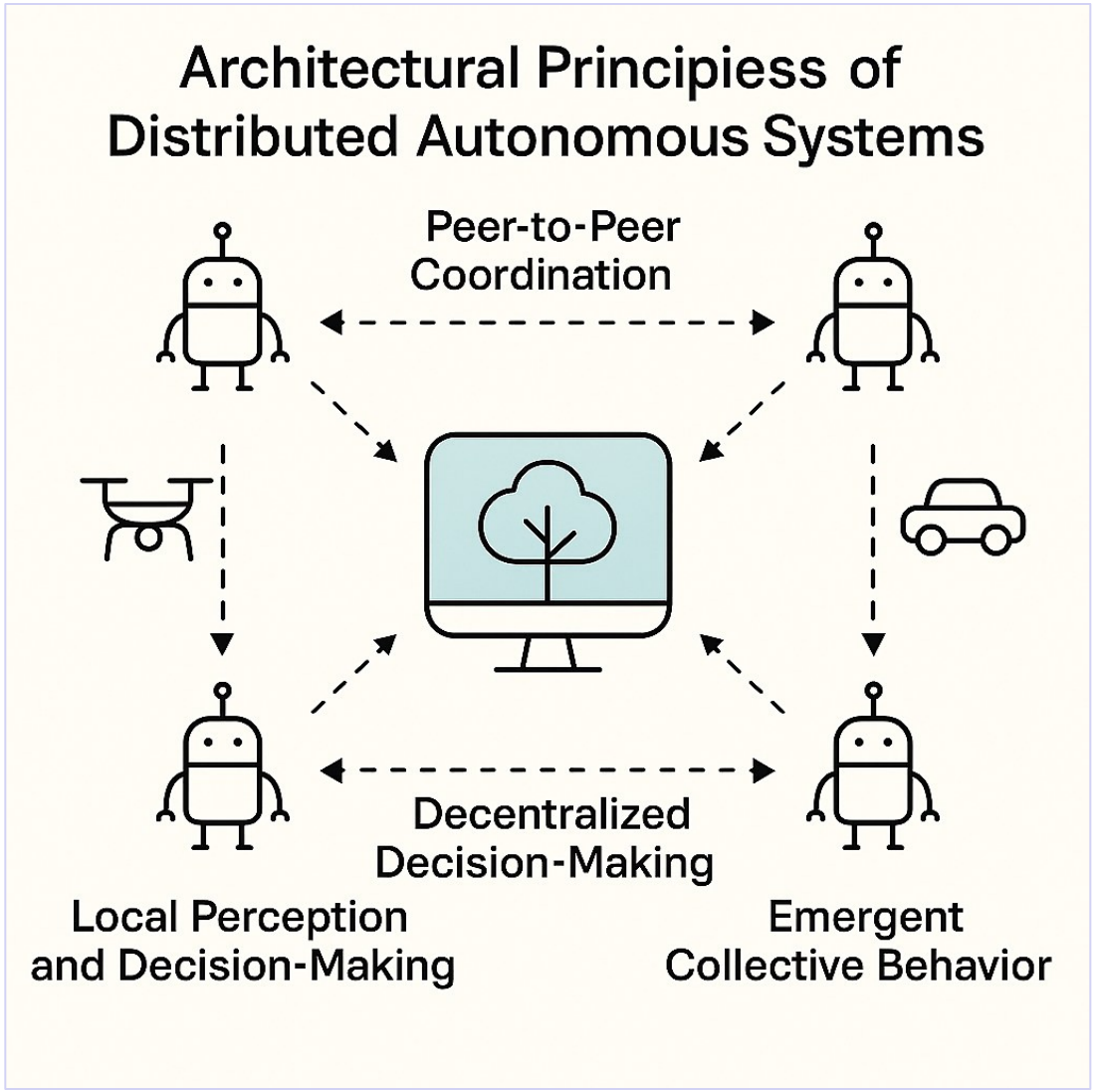

Neuromorphic Computing

von Neumann architecture

Transistors switch in nanoseconds

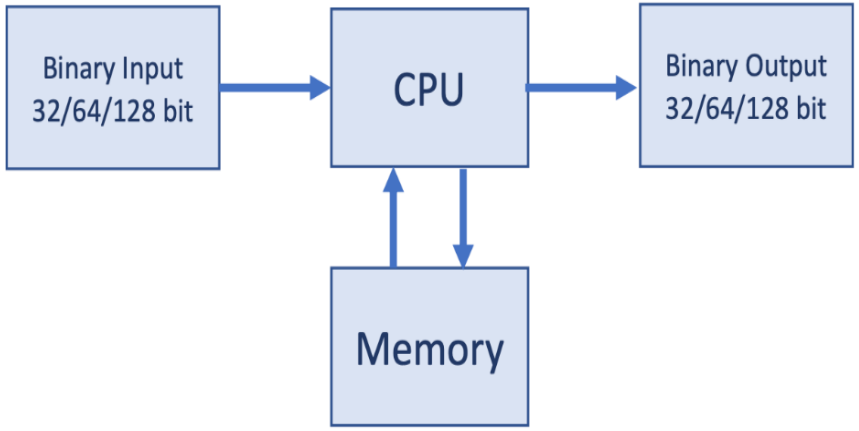

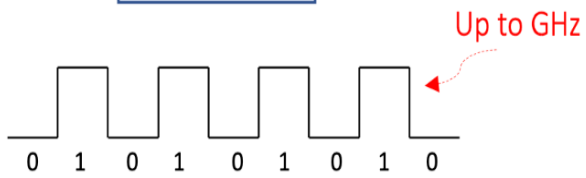

Signal in von Neumann architecture

Neuromorphic Computing

Neurons switch in milliseconds

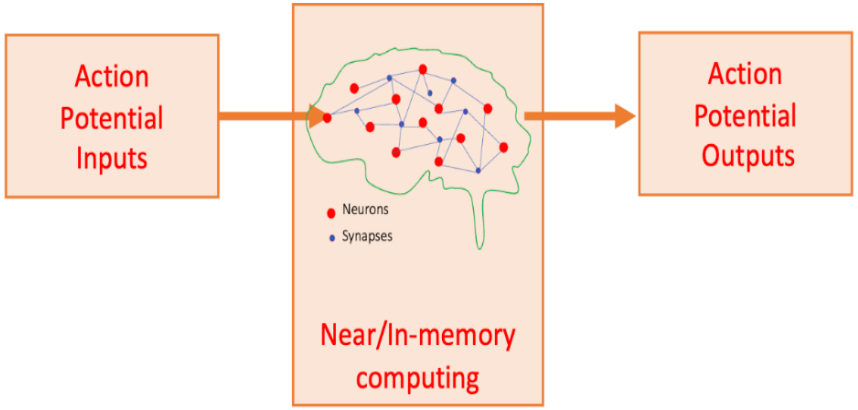

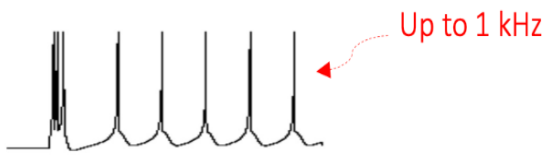

Signal in neuromorphic architecture

- SNN: synaptic weights and neuron behaviors usually are not fixed but evolve with timing-dependent dynamics.
- ANN: The synaptic weights and neuron functions are static after training

Serial computing, separated memory and computing unit, and digital information processing

In-memory computing, analog computing, and parallel computing/

benab@u-aizu.ac.jp

Neuromorphic Computing

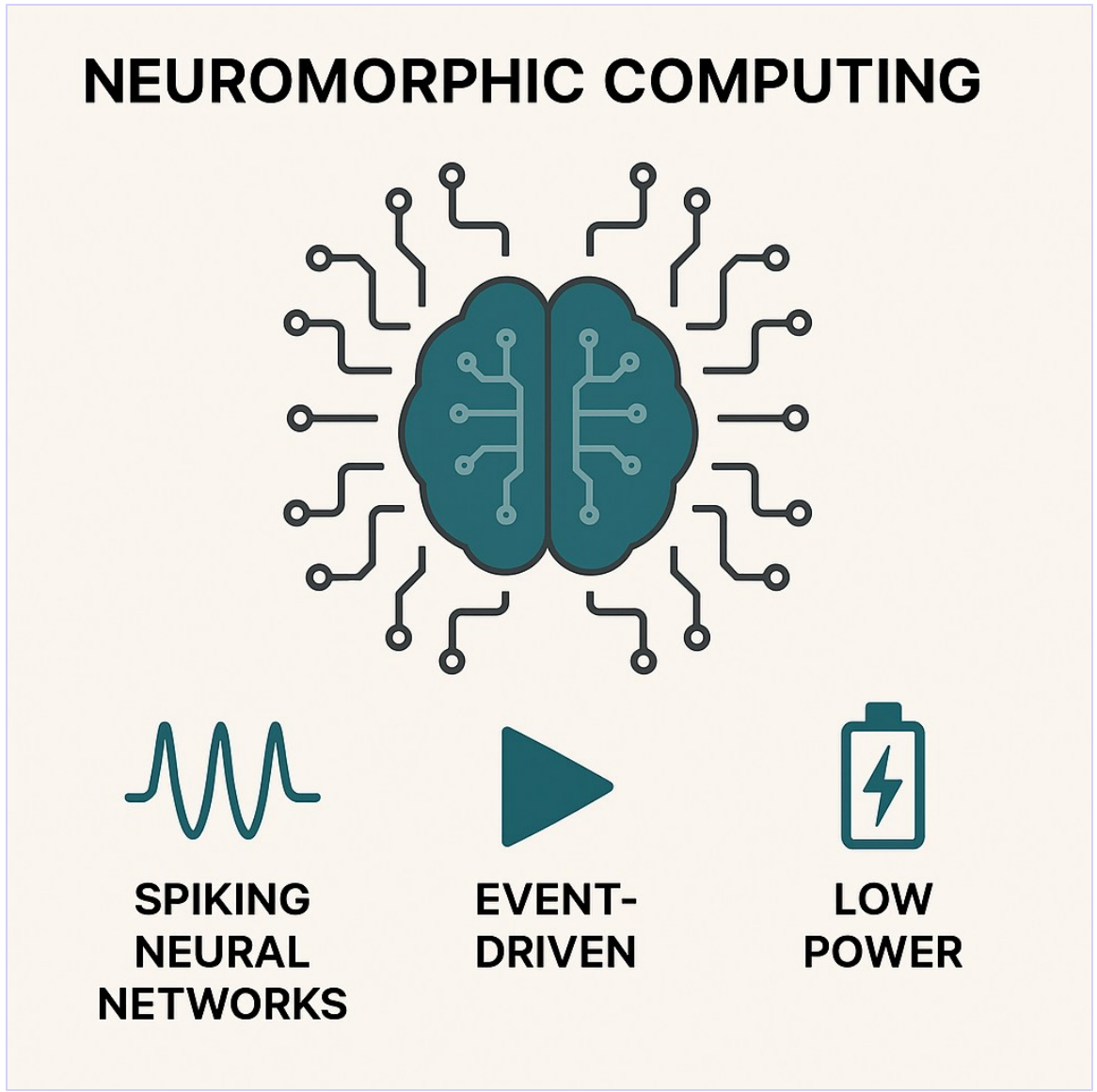

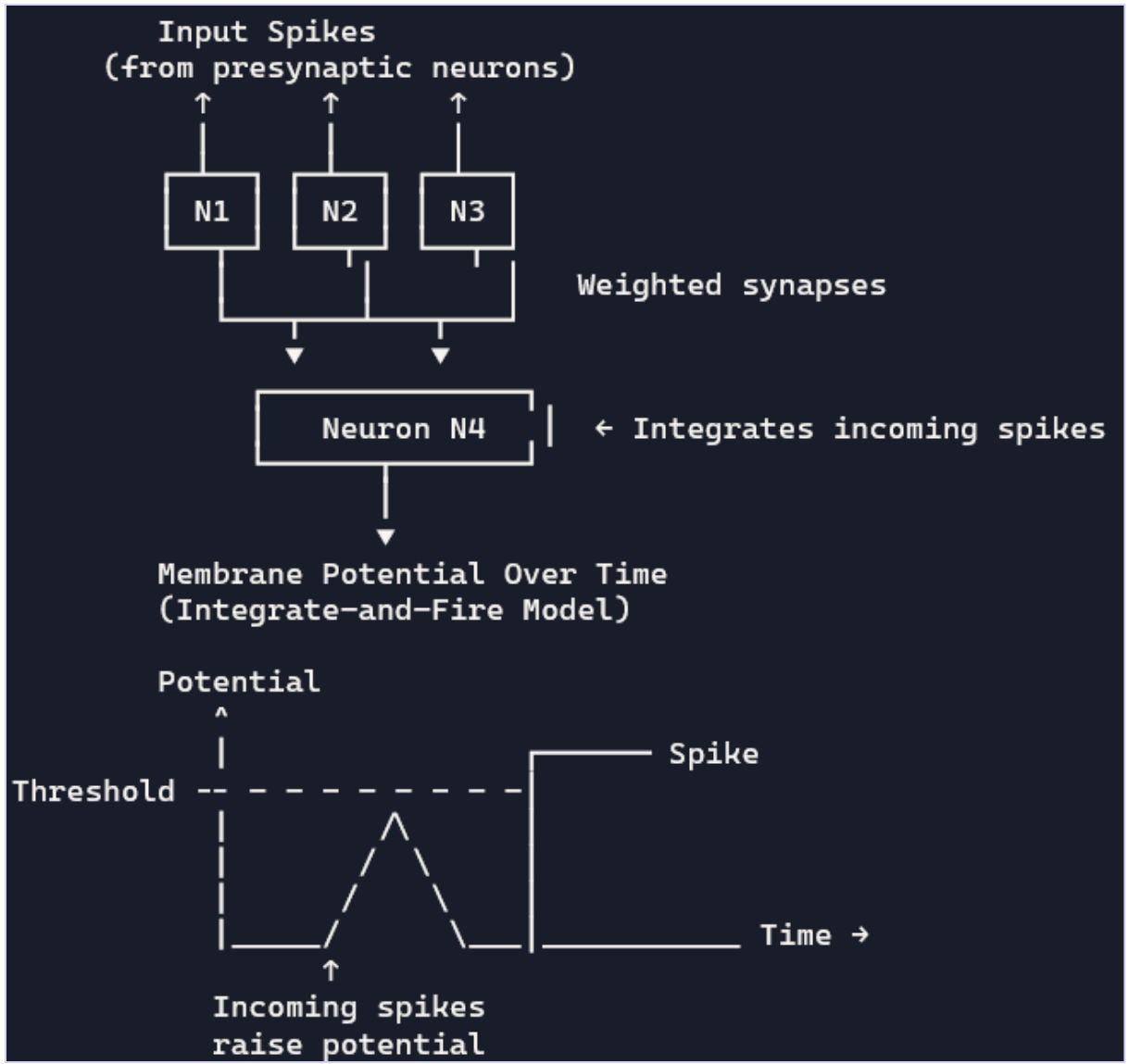

Neuromorphic Computing

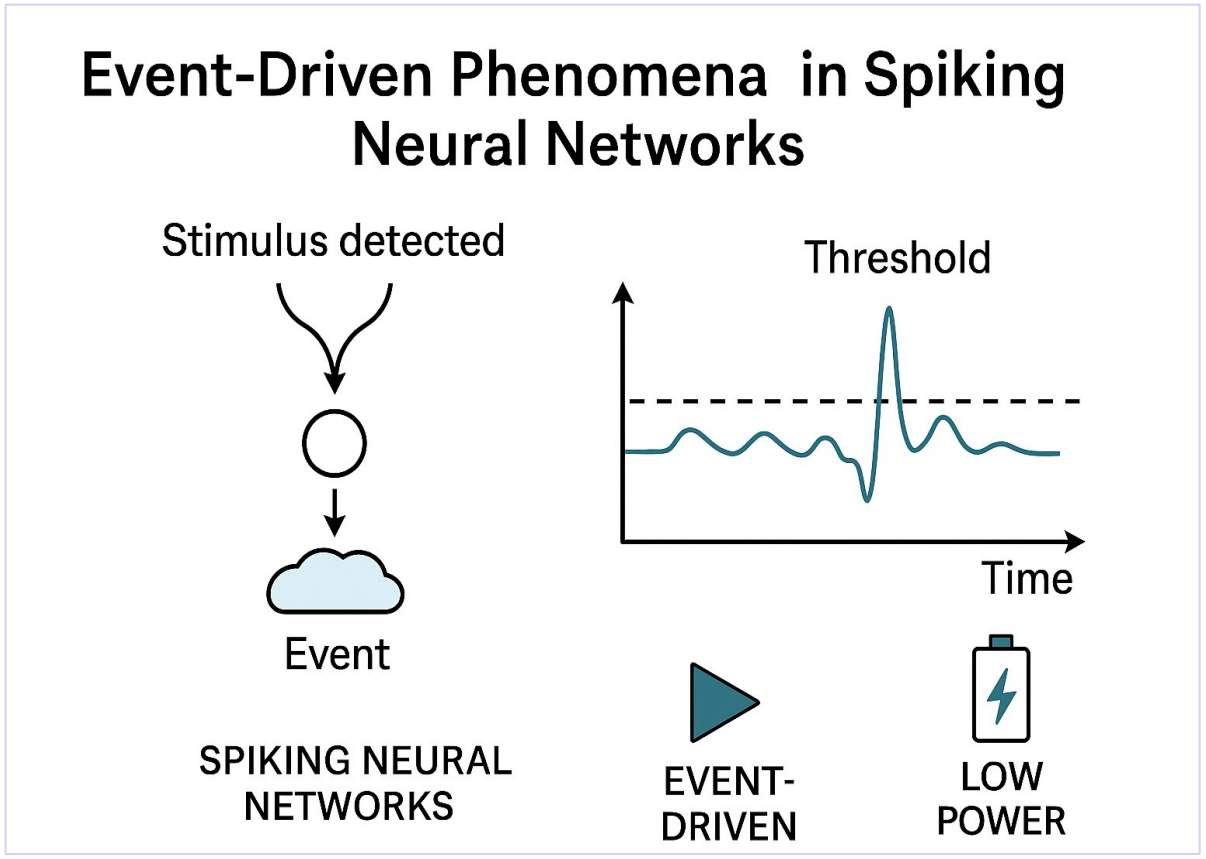

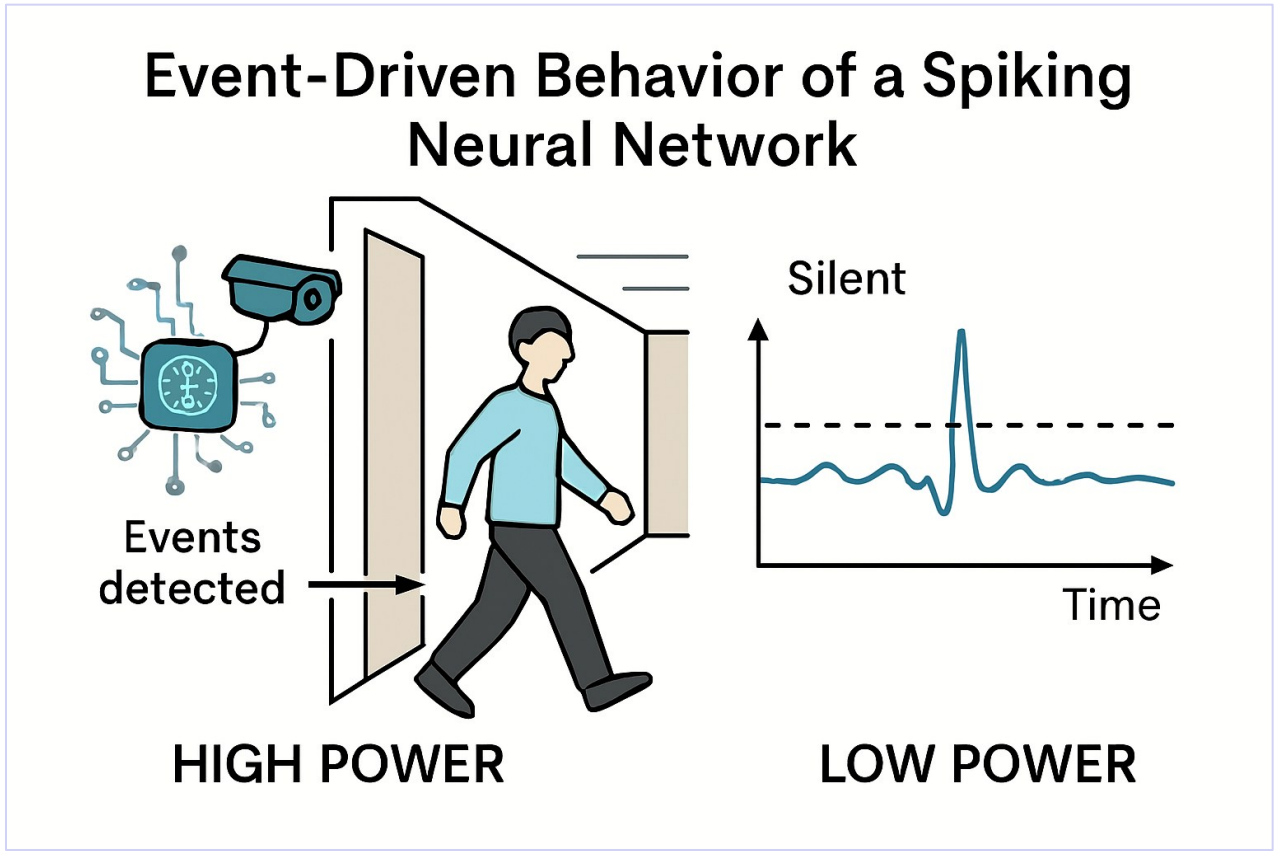

SNNs operate **only when events occur**—specifically, when a neuron receives a spike, and its membrane potential crosses a threshold. This is fundamentally different from traditional neural networks, which process data continuously across all neurons.

Neuromorphic Computing

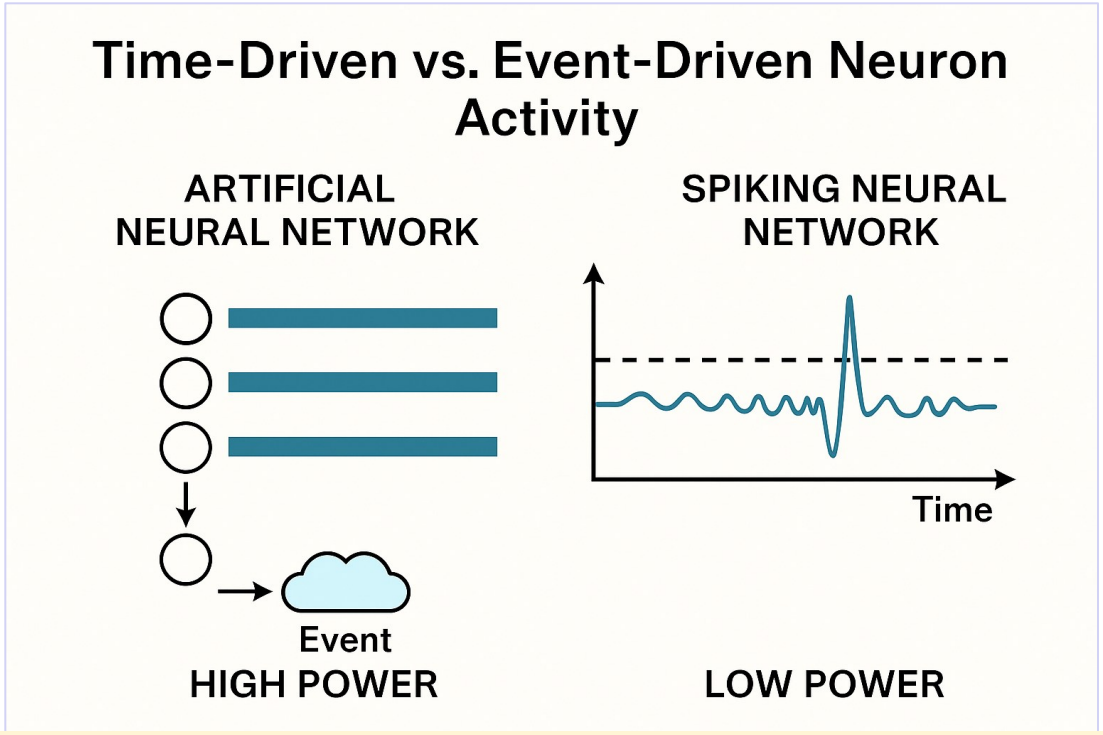

Feature	ANN (Time-Driven)	SNN (Event-Driven)
Neuron Activation	Continuous	Sparse
Computation Trigger	Clock cycles	Input spikes
Memory Access	Frequent	On-demand
Power Consumption	High	Low
Biological Plausibility	Low	High

ANNs process data in fixed time steps across all neurons, regardless of whether meaningful input is present.

SNNs only activate neurons when an input spike occurs—computation is triggered by events, not time.

➔ **SNNs avoid unnecessary computation, saving energy.**

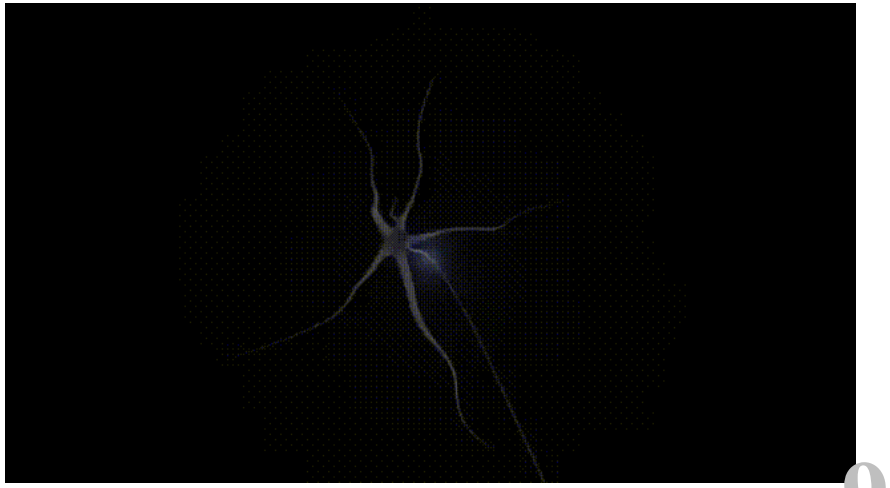

benab@u-aizu.ac.jp

Sparsity in Neural Networks

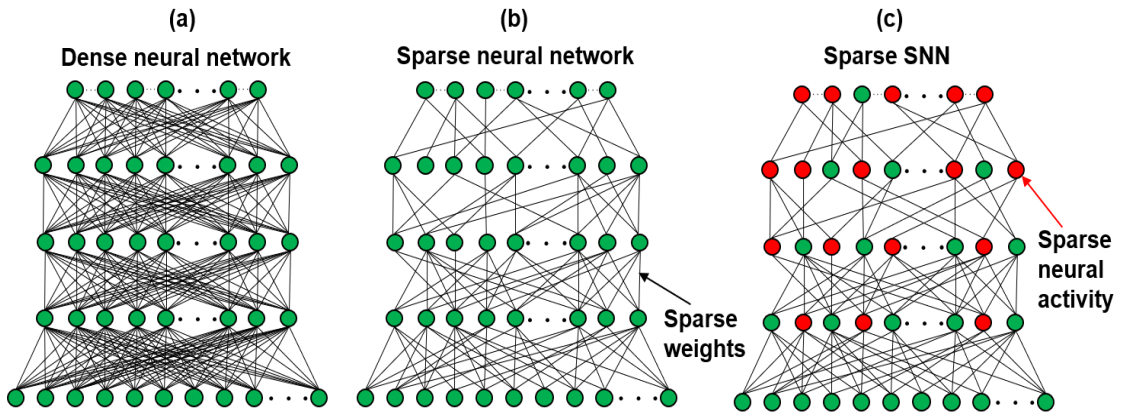

Illustration of sparsity in neural network

- Only 0.5% to 2% of neurons in the neocortex are active at any time [Lennie 2003]
- Only 1% to 5% of connections exist between two connected layers in the neocortex and 30% of those connections change every few days [Holmgren 2003]

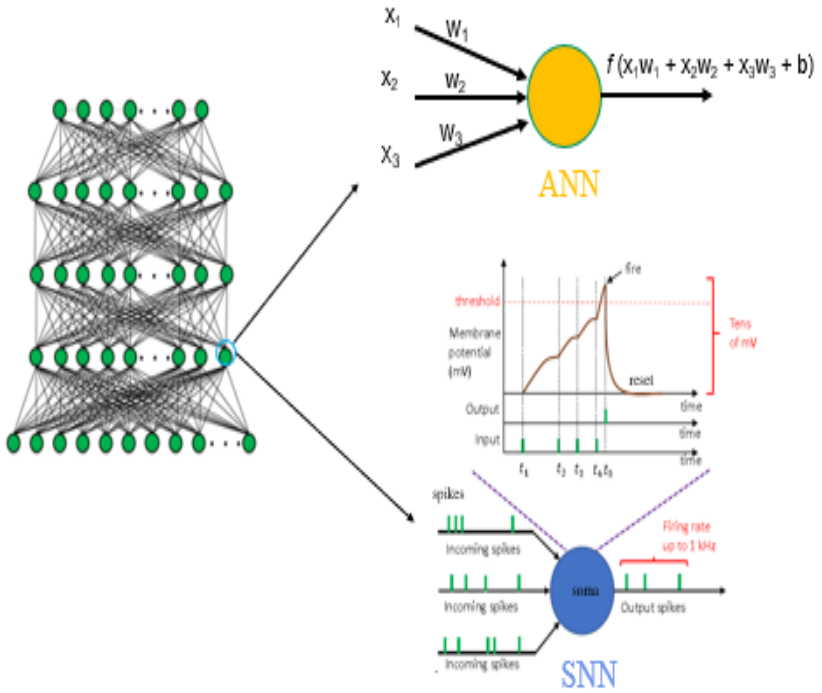

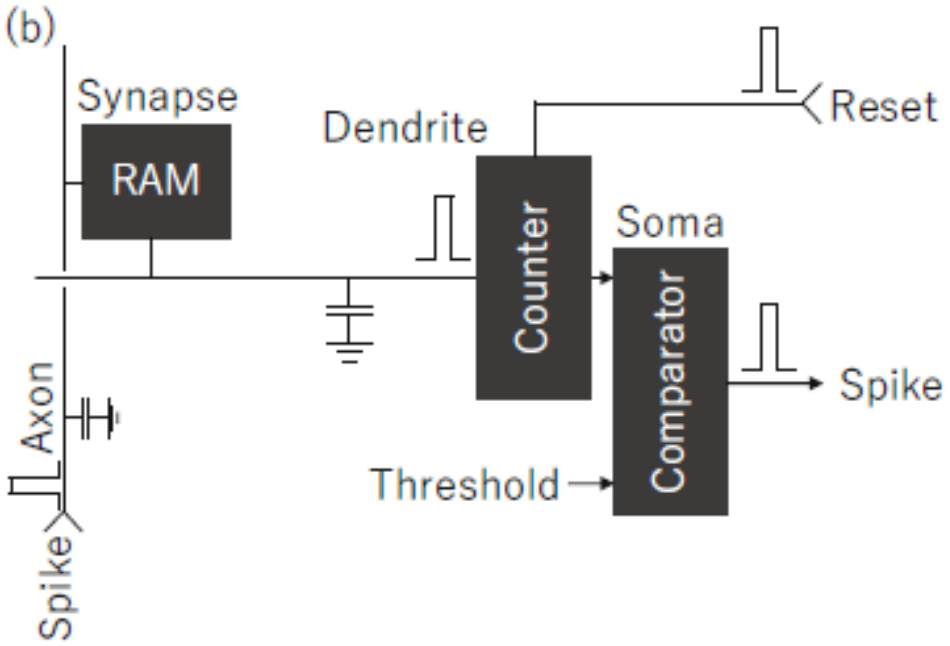

Digital silicon neuron implementation

Neuron Learning & AER

- Learning rules based on STDP specify changes in synaptic strength depending on the time interval between each pair of presynaptic and postsynaptic events.

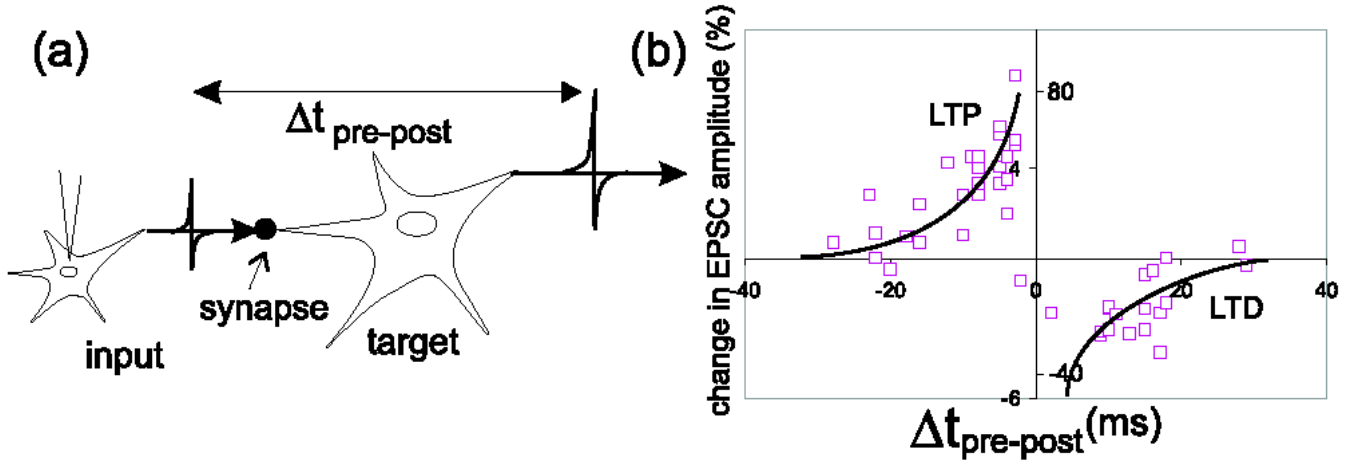

- If the presynaptic neuron fire **before** the postsynaptic neuron within a preceding 20ms, LTP occurs
- If the presynaptic neuron fire **after** the postsynaptic neuron within the following 20ms, LTD occurs

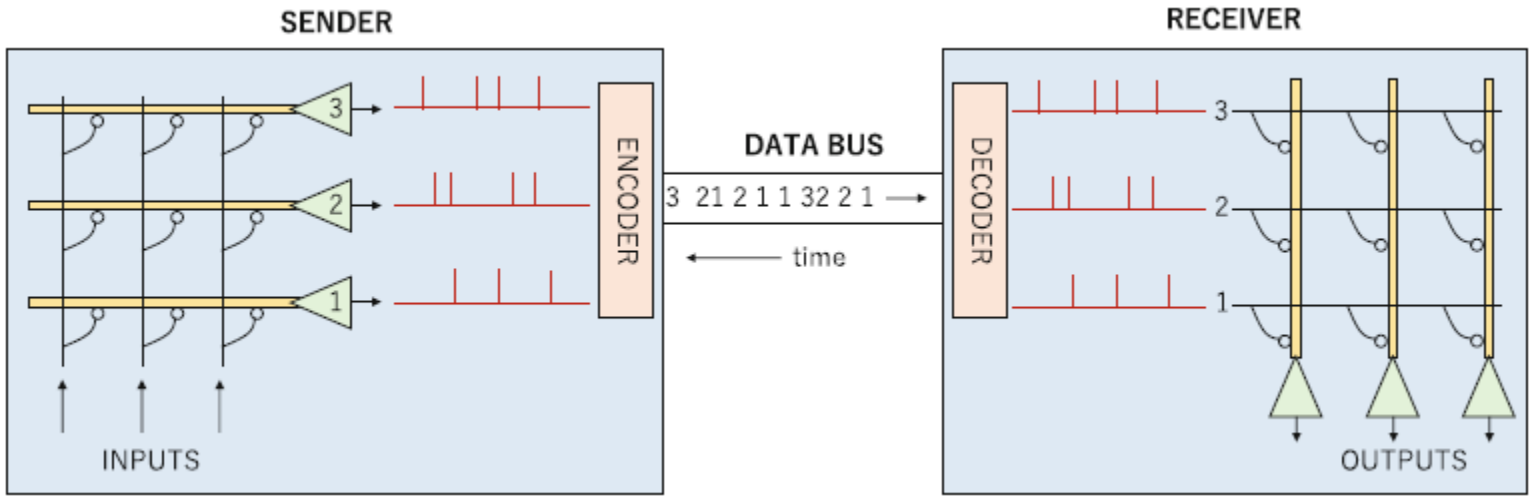

Address-event representation (AER) protocol

Low-power 3D-NoC-Baded Neuromorphic SoC

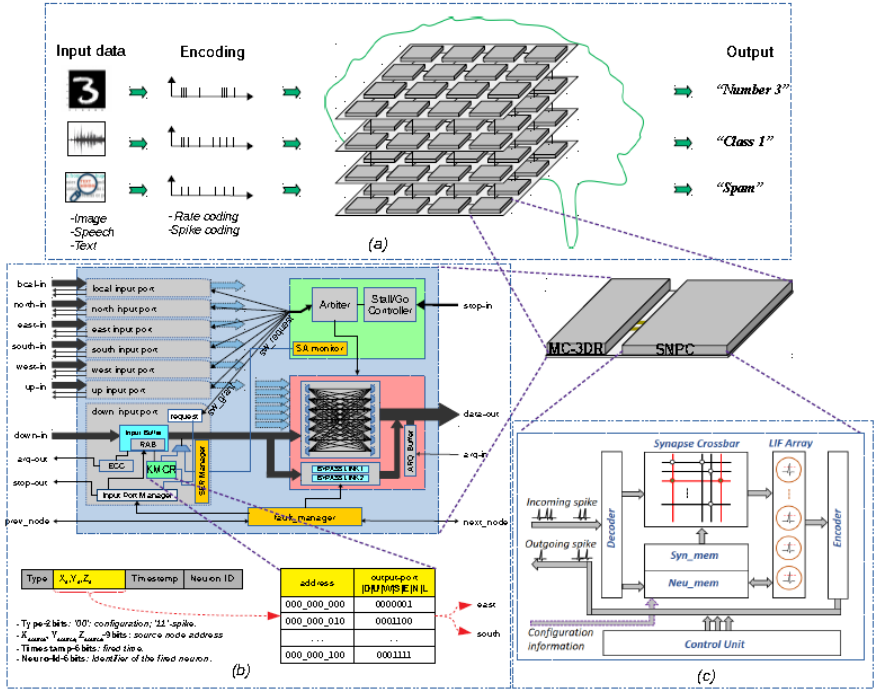

Fig. 5: System architecture: (a) 3DNoC-SNN organization, (b) Multicast router architecture (MC-3DR), (c) Spiking neuron processing core (SNPC).

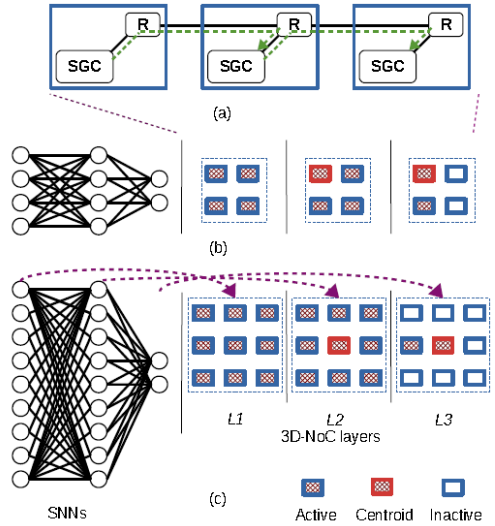

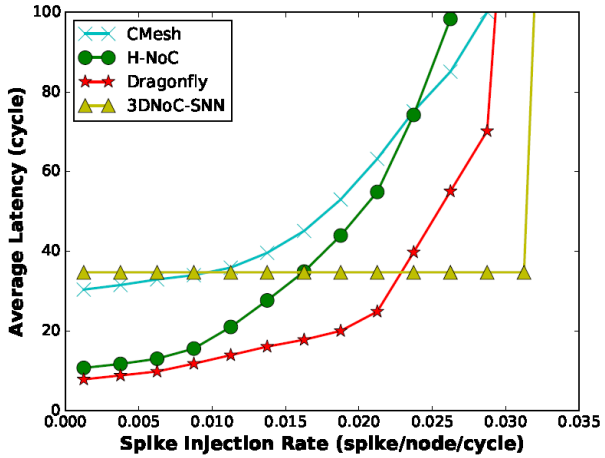

Evaluation Result

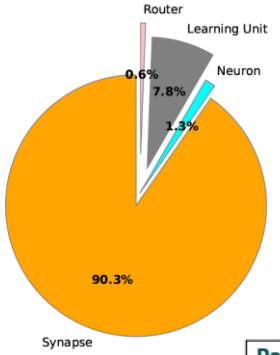

Area analysis of a NASH node

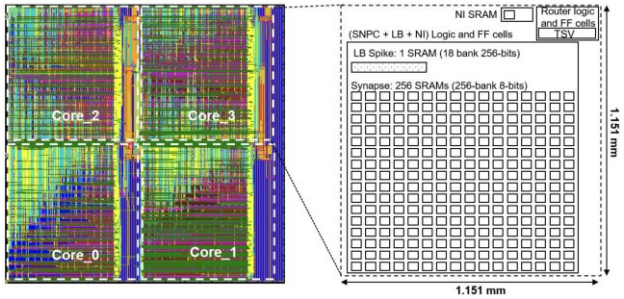

Parameter/System	XY-UB	XYZ-UB	SP-KMCR		FTSP-KMCR	
Architecture	Baseline	NASH	Baseline	NASH	Baseline	NASH
Area (mm^2)	1.312	1.316	1.322	1.322	1.320	1.325
Power (mW)	66.16	66.63	66.50	66.84	68.22	70.10

Design complexity comparison of NASH and Baseline nodes

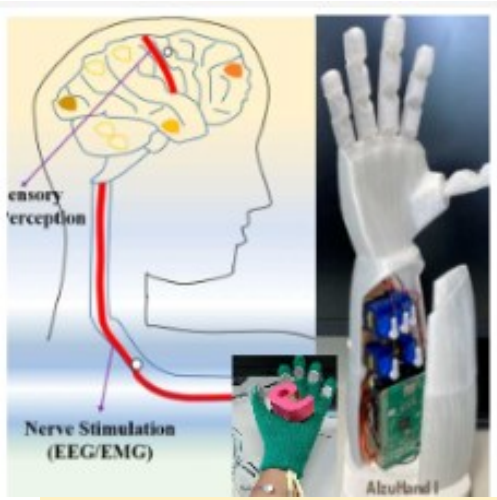

Deployment on Aizu Hand and Anthropomorphic Robot

https://web-ext.u-aizu.ac.jp/misc/neuro-eng/nash.htm

Distributed Autonomy + Neuromorphic Intelligence

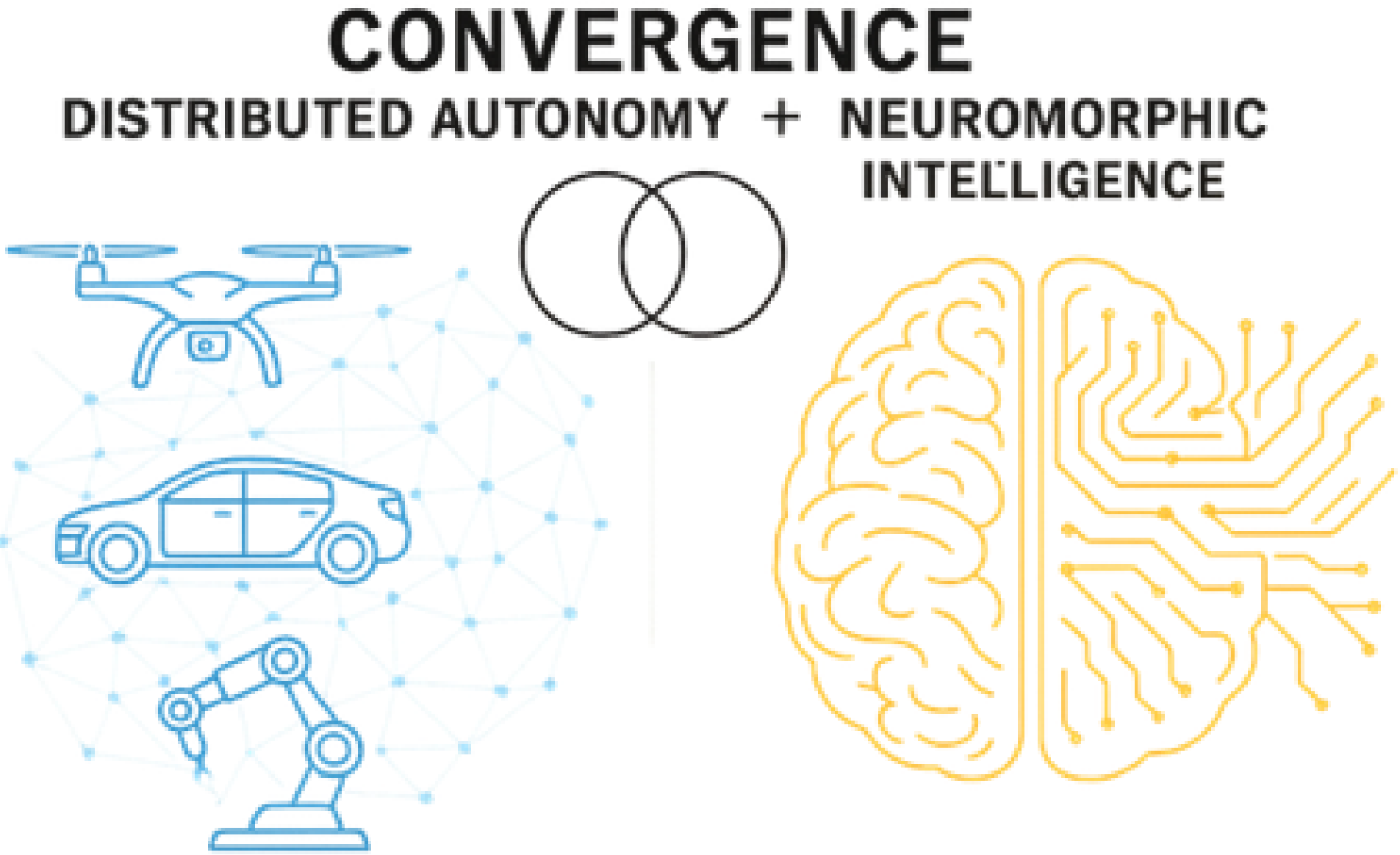

Distributed Autonomy + Neuromorphic Intelligence

How neuromorphic principles enhance distributed agents

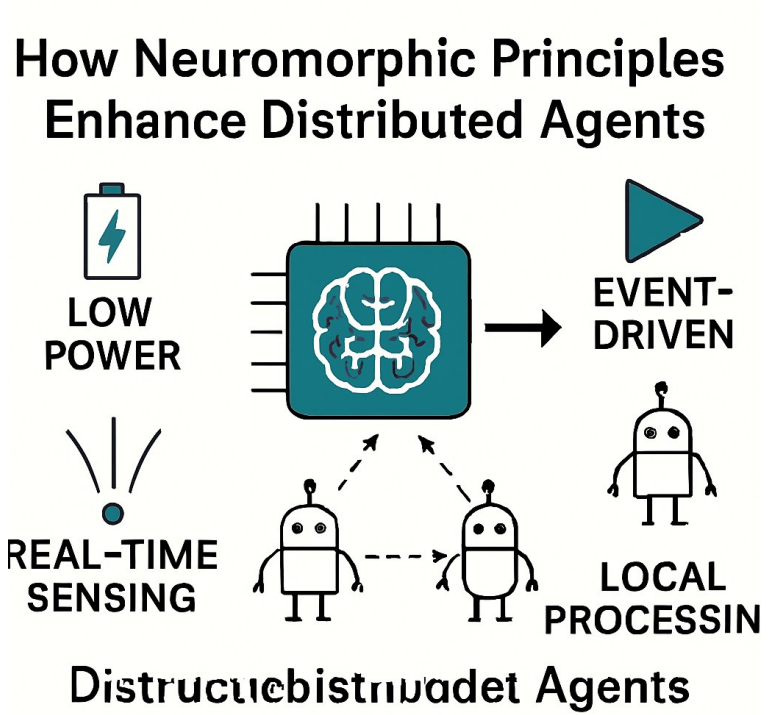

Feature	Traditional Agent	Neuromorphic Agent
Computation Model	Continuous	Event-driven
Power Consumption	High	Ultra-low
Learning	Centralized	Local & adaptive
Communication	Bandwidth-heavy	Sparse & efficient
Scalability	Limited	High

- ✓ Event-Driven Computation
- ✓ Spiking Neural Networks (SNNs
- ✓ Local Learning and Adaptation)

- ✓ Low-Power Hardware Integrator
- ✓ Scalable Decentralized Intelligence

Applications and Case Studies

- Robotics and swarm intelligence
- Robotics and swarm intelligence
- Environmental monitoring
- Space and planetary exploration
- Defense and security systems

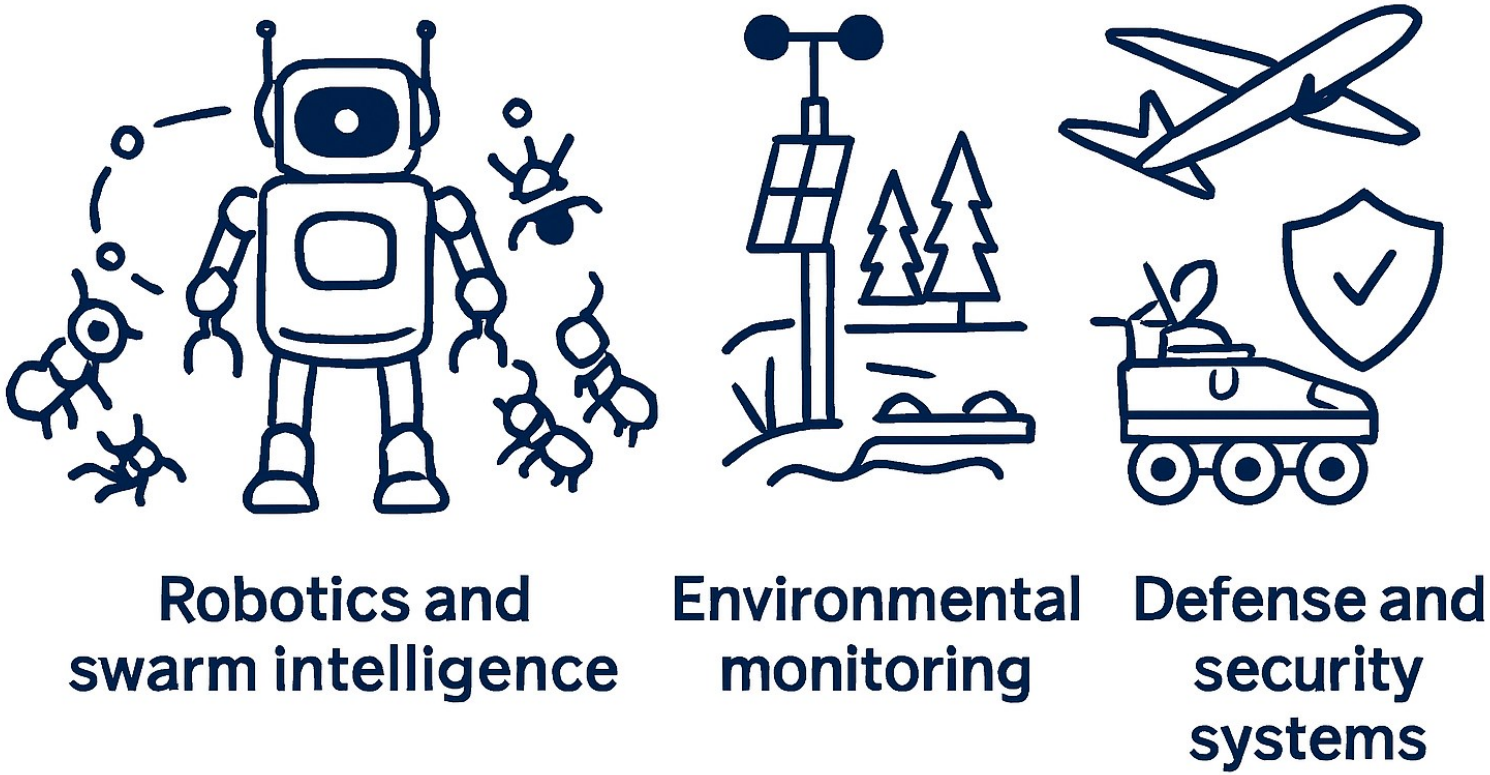

Real-World Deployment 1: Intelligent Off-Grid Energy Storage Powered by Distributed EV Autonomy

Smart Solar Carport: Off-Grid Energy Storage with AI and EV

Vision and Motivation/ビジョンと動機

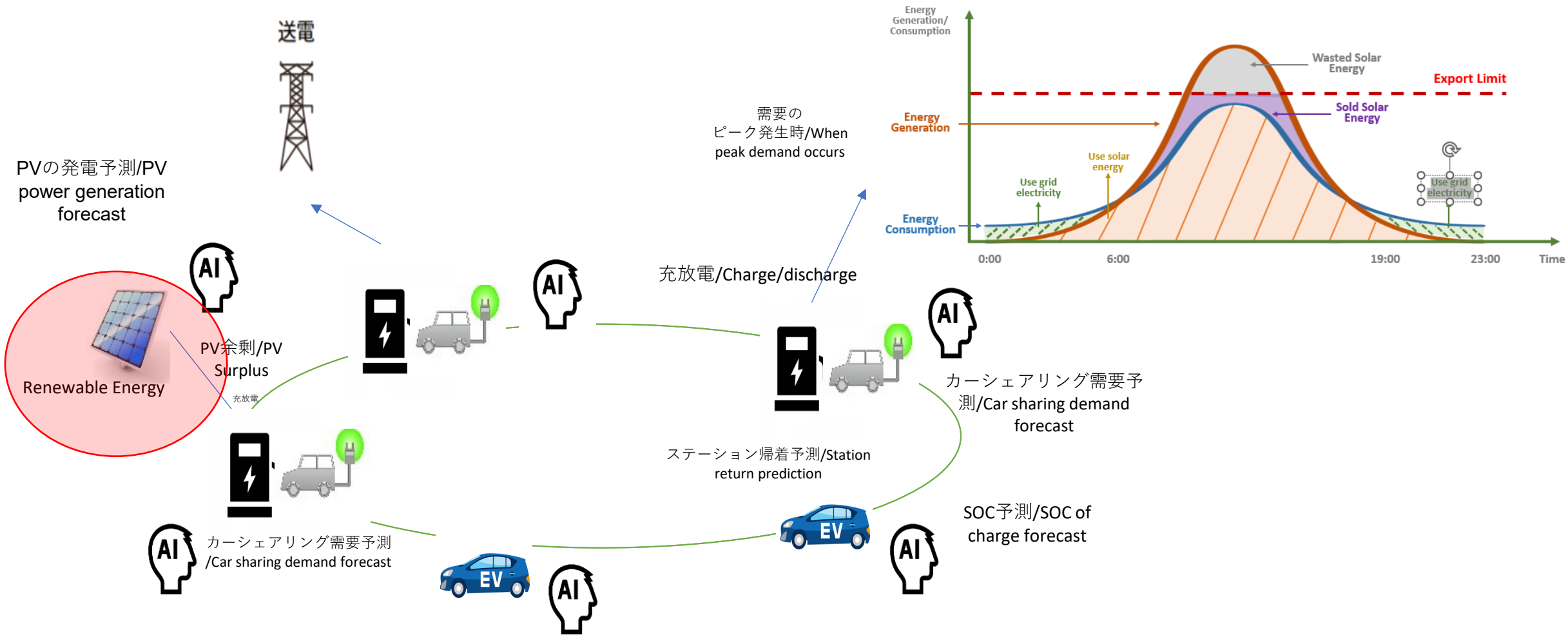

Smart Solar Carport: Off-Grid Energy Storage with AI and EV

System Overview

Solar panels
Average efficiency:
20–22% efficient.

Battery management system

① Store & Record harvested energy amount

② Upload data to the cloud

Cloud server

③ Read and transmit data

Inference server

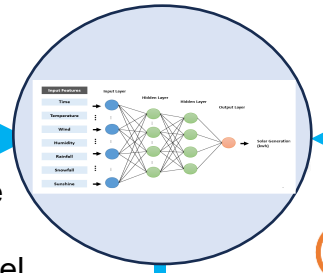

Weather API

AccuWeather APIs

④ Transmit **a)** weather information in the past (used for model training) and **b)** future weather forecast (used for model inference)

⑤ Predict the solar energy generation and display the result on the UI.

Software tool for solar power generation prediction

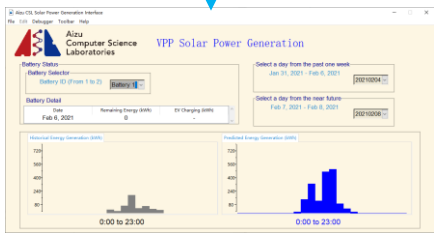

Smart Solar Carport: Off-Grid Energy Storage with AI and EV

System Overview

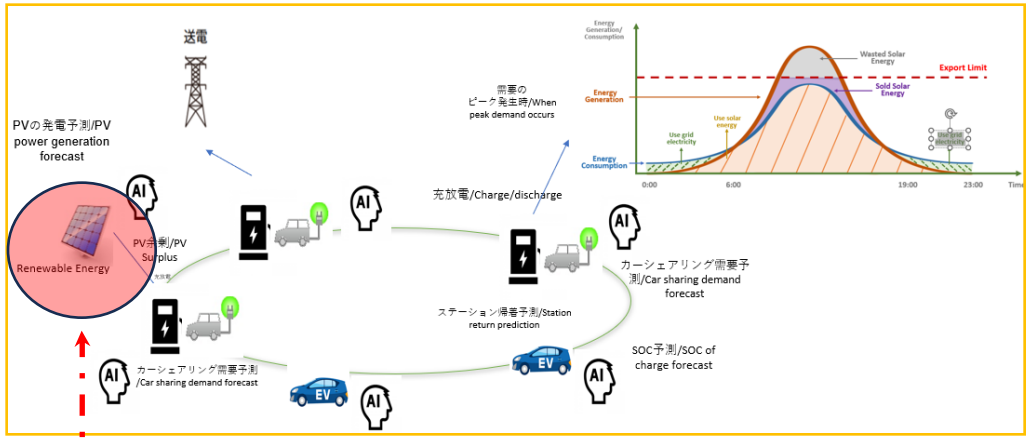

1. PVの発電予測/PV power generation forecast

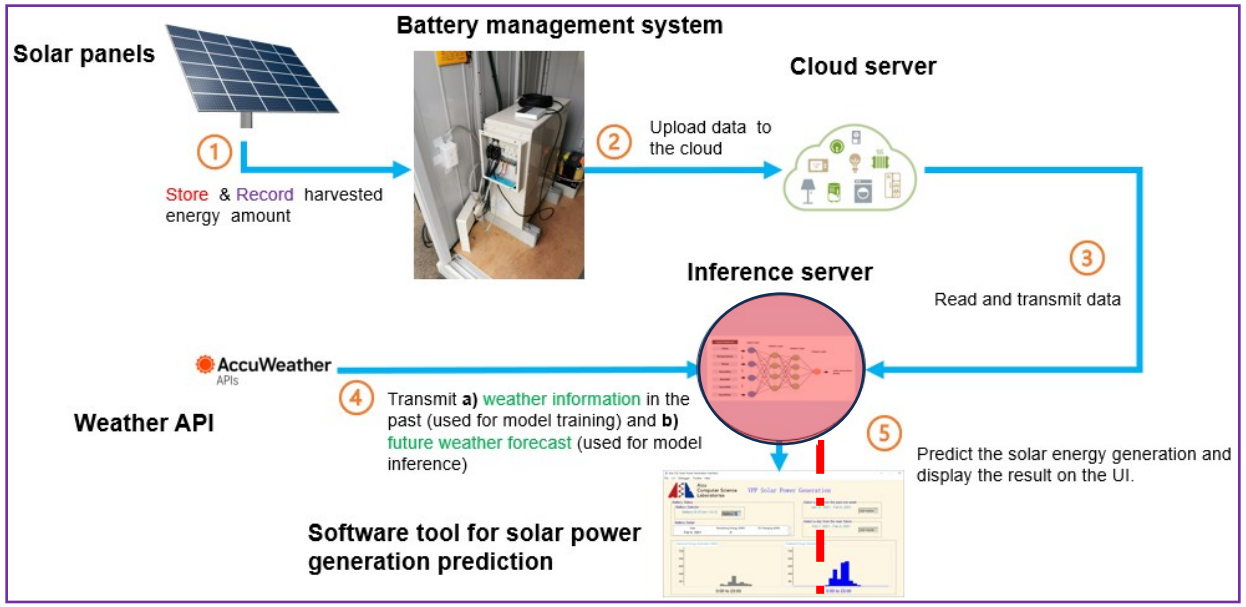

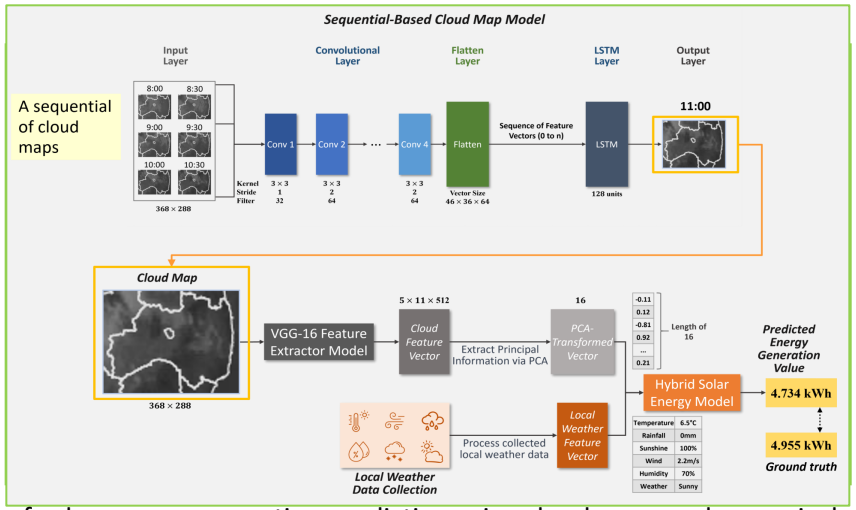

Workflow of solar energy generation prediction using cloud maps and numerical weather data.

Smart Solar Carport: Off-Grid Energy Storage with AI and EV

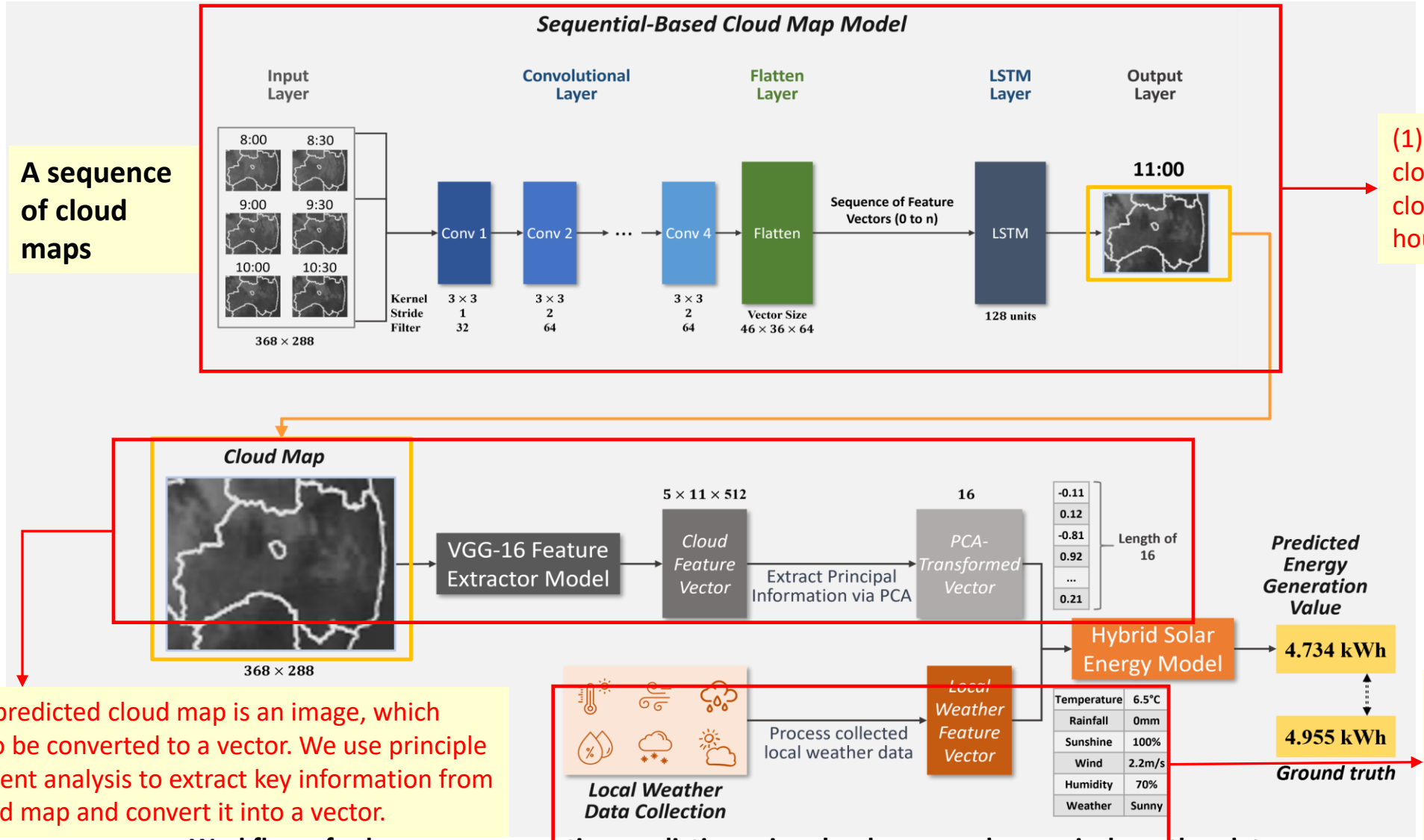

Workflow of solar energy generation prediction using cloud maps and numerical weather data.

For cloud map: Japan Meteorological Agency, "Weather Satellite Himawari," accessed Nov. 25, 2025, https://www.jma.go.jp/bosai/map.html
For weather data: Japan Meteorological Agency, "Historical weather data," accessed Nov. 25, 2025, https://www.data.jma.go.jp/risk/obsdl/index.php

Smart Solar Carport: Off-Grid Energy Storage with AI and EV

System Overview

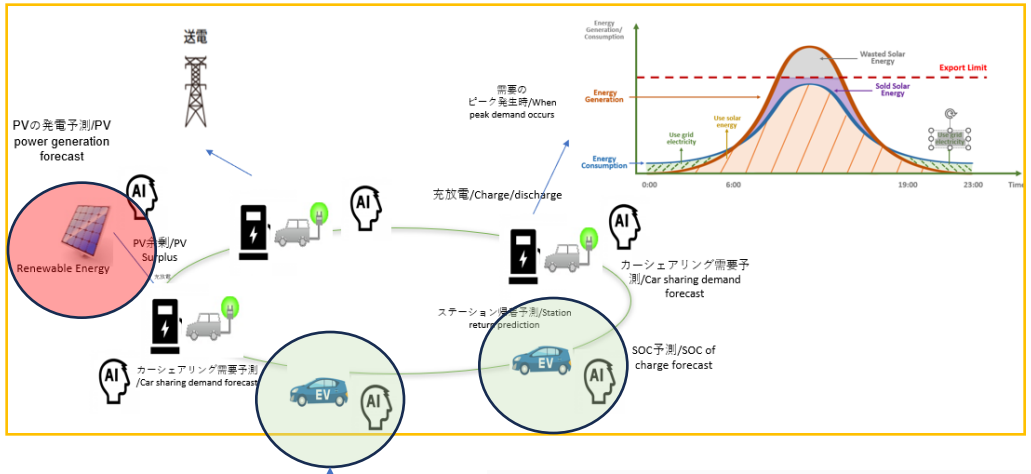

EV Power Consumption Prediction

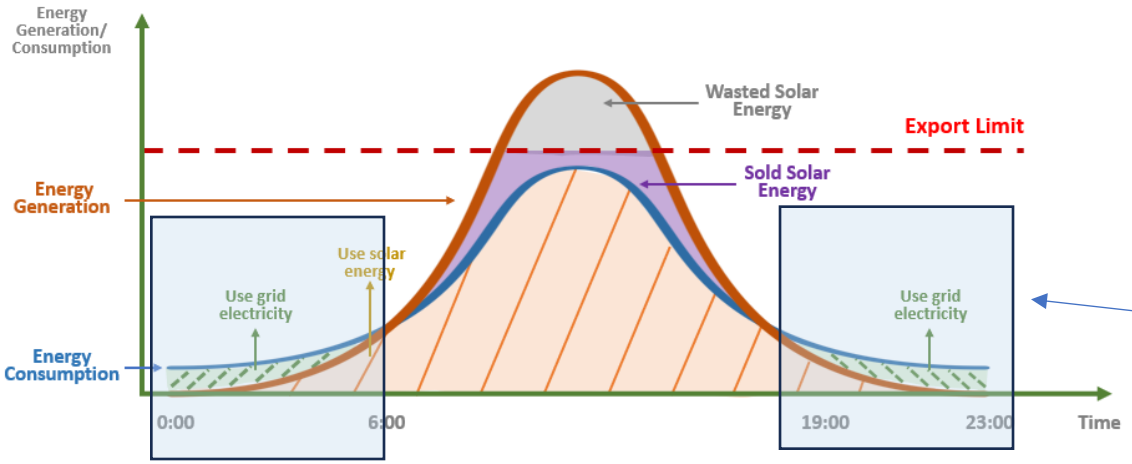

EV discharge period

2. EV Power Consumption Prediction

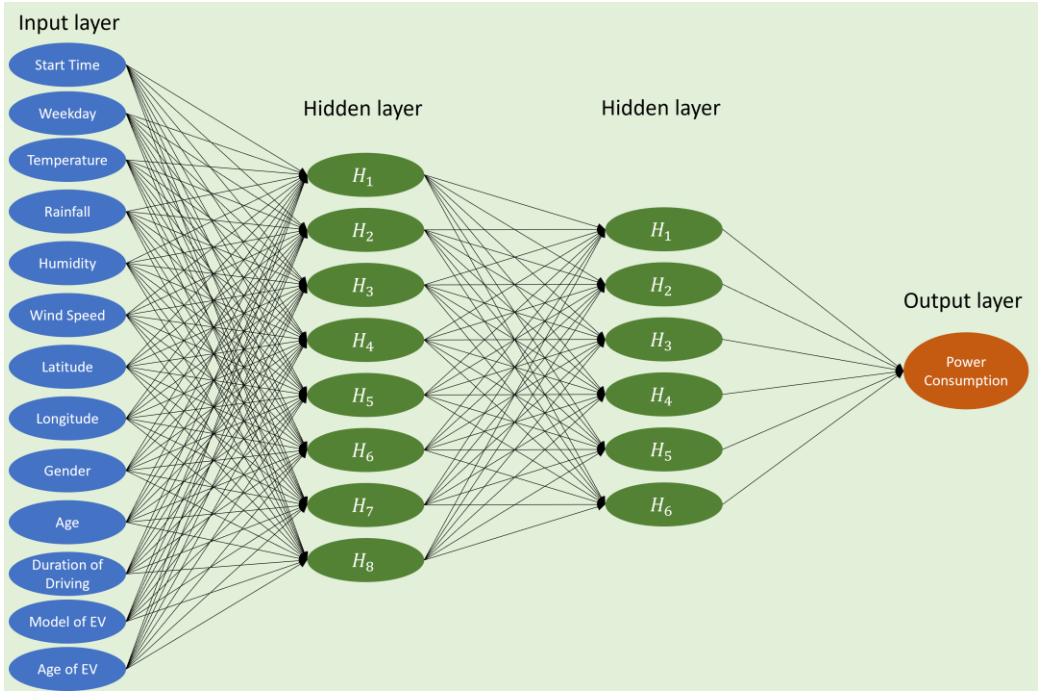

Smart Solar Carport: Off-Grid Energy Storage with AI and EV

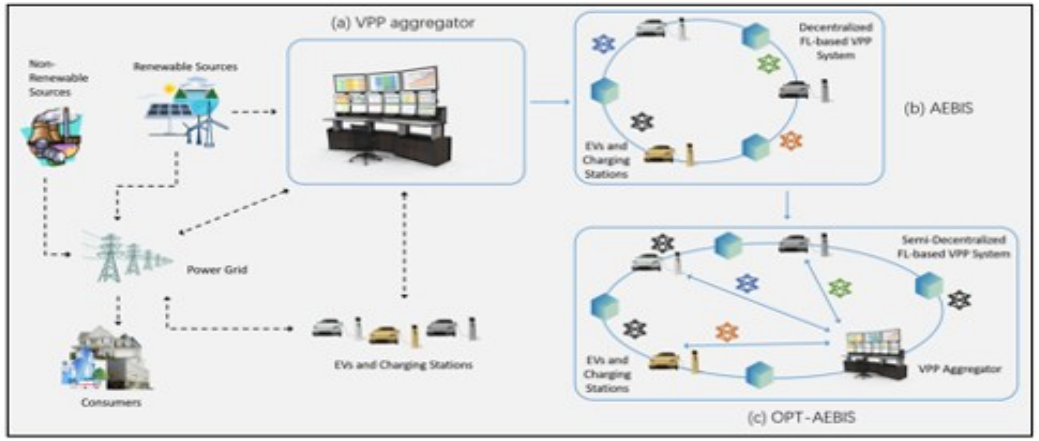

Fig. 1. Virtual Power Plant (VPP): (a) conventional VPP aggregator, (b) AEBIS, (c) optimized AEBIS (O-AEBIS).

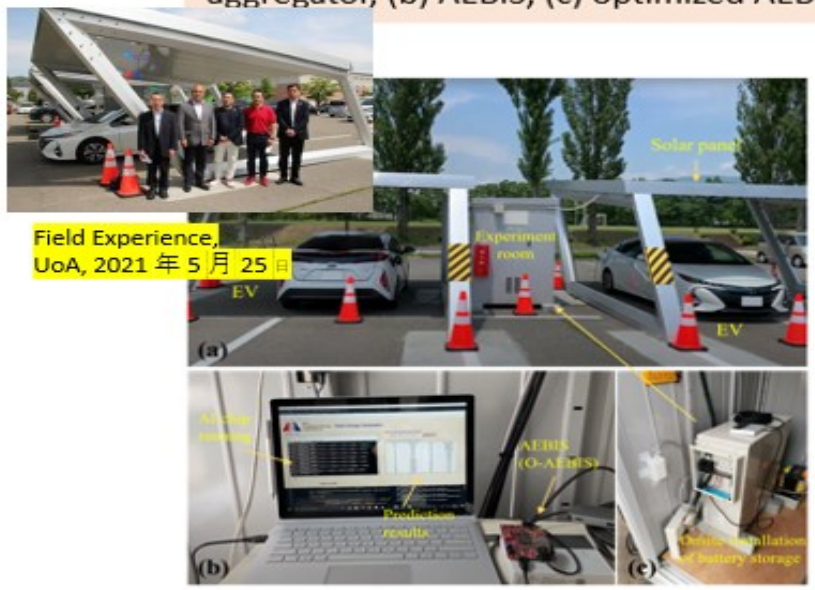

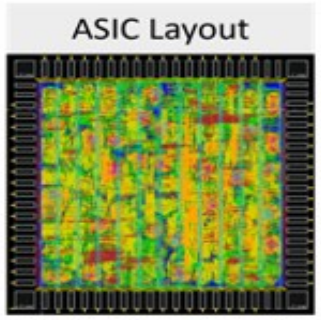

Area	0.265 mm²
Voltage	1.1 V
Power	318.224 mw
Temperature	25°C

Fig. 5. A demonstration of the energy management system based on our system named AEBIS and its optimized version O-AEBIS.

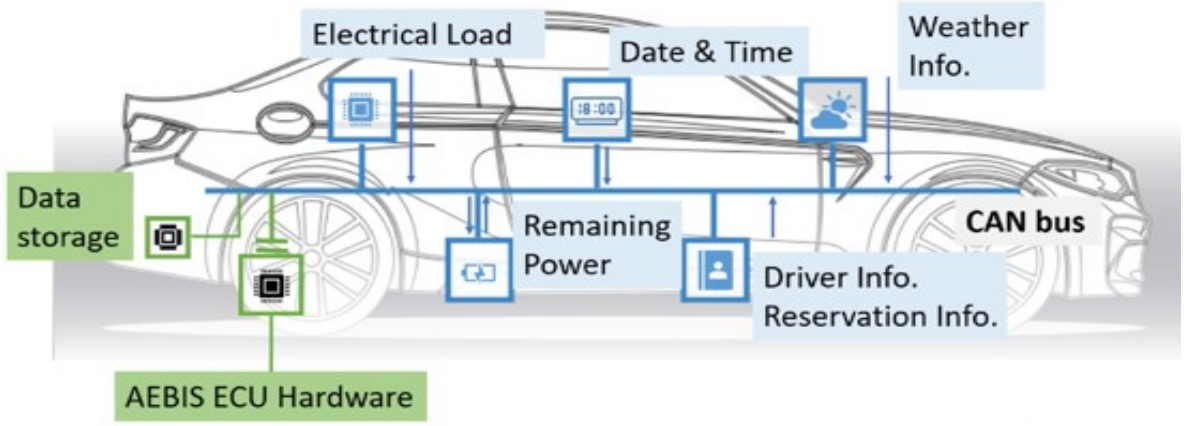

Fig. 2. Neural Network for Power Consumption Prediction of Electric Vehicle (EV).

Name	BRAM_18K	DSP48E	FF	LUT
Expression	-	-	0	493
Instance	-	5	414	950
Memory	2	-	320	20
Multiplexer	-	-	-	627
Register	-	-	454	-
Total	2	5	1188	2090
Available	120	80	35200	17600
Utilization (%)	1	6	3	11
Weights	**Memory required**			
Weights	568 Bytes			
Biases	60 Bytes			
Inputs	44 Bytes			
Total	672 Bytes			

Fig. 6. Hardware complexity of power consumption prediction system on the Zynq-7010 FPGA. The system utilized 3% of the FF, 11% of the LUT, 6% of the DSP48, and approximately 1% 18k BRAM.

benab@u-aizu.ac.jp

Smart Solar Carport: Off-Grid Energy Storage with AI and EV

On-site Field Experiment, UoA, 2021

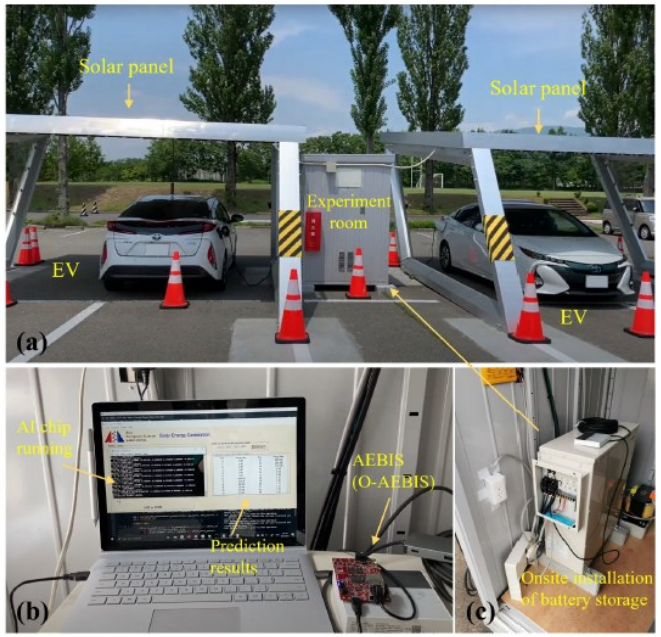

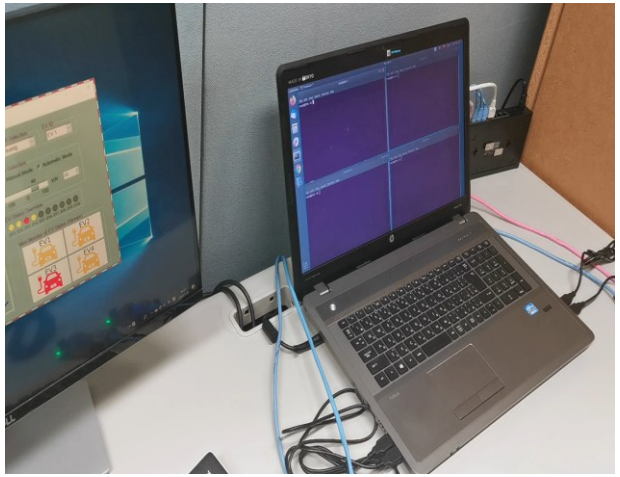

Software Tool – EV Charge/Discharge Status Display

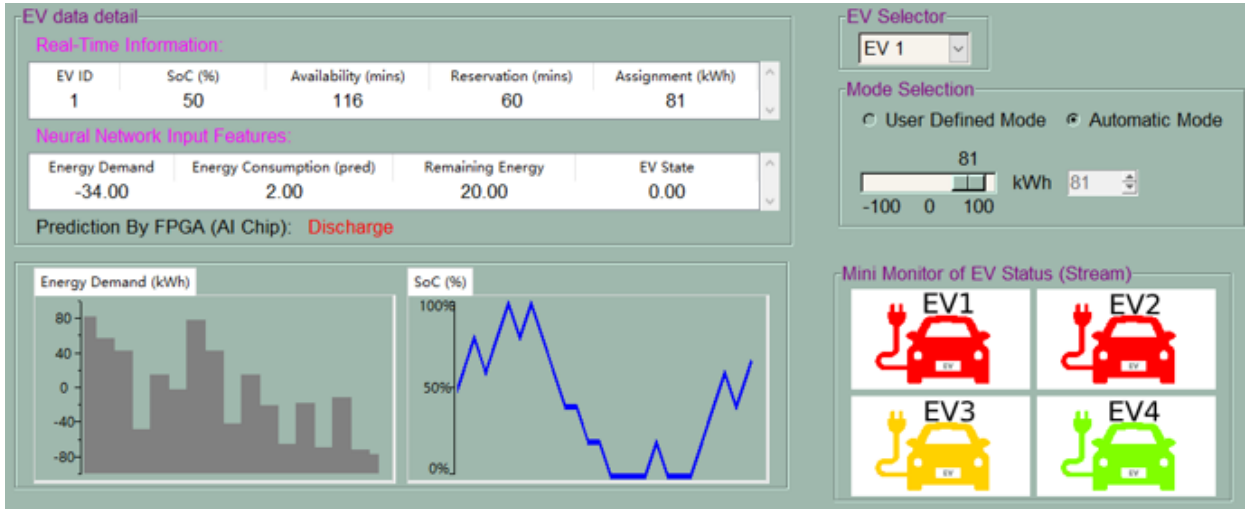

Hardware Experiments

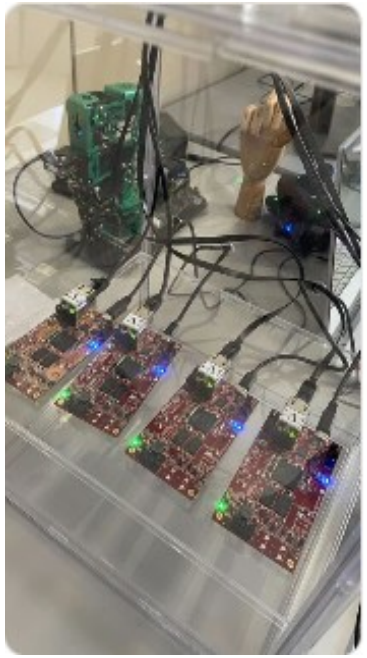

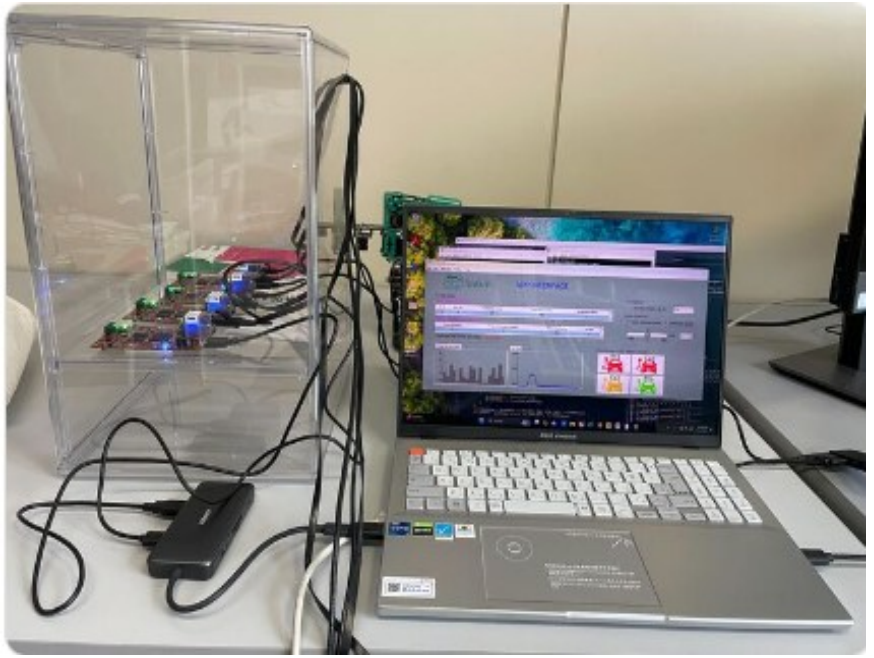

Smart Solar Carport: Off-Grid Energy Storage with AI and EV

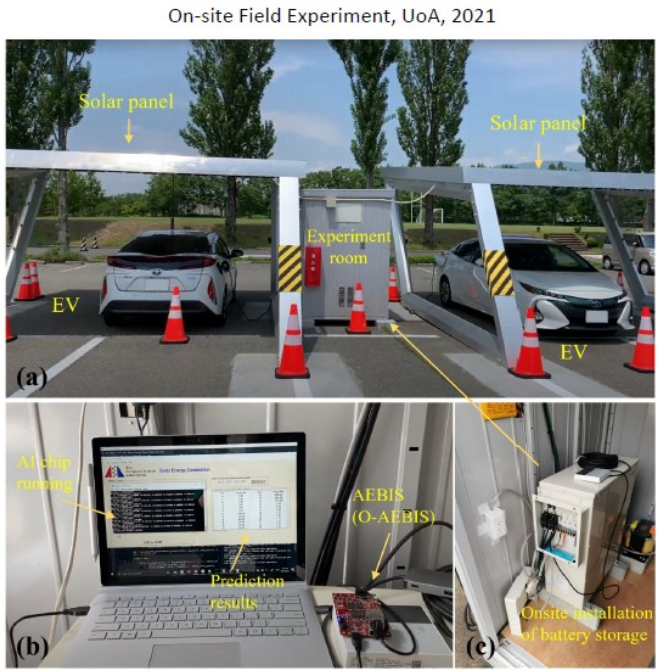

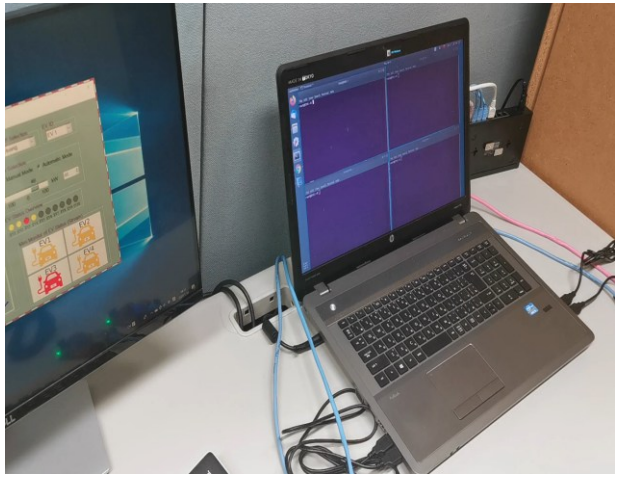

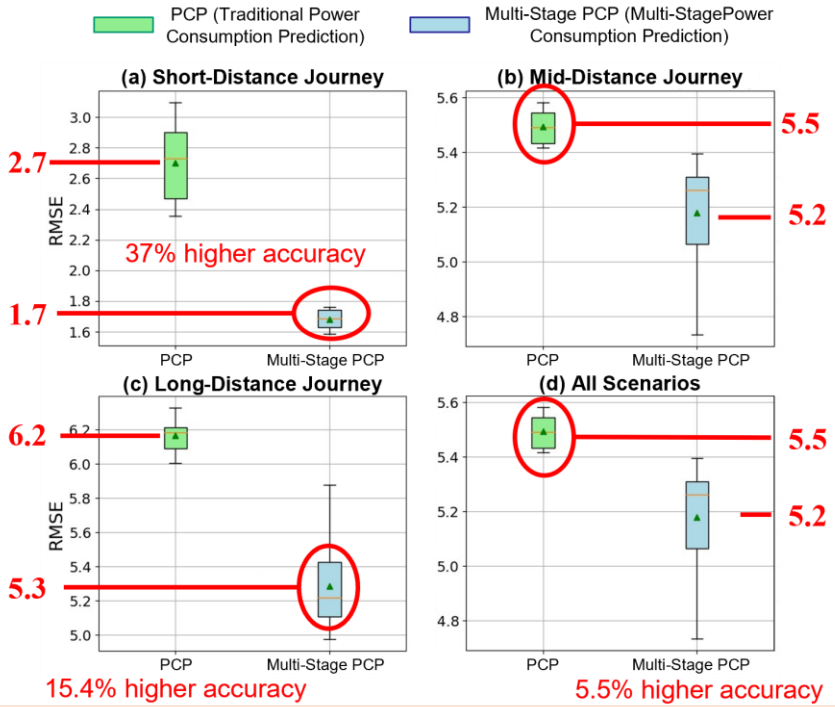

The multi-stage prediction method achieves better performance, increasing EV power consumption prediction accuracy by 5.5% across all scenarios compared to the baseline method.

Cloud Map Prediction

Table 2. Evaluation of the cloud prediction method using Fukushima cloud maps (comparative image pairs) [1].

Forecast Interval	Avg. MSE	Avg. PSNR	Avg. SSIM
30 minutes	277.30	23.75	0.893
1 hour	297.35	23.57	0.891
1.5 hours	309.49	23.53	0.892
2 hours	452.64	21.88	0.884

Table 3. Evaluation of the super-resolution-based cloud prediction method using Fukushima cloud maps (comparative image pairs) [1].

Forecast Interval	Avg. MSE	Avg. PSNR	Avg. SSIM
30 minutes	2056.39	16.52	0.909
1 hour	1906.75	16.87	0.914
1.5 hours	1863.41	16.68	0.916
2 hours	1578.94	17.89	0.926

Robust performance of the cloud map prediction with high accuracy and structural similarity. The cloud map prediction benefits from super-resolution. Combining the cloud map with numerical meteorological data maintains the accuracy

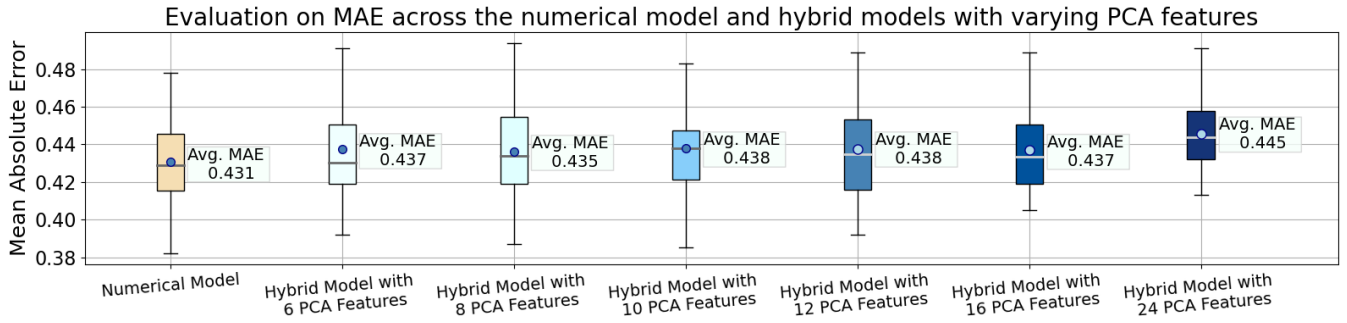

Solar Energy Generation Prediction

[Japan Meteorological Agency, "Weather Satellite Himawari," accessed Nov. 25, 2025, https://www.jma.go.jp/bosai/map.html

AI Enabled Energy Trading in Distributed Ve2G Network

On-site Field Experiment, UoA, 2021

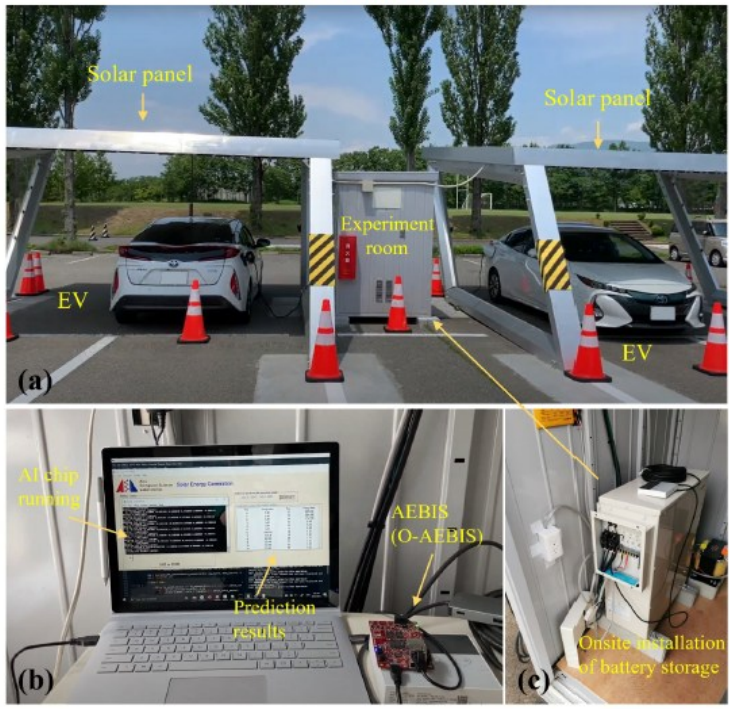

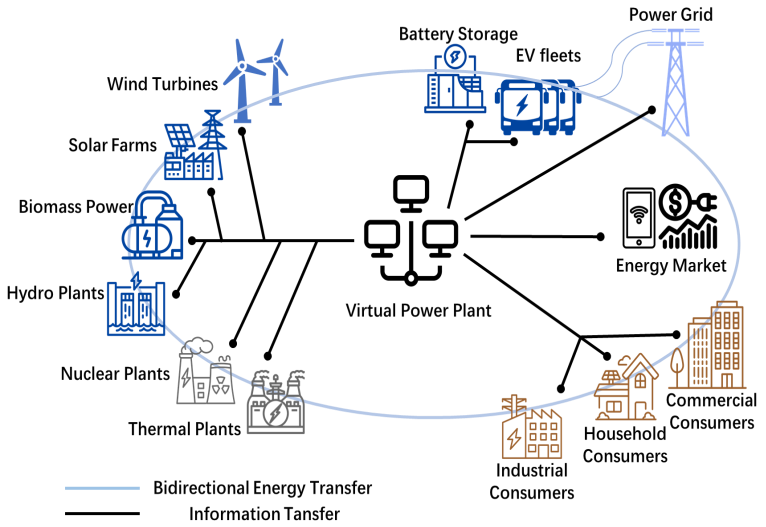

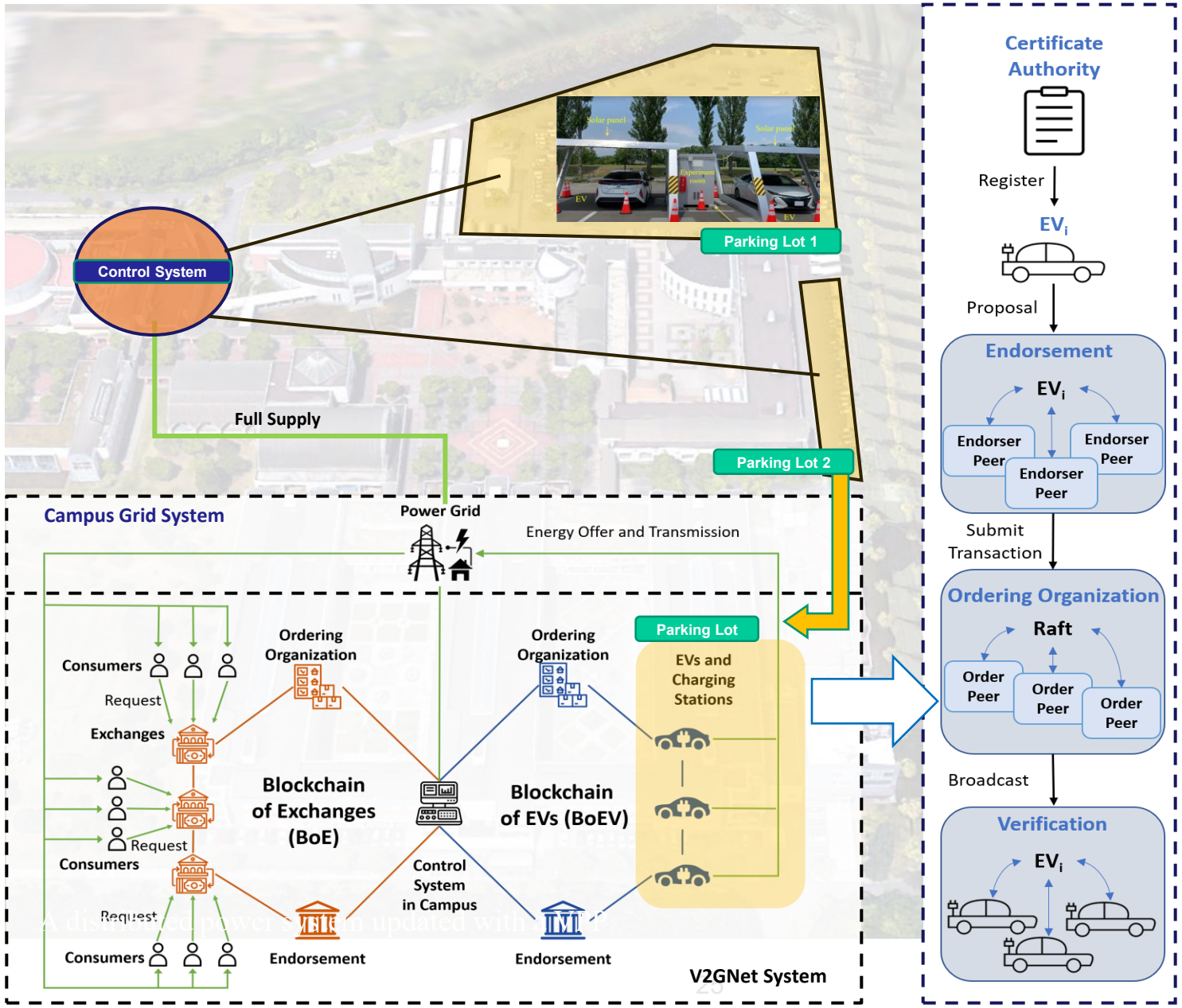

V2G Energy Trading: Building Trust in the Grid

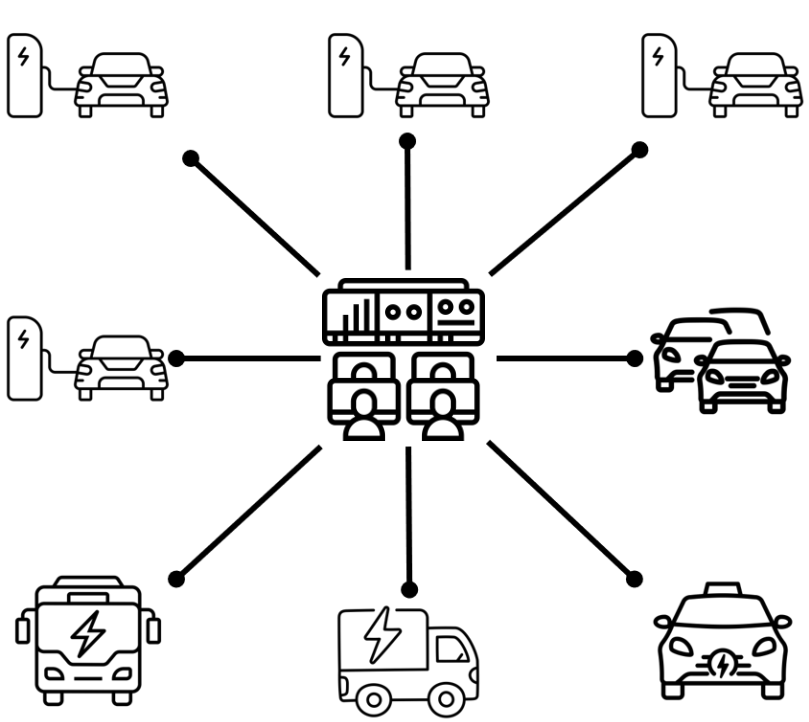

centralized

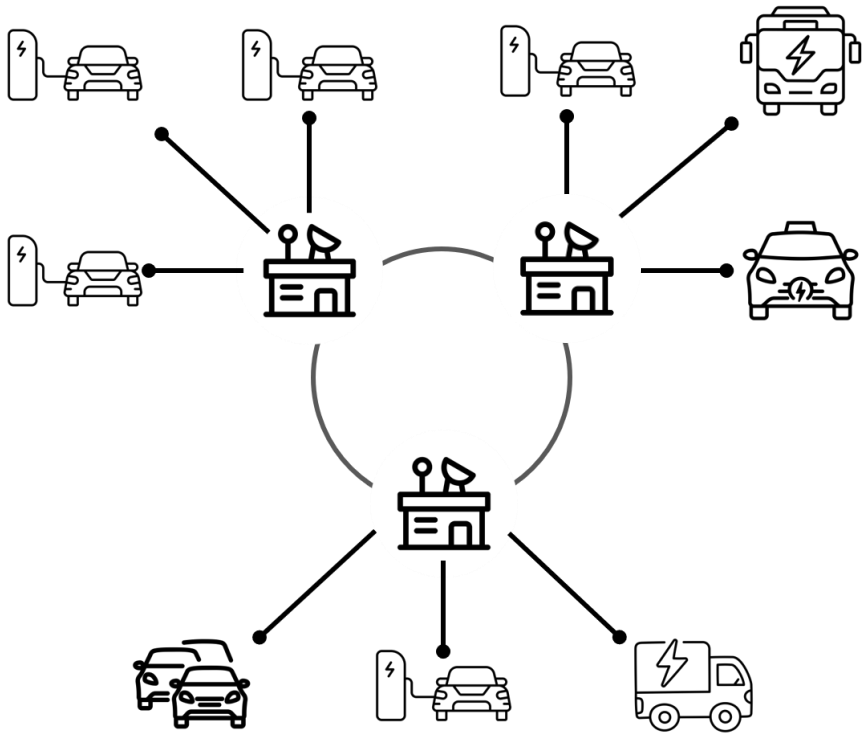

decentralized

Centralized and decentralized energy trading system networks.
Its objective is to optimize efficiency, security, privacy, and scalability.

V2G Energy Trading: Building Trust in the Grid

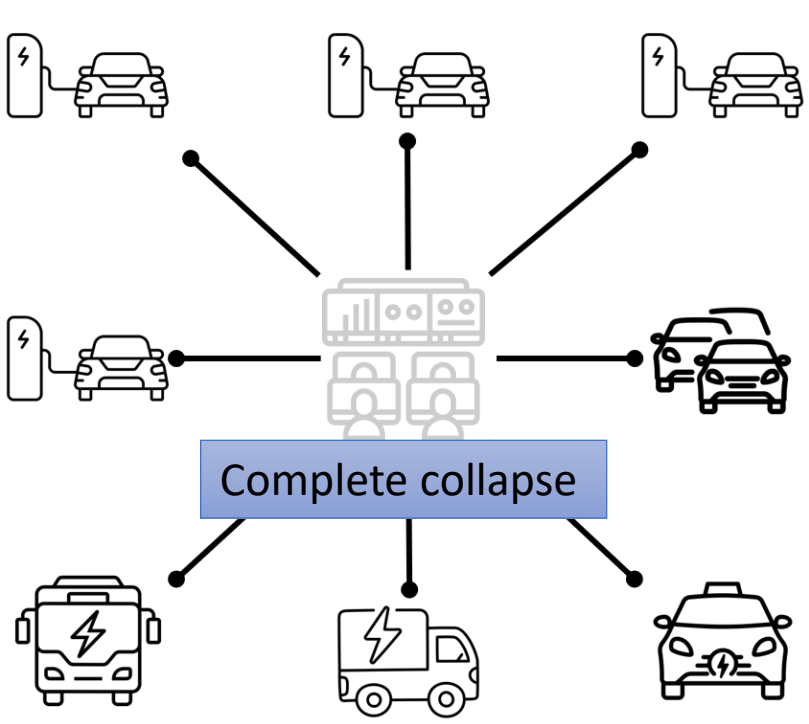

centralized

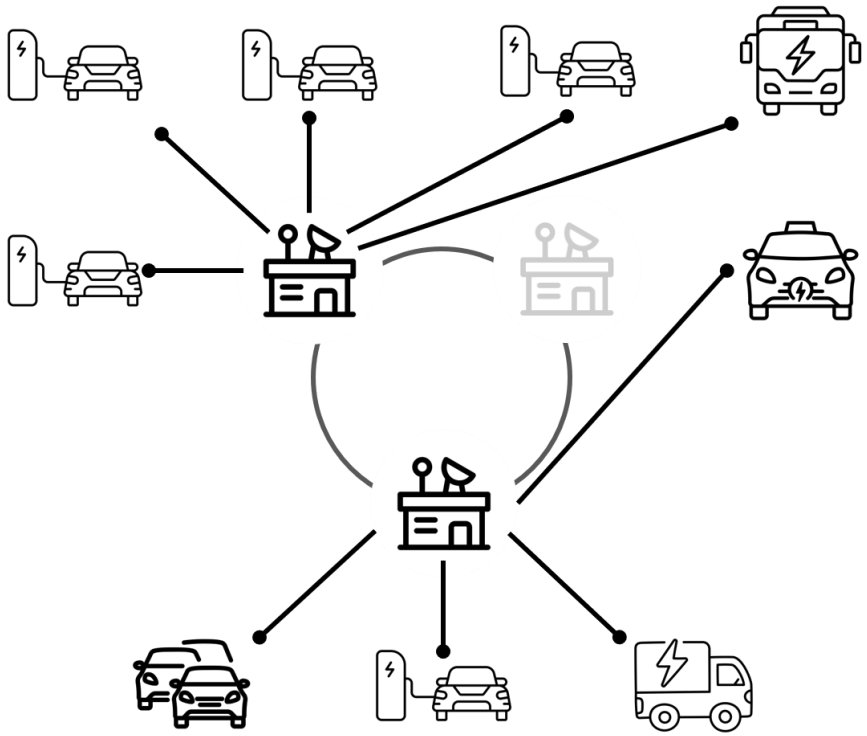

decentralized

Centralized and decentralized energy trading system networks. Its objective is to optimize efficiency, security, privacy, and scalability.

V2G Energy Trading: Building Trust in the Grid

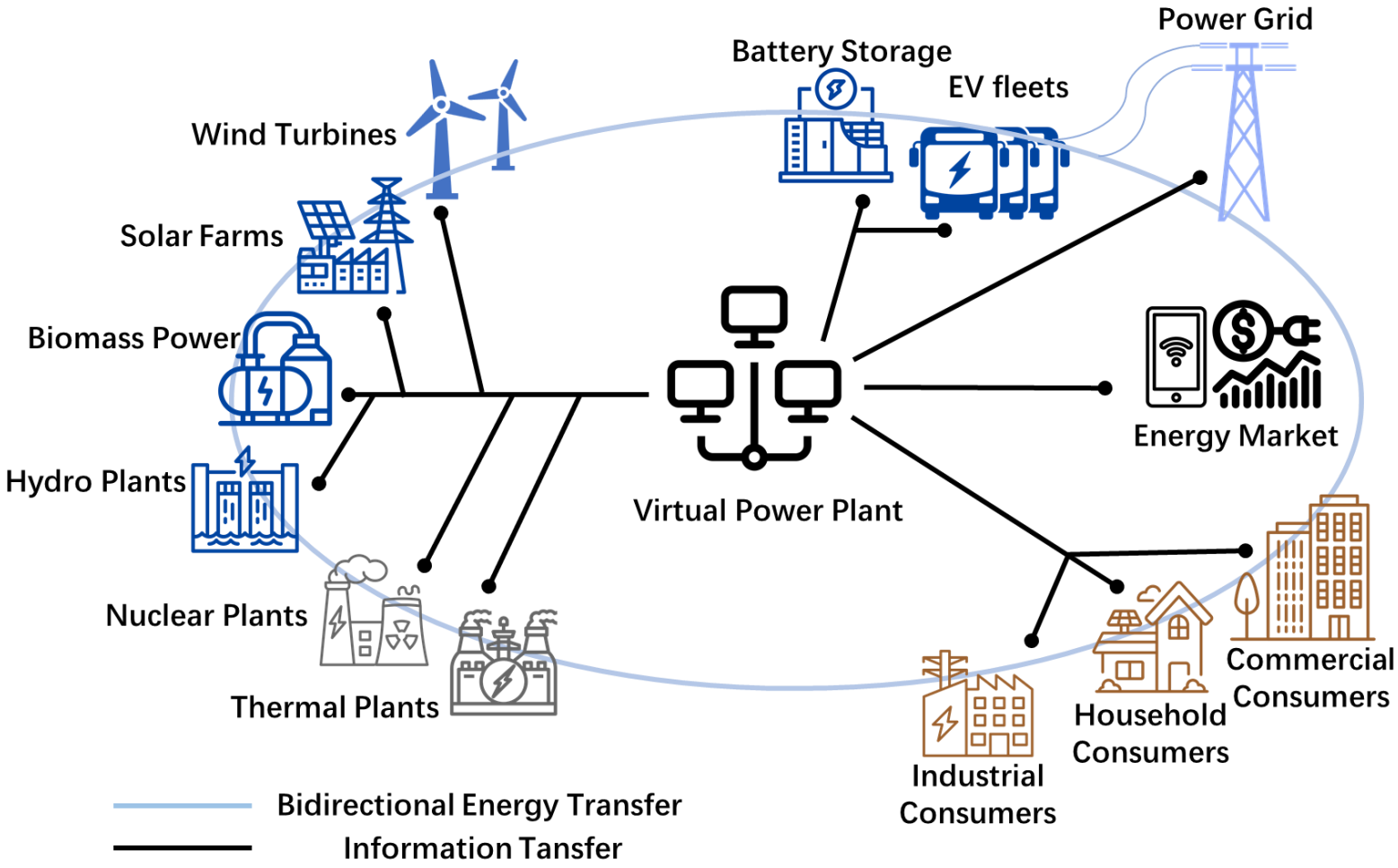

Illustration of a distributed power system updated with a VPP and energy storage departments.
The grid turns from the center of the system to a necessary ancillary part.
The VPP now serves as an information processing center, integrating the power grid, energy market, renewable and non-renewable resources, energy storage systems, and energy consumers.

V2G Energy Trading: Building Trust in the Grid

- Each campus' V2G control system (CS) works as an information mediator between energy consumers and EV suppliers.
- Each consumer connects and submits the energy request to the energy exchange.
- In BoEV, the offer lists (EVs to CS) and notification of discharge tasks (CS to EVs) are transmitted.
- Only necessary trading data is uploaded to keep privacy and shorten the chaining latency.

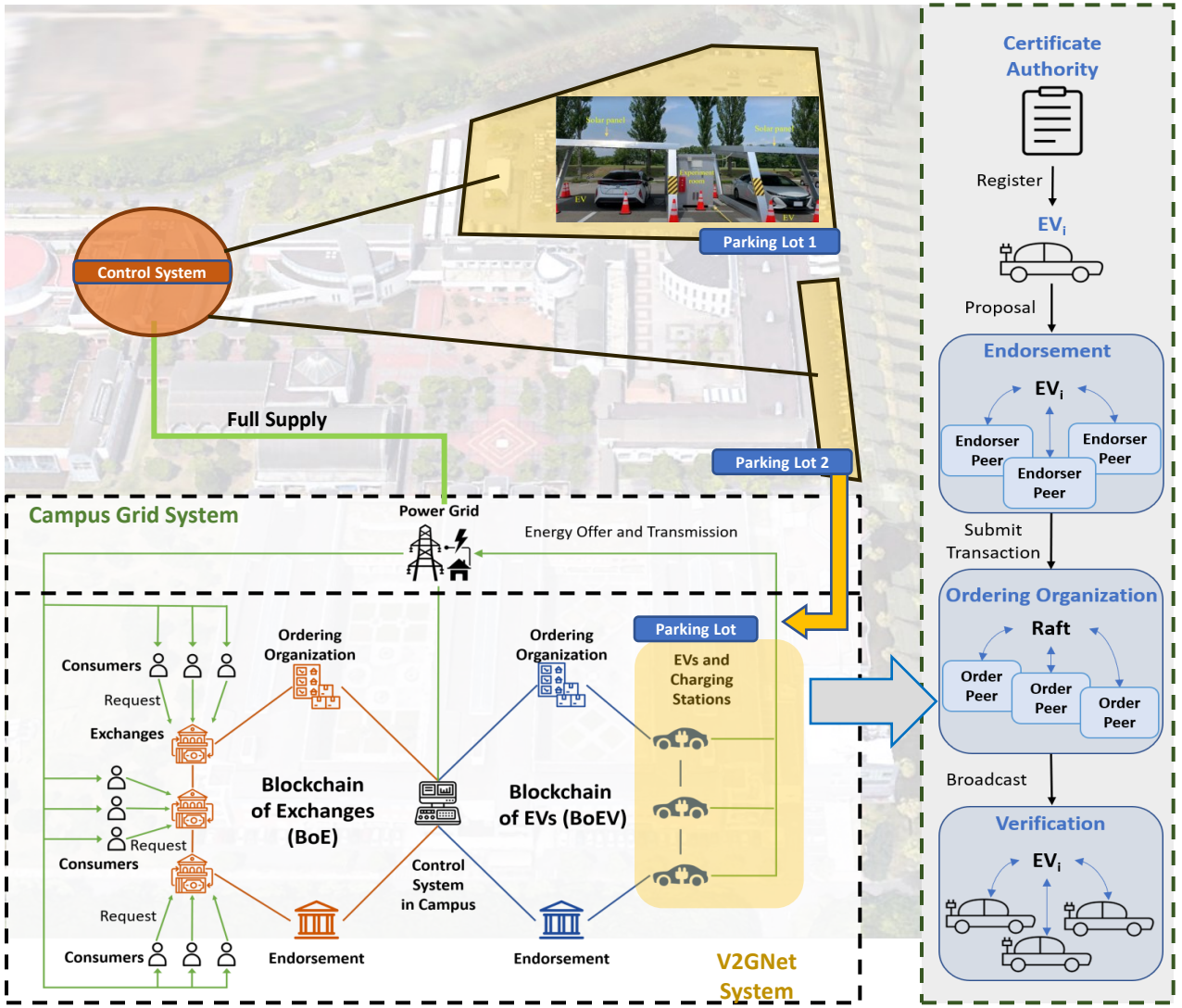

Overview of V2GNet for energy trading in a campus V2G network.

V2G Energy Trading: Building Trust in the Grid

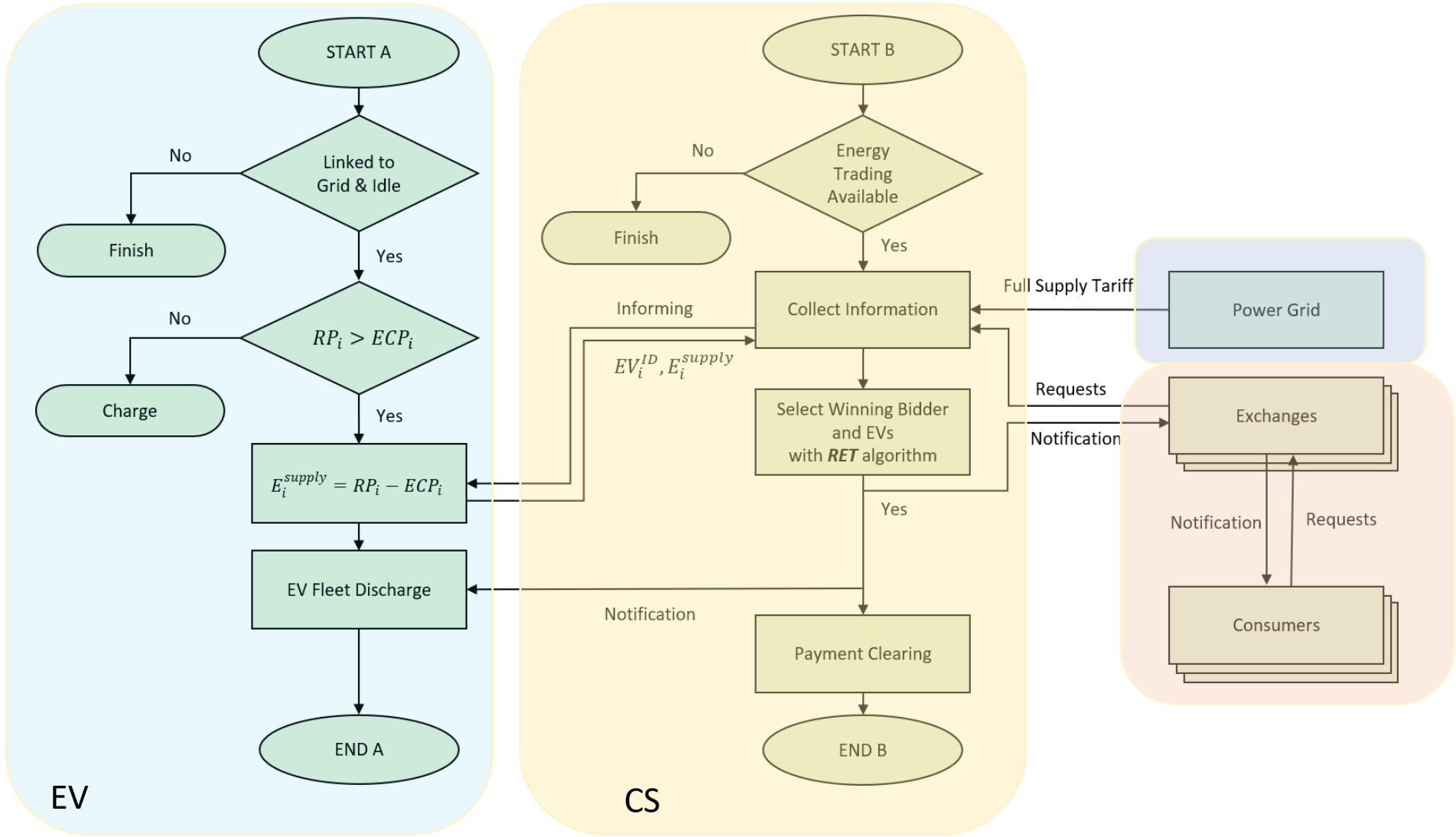

Flowchart for V2GNet Trading Algorithm.

benab@u-aizu.ac.jp

V2G Energy Trading: Building Trust in the Grid

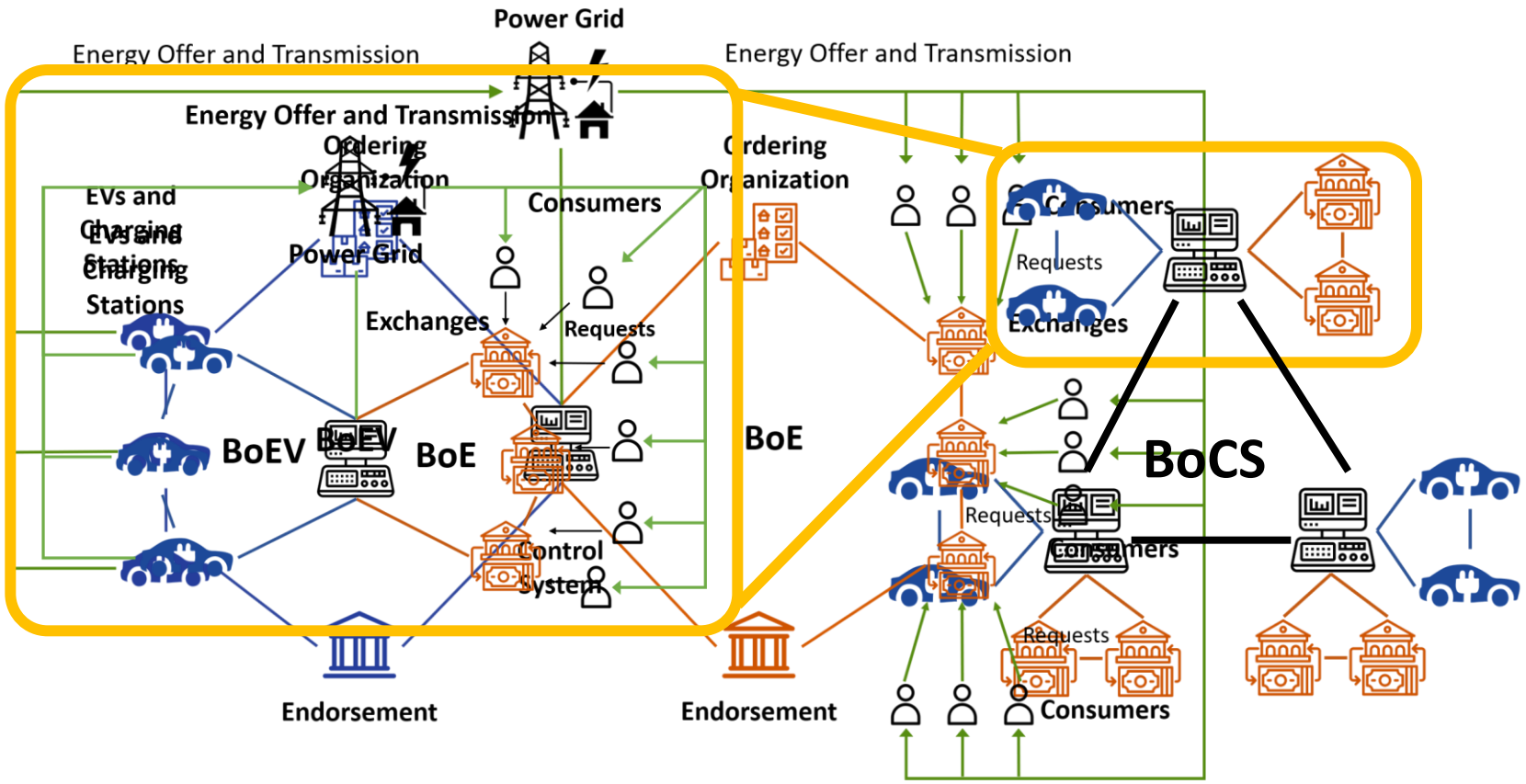

Overview of the proposed blockchain of campus control systems (BoCS) among campuses based on the CS of each V2GNet.

- The BoCS is where inter-campus energy trading is planned and recorded, and each CS is a node of the BoCS. Besides, each campus's CS serves as a blockchain connection between the BoEV and the BoE for that campus.

V2G Energy Trading: Building Trust in the Grid

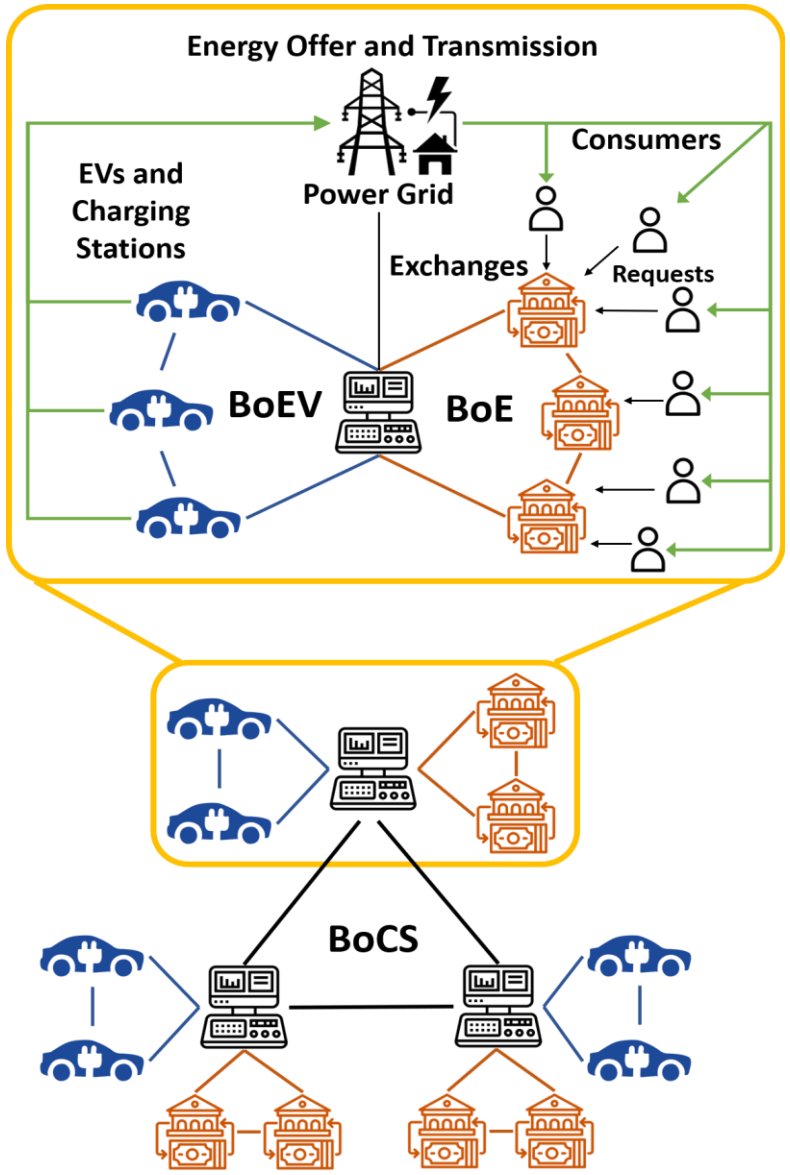

1. Upload unselected EV suppliers and energy requests.
2. Download the overall request list and EV supplier list.
3. Compete on trading planning SRET mechanism and uploading the outcome back to BoCS.
4. Download and record the new block from BoCS. Arrange energy trading accordingly.

Overview of the proposed blockchain of campus control systems (BoCS) among campuses based on the CS of each V2GNet.

V2G Energy Trading: Building Trust in the Grid

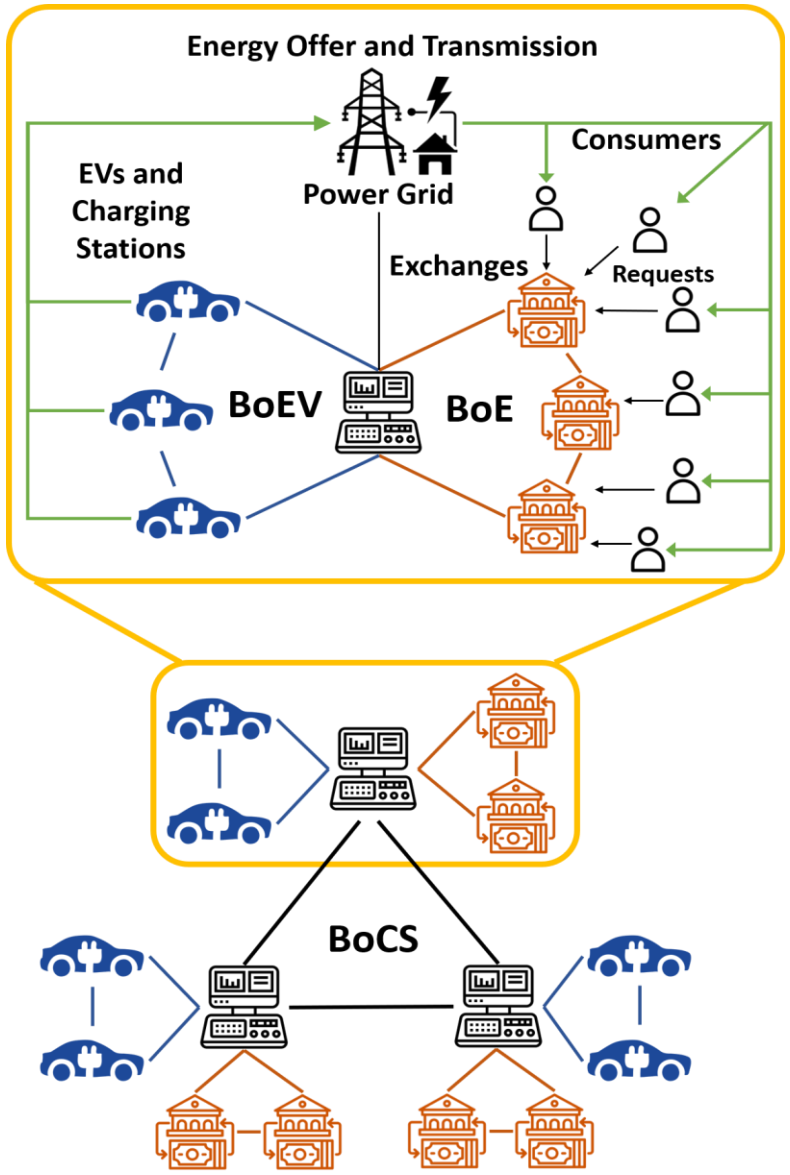

1. **The initial step in BoCS begins once any CS completes and uploads the local trading plan to its BoE and BoEV. The CS packs the data for its unselected EVs and requests into a transaction, then broadcasts it on BoCS. Once enough transactions are collected within any pool, the corresponding CS dispatch them for endorsement and ordering, then package into a block. The block is broadcast across BoCS for verification.**
2. Download the overall request list and EV supplier list.
3. Compete on trading planning SRET mechanism and uploading the outcome back to BoCS.
4. Download and record the new block from BoCS. Arrange energy trading accordingly.

Overview of the proposed blockchain of campus control systems (BoCS) among campuses based on the CS of each V2GNet.

V2G Energy Trading: Building Trust in the Grid

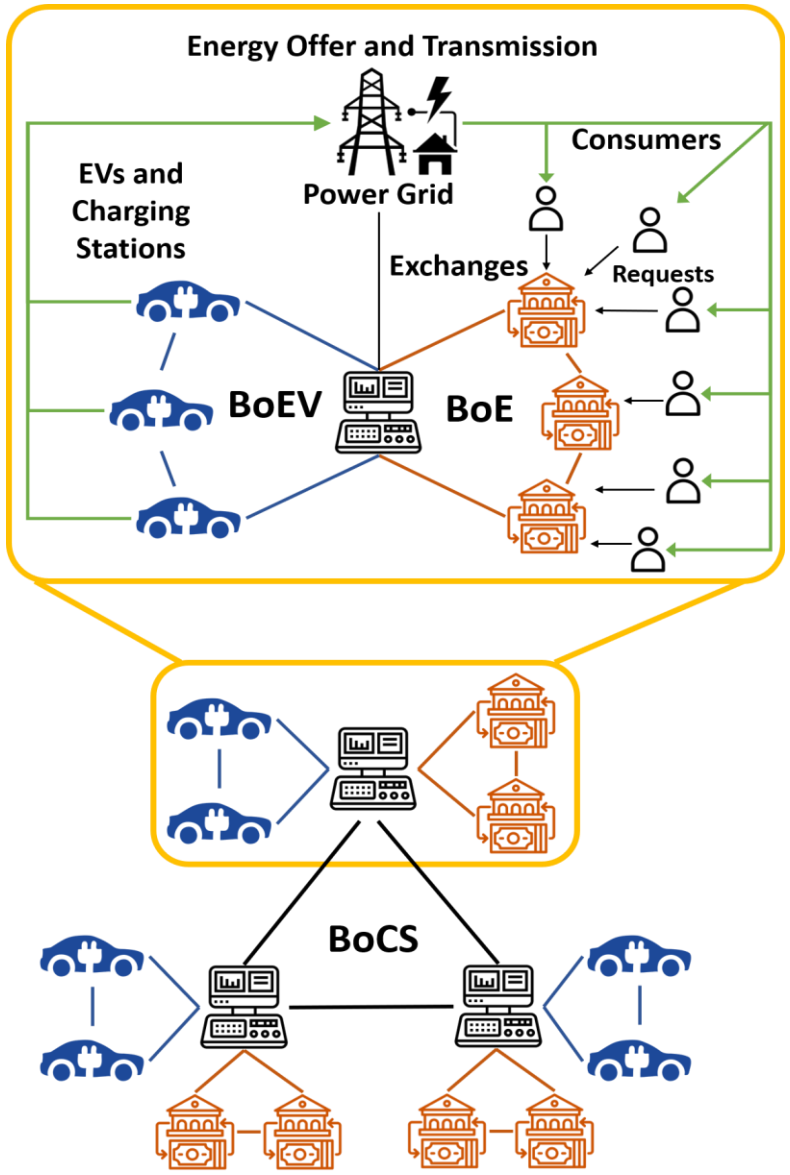

1. Upload unselected EV suppliers and energy requests.
2. **After the block is verified, each node of the BoCS proceeds to download the block, extracting the associated lists and consolidating these lists into an overall request list and an overall EV supplier list.**
3. Compete on trading planning SRET mechanism and uploading the outcome back to BoCS.
4. Download and record the new block from BoCS. Arrange energy trading accordingly.

Overview of the proposed blockchain of campus control systems (BoCS) among campuses based on the CS of each V2GNet.

V2G Energy Trading: Building Trust in the Grid

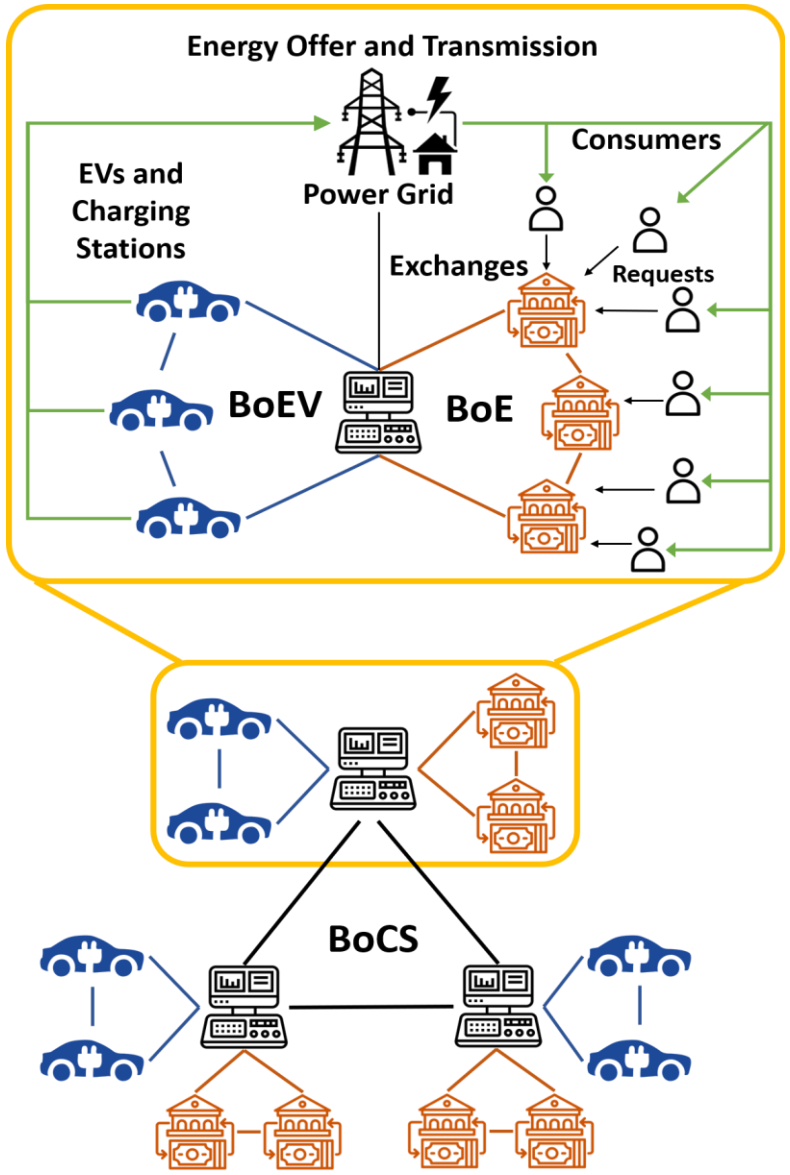

1. Upload unselected EV suppliers and energy requests.
2. Download the overall request list and EV supplier list.
3. Compete on trading planning SRET mechanism and uploading the outcome back to BoCS.
4. **The new block is downloaded and permanently recorded by all CS nodes of BoCS network. From the block, each CS extracts the cross-campus energy trading outcomes and notifies the relevant consumers and EVs of their specific trading details accordingly.**

Overview of the proposed blockchain of campus control systems (BoCS) among campuses based on the CS of each V2GNet.

V2G Energy Trading: Building Trust in the Grid

The number of requests and EVs is equal, and demand can be almost entirely covered
要求数とEVの台数は同数であり、需要はほぼ完全に賄うことができます。

The number of EVs is half, but they can still cover more than 60% of demand.
EVの台数は半分ですが、それでも需要の60%以上を賄うことができます。

Achieves 45% more total profit of a single energy trading round, compared to the baseline methods.
基準手法と比較して、単一のエネルギー取引ラウンドにおいて総利益を45%多く達成します。

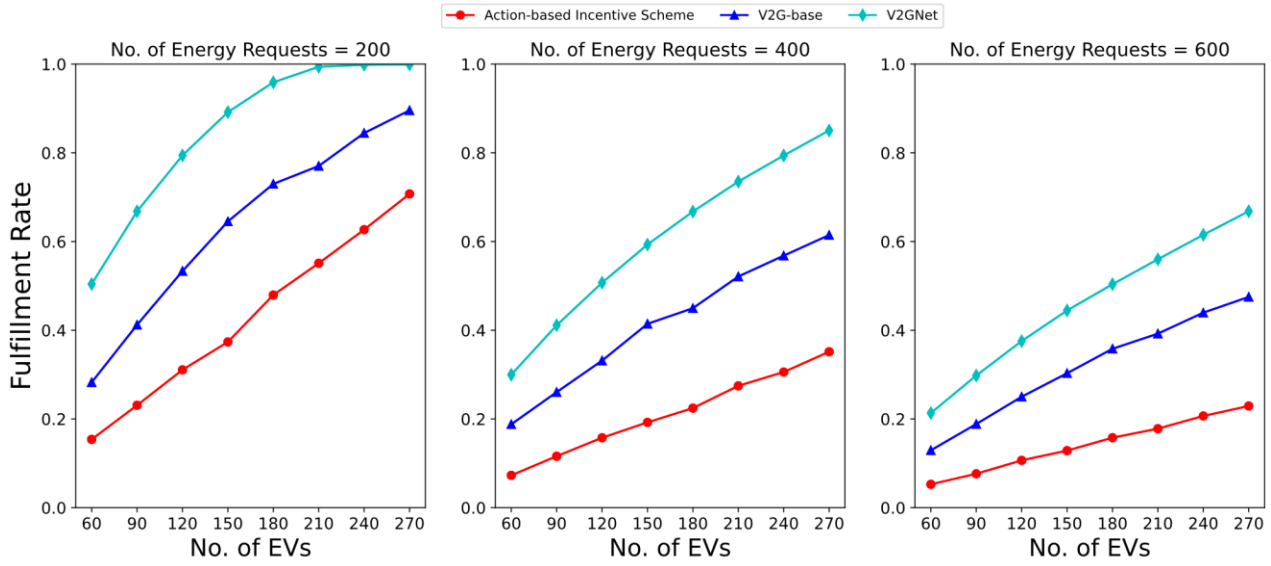

Evaluation of the fulfillment rate of a single energy trading round across three trading strategies.

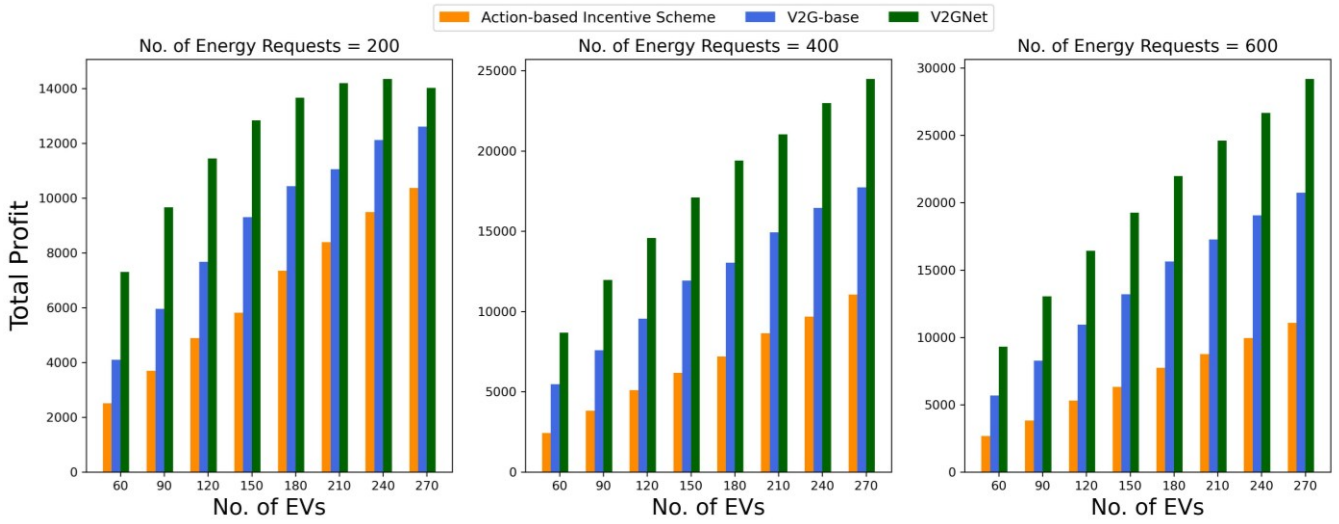

Evaluation of the total profit (JPY) of a single energy trading round across three trading strategies.

An **action-based incentive scheme** in EV grid energy trading rewards electric vehicle (EV) owners or aggregators for their actual participation and actions in energy trading—such as charging, discharging, or providing grid services—rather than just for availability.

Y. Liang, Z. Wang and A. B. Abdallah, "V2GNet: Robust Blockchain-Based Energy Trading Method and Implementation in Vehicle-to-Grid Network," in IEEE Access, 2022
.Liang, Z. Wang and A. B. Abdallah, "Robust Vehicle-to-Grid Energy Trading Method Based on Smart Forecast and Multi-Blockchain Network," in IEEE Access, 2024

Evaluation Results

Input Feature	Value	Unit
Discharge Power	0 to 10	kWh, Float
Charge Power	15	kWh, Int
Driving Power	10	kWh, Int
Driving Time Slot	20 to 22	-, Float
Charge Time Slot	20 to 21	-, Float
Request Time Slot	21 to 22	-, Float
No. of Energy Exchange	3	-, Int
No. of Malicious Exchanges	1	-, Int
No. of Malicious Consumers	1, 5, 10, 20, 50	-, Int
EV State	Idle, Charging, Driving	-, Int
Battery Capacity	60	kWh, Int
Requests Capacity	0 to 10	kWh, Float
Maximum No. of Requests from One Malicious Consumer	10	-, Int
Bid Price	22.39 to 42.84	JPY, Float

[1] The currency code for the Japanese Yen is JPY.

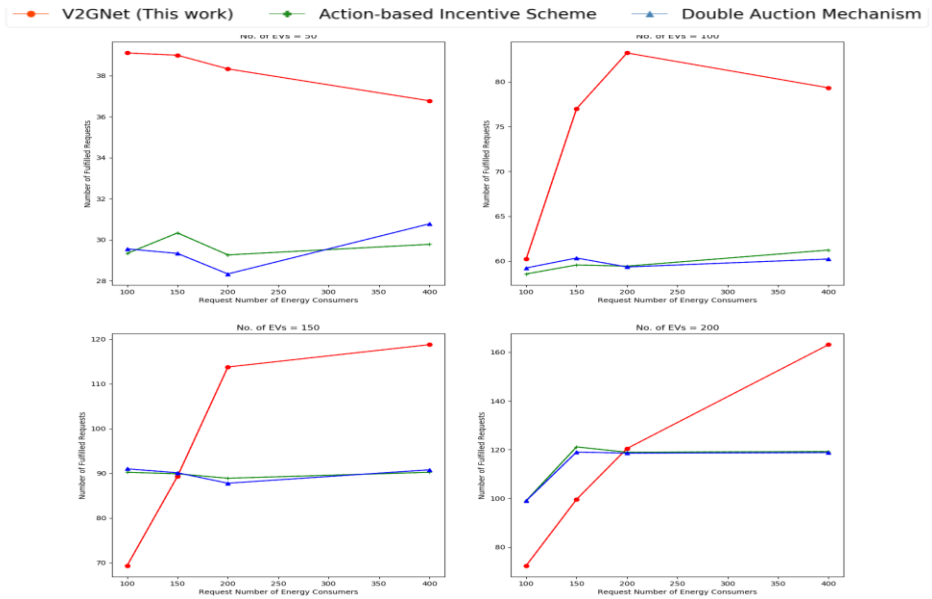

V2GFTN Energy Trading Results : Time cost ratios

Table 3. The **total time consumption** of an energy trading round across four trading strategies: 1) the action-based incentive scheme; 2) V2GNet; 3) double time boundaries scheme within V2GFTN; 4) single time boundary scheme within V2GFTN..

Time Consumption (s)		No. of EVs															
		Action-Based Incentive Scheme				V2GNet				Double Time Boundary (This Work)				Single Time Boundary (This Work)			
		60	90	120	150	60	90	120	150	60	90	120	150	60	90	120	150
No. of Requests	200	1.79	3.36	5.88	8.54	4.45	6.75	7.33	9.49	3.78	7.73	13.92	21.65	7.47	19.44	43.67	73.92
	400	1.84	3.37	5.84	8.53	4.21	7.37	9.49	10.56	3.44	7.40	13.13	21.09	7.25	19.90	41.10	73.44
	600	1.97	3.26	5.78	8.59	6.71	8.26	7.55	10.02	3.30	7.30	12.83	20.39	7.12	19.50	43.03	71.76

Time Consumption (s)		No. of EVs															
		Action-Based Incentive Scheme				V2GNet				Double Time Boundary (This Work)				Single Time Boundary (This Work)			
		180	210	240	270	180	210	240	270	180	210	240	270	180	210	240	270
No. of Requests	200	12.48	17.09	22.15	29.87	14.04	19.22	25.62	30.50	30.92	41.78	54.30	66.23	113.90	176.27	249.86	340.09
	400	12.31	16.72	21.67	28.22	17.42	19.34	22.60	29.45	29.95	40.65	53.64	69.04	119.70	167.19	253.91	375.00
	600	12.39	16.59	25.52	28.91	12.97	16.92	22.07	30.12	29.30	40.55	53.46	77.80	117.84	176.44	248.36	338.12

The time consumption is the total time CS spend on trading planning for a whole energy trading round of the V2G system. In our hour-ahead V2G trading system, the upper limit of time consumption turns out to be 1 hour.

The multi-blockchain processing time makes the most of the overall time cost of V2GFTN. And getting notifications from cross-campus V2G trading on the BoCS takes more time than from V2G trading within a single campus from the CS. This is because the BoCS takes extra time to upload and download the data of the remaining EVs and requests.

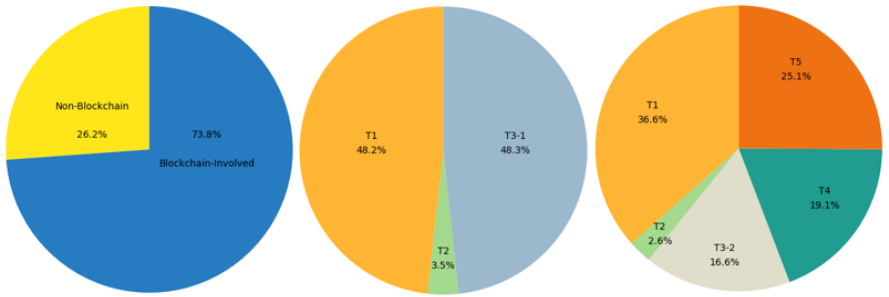

(a) Time ratio of blockchain-involved and non-blockchain process.

(b) Time ratio of Phase 1, Phase 2, and Phase 3-1 for BoE and BoEV.

(c) Time cost ratio of Phase 1 to Phase 5 for BoE, BoEV, and BoCS.

Figure 26. Comparative analysis of **time cost ratios** in different scenarios.

Real-World Deployment 2: Distributed AI-Driven HW–SW Platform Transforming Medical Applications

benab@u-aizu.ac.jp

Distributed AI-Powered HW-SW Platform for Pneumonia Detection

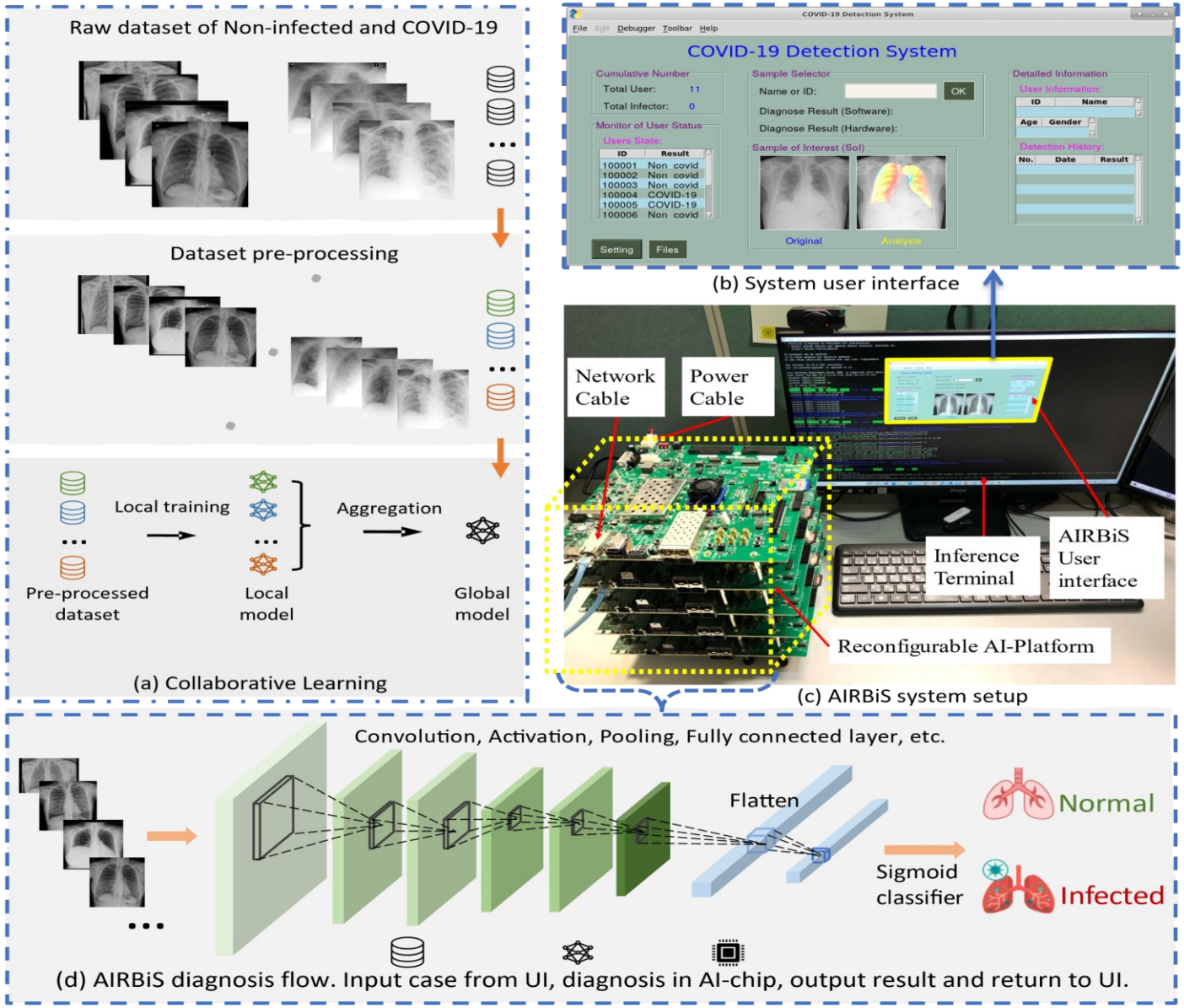

Table 7.3. FPGA Resource Utilization Estimates.

Resource	Utilization		Available	Utilization (%)	
	ANN	SNN		ANN	SNN
LUT	54,585	27,288	274,080	19.9	9.9
LUTRAM	3668	2048	144,000	2.5	1.28
FF	53,035	37,098	548,160	9.7	6.77
BRAM	824	0	912	90.4	0
DSP	35	0	2520	1.4	0
BUFG	4	18	404	1.0	4.45
MMCM	1	0	4	25	0

Table 7.4. Hardware Complexity.

Core/Parameter	Area (mm^2)		Power (mW)	
	SNN	ANN	SNN	ANN
Convolution core	0.0748	0.0755	0.007	0.011

Table 7.2. Dataset description.

Label	Class	Train	Test
COVID	COVID	2870	700
	COVID(Augmented)	14,349	-
Non-COVID	Normal	9791	400
	Lung_Opacity	5762	250
	Viral_Pneumonia	1288	50
Sum		34,060	1400

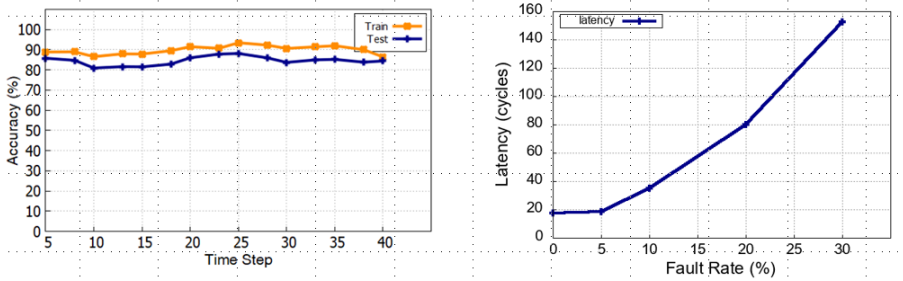

(a) Detection accuracy over various time-steps (b) Detection Latency over various fault-rate

Figure 7.6. Accuracy and fault-rate evaluation result

benab@u-aizu.ac.jp

Architecture of 3D-NoC-based Neuromorphic Pneumonia Detection System

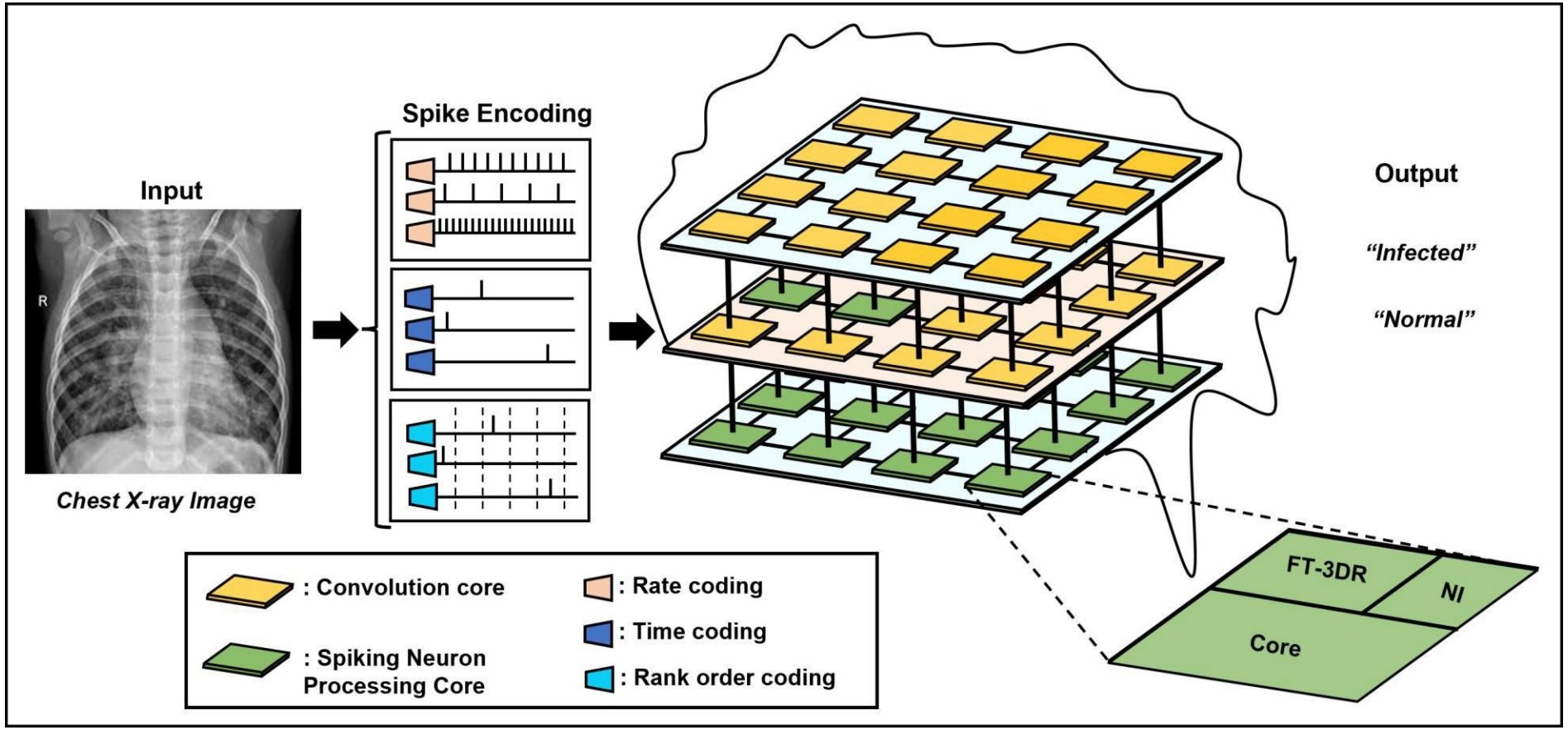

Figure 7.1. High level view of 3D-NoC-based neuromorphic pneumonia detection system.

Jiangkun Wang, Ogbodo Mark Ikechukwu, Khanh N. Dang, and Abderazek Ben Abdallah. ‘S k -Event X-ray Image Classification for 3D-NoC-Based Neuromorphic Pneumonia , Detection, Electronics, vol. 11, no. 24, p. 4157, 2022. doi: 10.3390/electronics11244157.

Architecture of 3D-NoC-based Neuromorphic Pneumonia Detection System

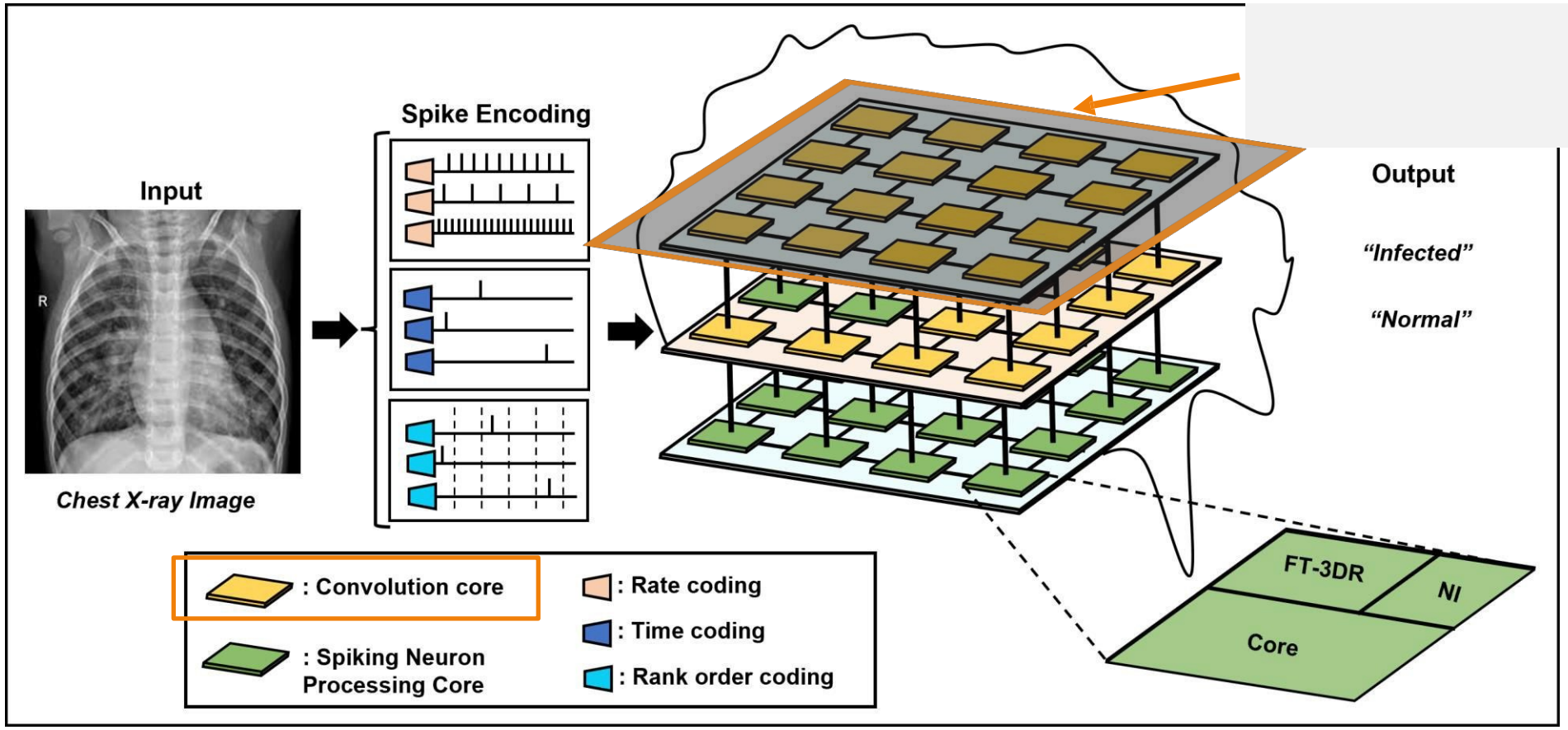

Figure 7.1. High level view of 3D-NoC-based neuromorphic pneumonia detection system.

Jiangkun Wang, Ogbodo Mark Ikechukwu, Khanh N. Dang, and Abderazek Ben Abdallah. ‘S k -Event X-ray Image Classification for 3D-NoC-Based Neuromorphic Pneumonia , Detection, Electronics, vol. 11, no. 24, p. 4157, 2022. doi: 10.3390/electronics11244157.

Architecture of 3D-NoC-based Neuromorphic Pneumonia Detection System

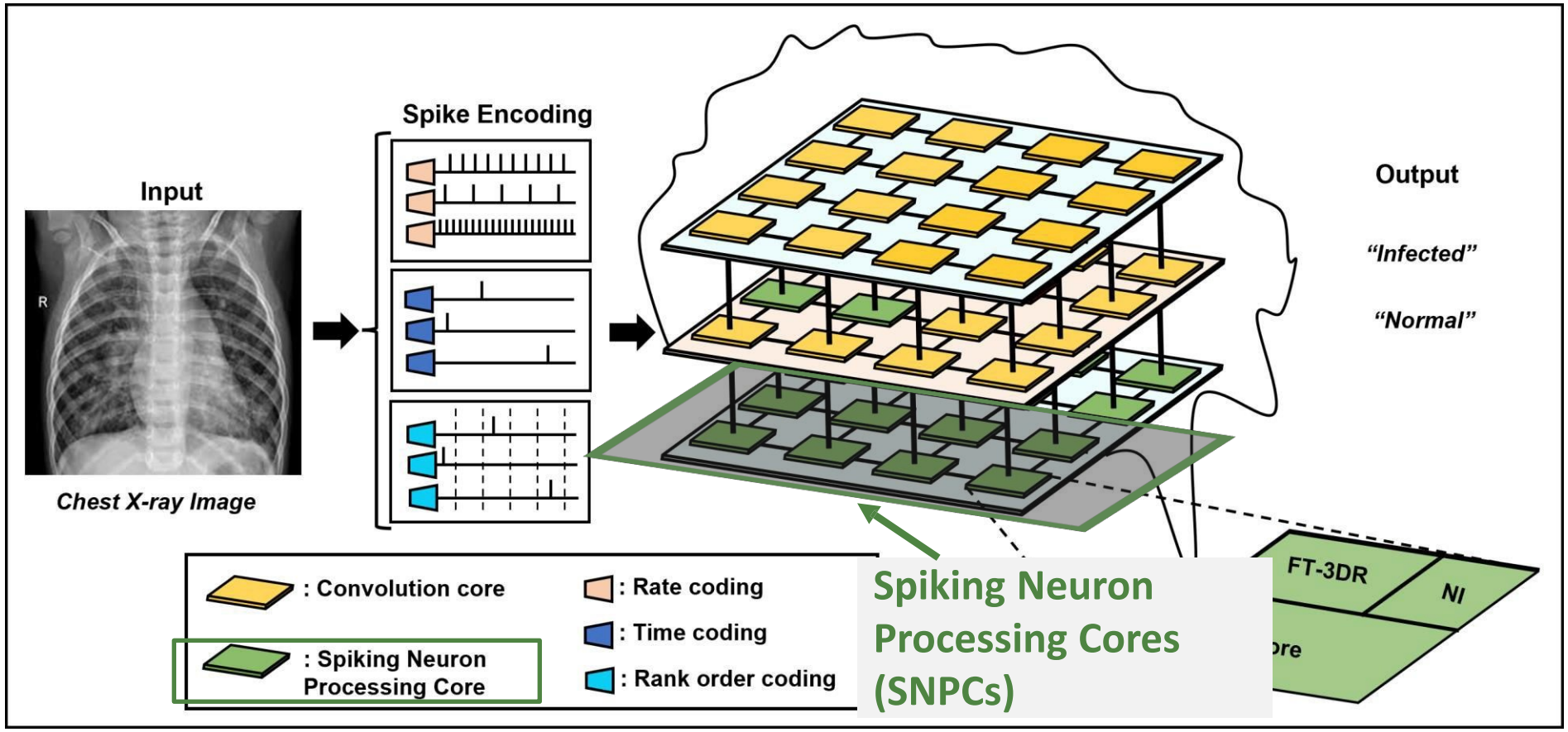

Figure 7.1. High level view of 3D-NoC-based neuromorphic pneumonia detection system.

Jiangkun Wang, Ogbodo Mark Ikechukwu, Khanh N. Dang, and Abderazek Ben Abdallah. 'S k -Event X-ray Image Classification for 3D-NoC-Based Neuromorphic Pneumonia , Detection, Electronics, vol. 11, no. 24, p. 4157, 2022. doi: 10.3390/electronics11244157.

Architecture of 3D-NoC-based Neuromorphic Pneumonia Detection System

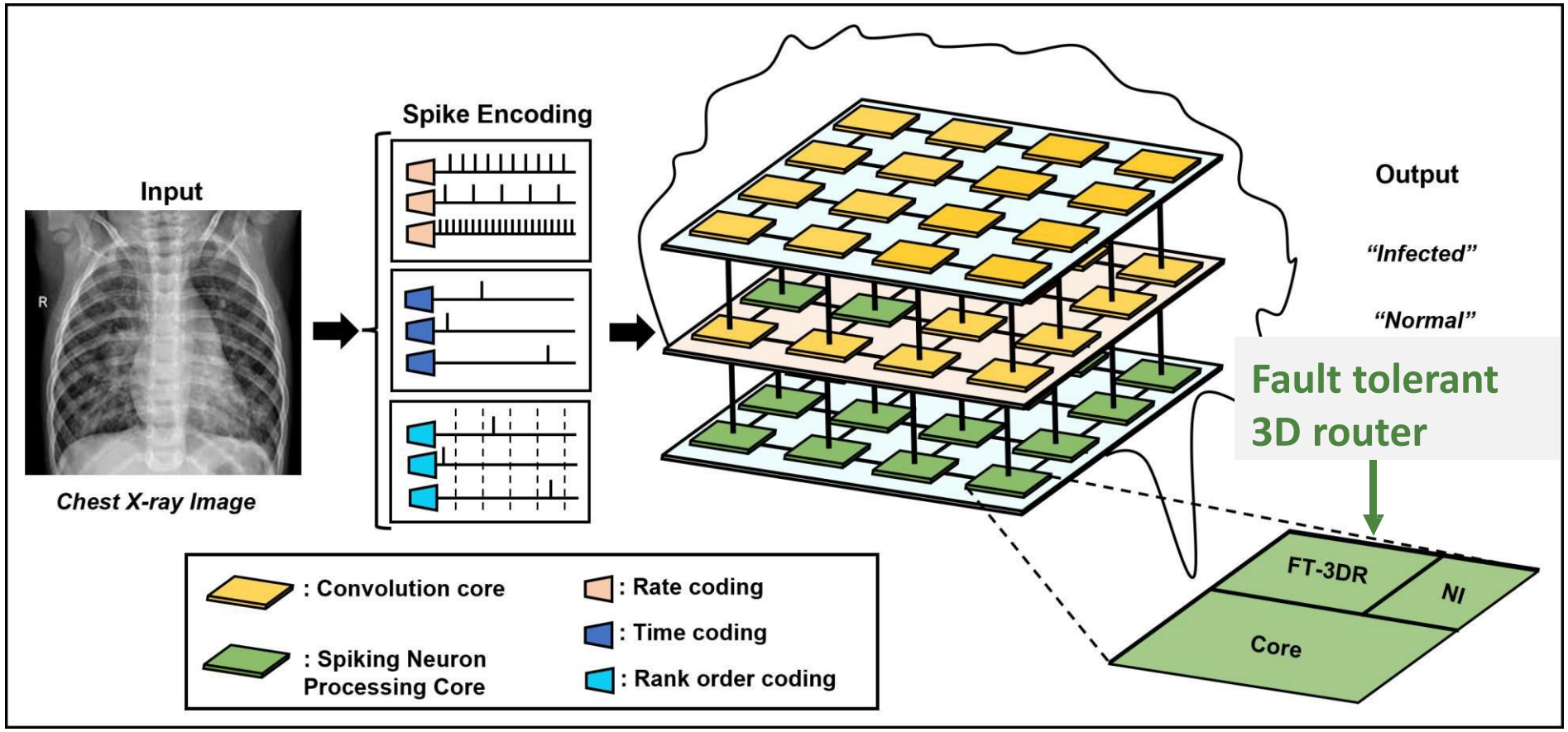

Figure 7.1. High level view of 3D-NoC-based neuromorphic pneumonia detection system.

Jiangkun Wang, Ogbodo Mark Ikechukwu, Khanh N. Dang, and Abderazek Ben Abdallah. ‘S k -Event X-ray Image Classification for 3D-NoC-Based Neuromorphic Pneumonia , Detection, Electronics, vol. 11, no. 24, p. 4157, 2022. doi: 10.3390/electronics11244157.

Architecture of 3D-NoC-based Neuromorphic Pneumonia Detection System

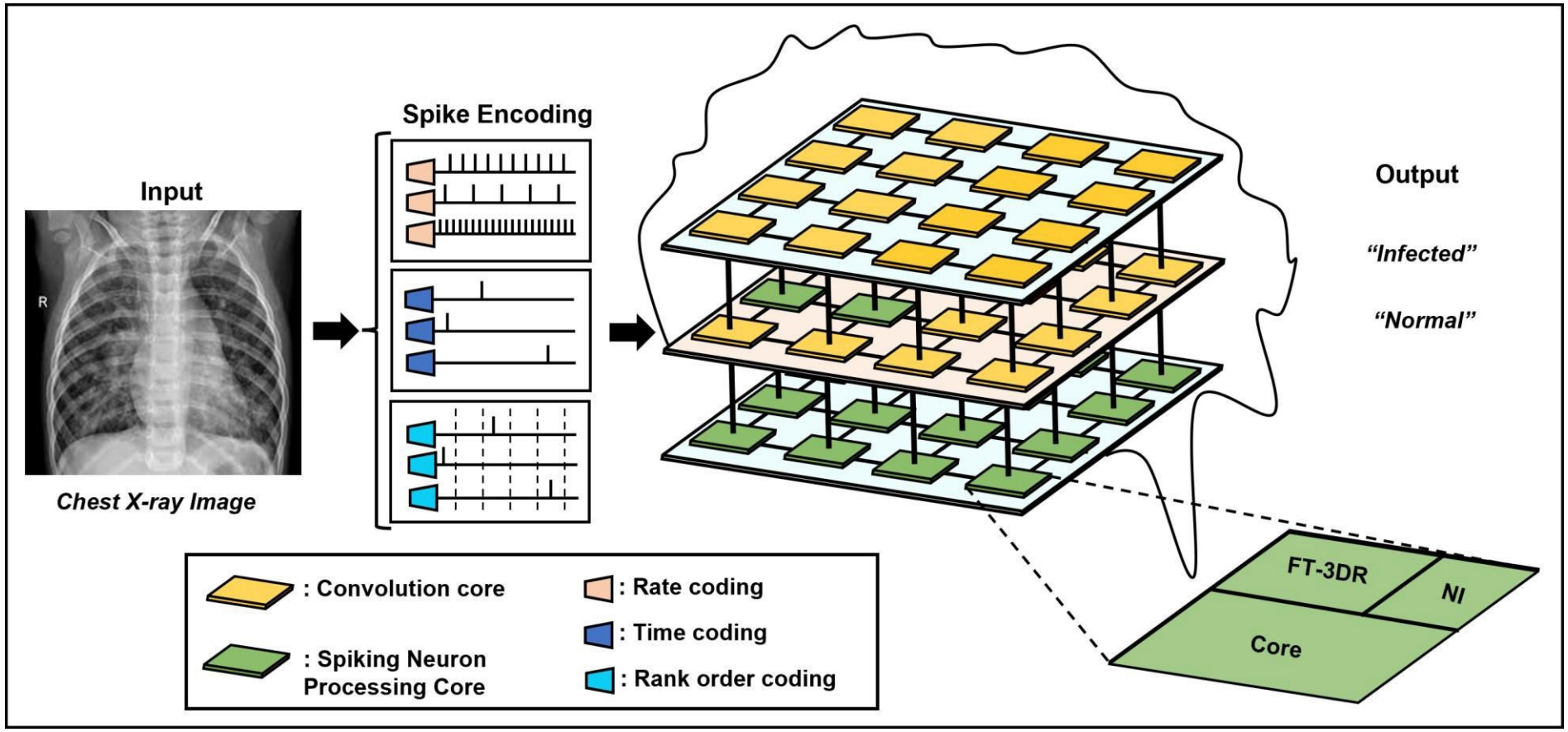

Figure 7.1. High level view of 3D-NoC-based neuromorphic pneumonia detection system.

Jiangkun Wang, Ogbodo Mark Ikechukwu, Khanh N. Dang, and Abderazek Ben Abdallah. ‘S k -Event X-ray Image Classification for 3D-NoC-Based Neuromorphic Pneumonia , Detection, Electronics, vol. 11, no. 24, p. 4157, 2022. doi: 10.3390/electronics11244157.

Mapping of SNN model on 3D-NoC-based neuromorphic system

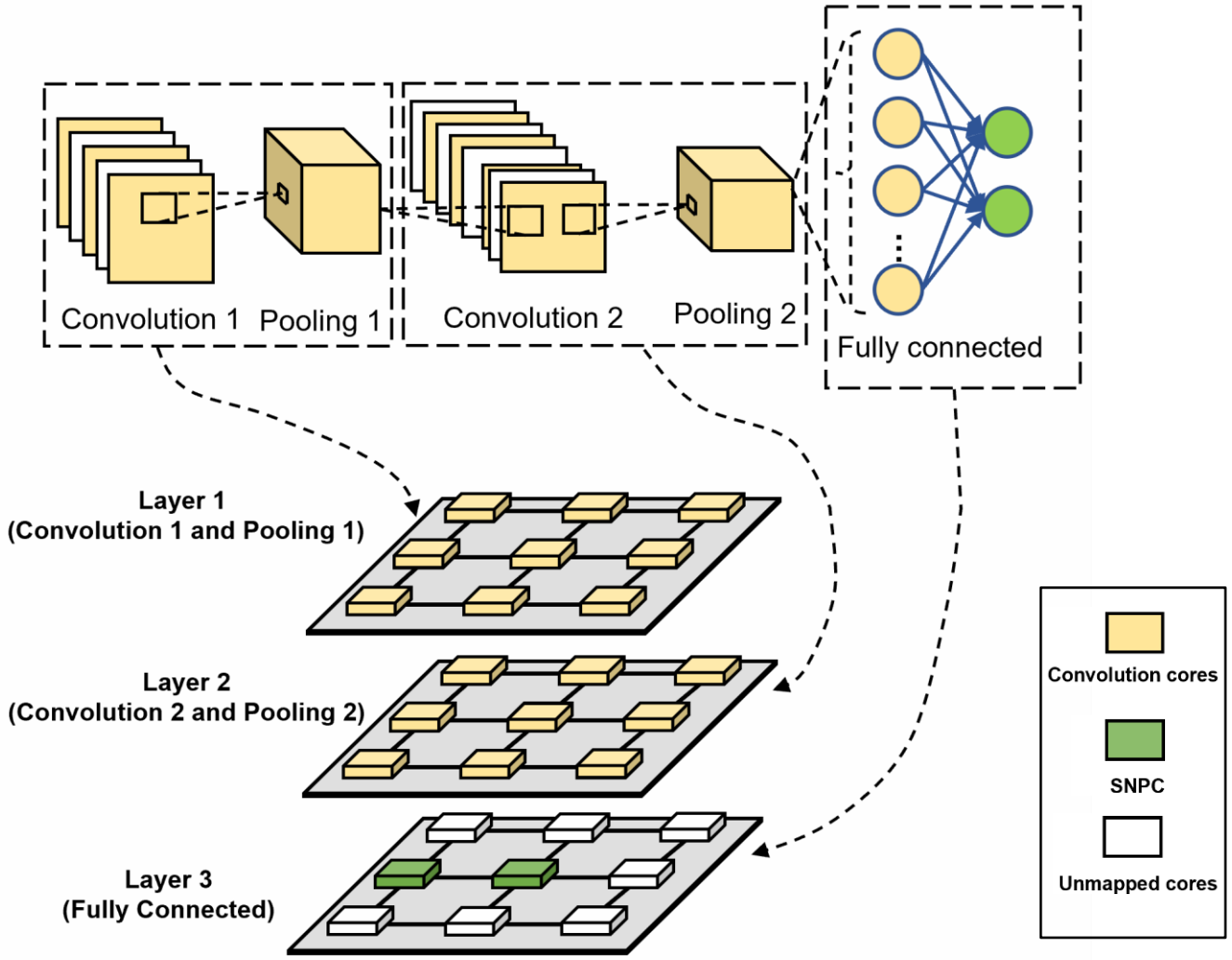

Figure 7.5. Layer-based mapping of SNN model on 3D-NoC-based neuromorphic system.

Related Journal Paper: Jiangkun Wang, Ogbodo Mark Ikechukwu, Khanh N. Dang, and Abderazek Ben Abdallah. 'Spike-Event X-ray Image Classification for 3D-NoC-Based Neuromorphic Pneumonia Detection', Electronics, vol. 11, no. 24, p. 4157, 2022. doi: 10.3390/electronics11244157.

Mapping of SNN model on 3D-NoC-based neuromorphic system

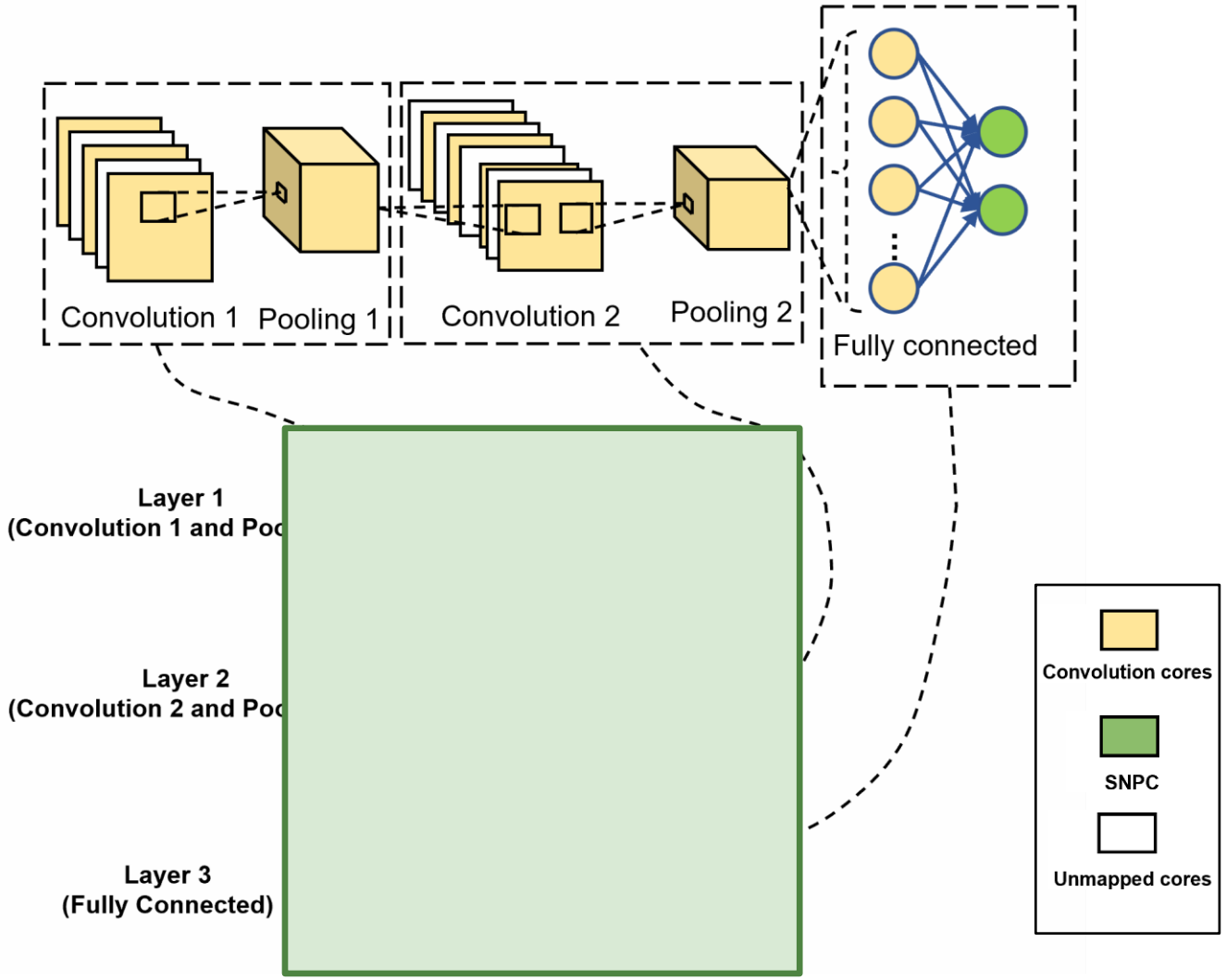

Figure 7.5. Layer-based mapping of SNN model on 3D-NoC-based neuromorphic system.

Related Journal Paper: Jiangkun Wang, Ogbodo Mark Ikechukwu, Khanh N. Dang, and Abderazek Ben Abdallah. 'Spike-Event X-ray Image Classification for 3D-NoC-Based Neuromorphic Pneumonia Detection', Electronics, vol. 11, no. 24, p. 4157, 2022. doi: 10.3390/electronics11244157.

Mapping of SNN model on 3D-NoC-based neuromorphic system

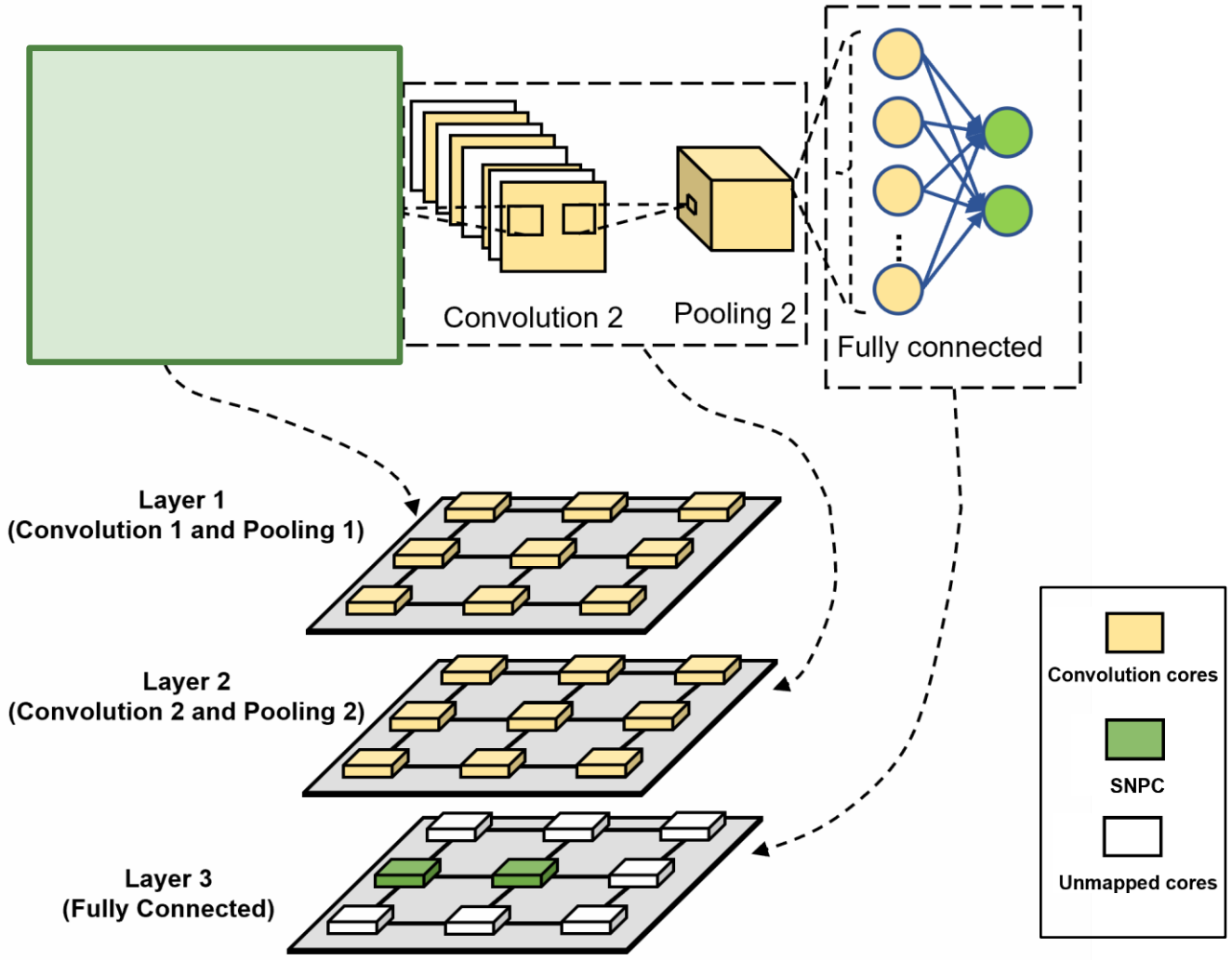

Figure 7.5. Layer-based mapping of SNN model on 3D-NoC-based neuromorphic system.

Related Journal Paper: Jiangkun Wang, Ogbodo Mark Ikechukwu, Khanh N. Dang, and Abderazek Ben Abdallah. 'Spike-Event X-ray Image Classification for 3D-NoC-Based Neuromorphic Pneumonia Detection', Electronics, vol. 11, no. 24, p. 4157, 2022. doi: 10.3390/electronics11244157.

Mapping of SNN model on 3D-NoC-based neuromorphic system

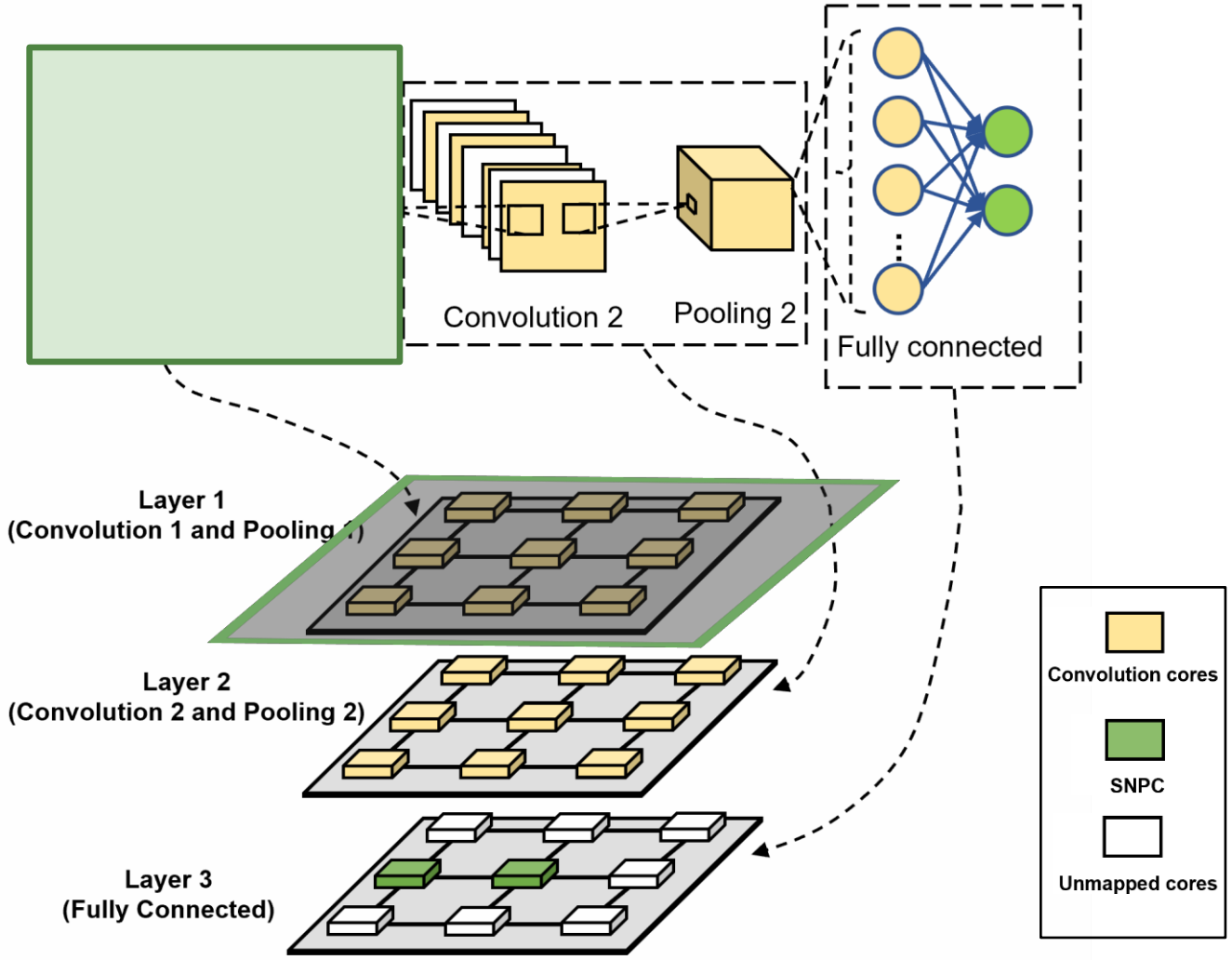

Figure 7.5. Layer-based mapping of SNN model on 3D-NoC-based neuromorphic system.

Related Journal Paper: Jiangkun Wang, Ogbodo Mark Ikechukwu, Khanh N. Dang, and Abderazek Ben Abdallah. 'Spike-Event X-ray Image Classification for 3D-NoC-Based Neuromorphic Pneumonia Detection', Electronics, vol. 11, no 24, p. 4157, 2022. doi: 10.3390/electronics11244157.

Mapping of SNN model on 3D-NoC-based neuromorphic system

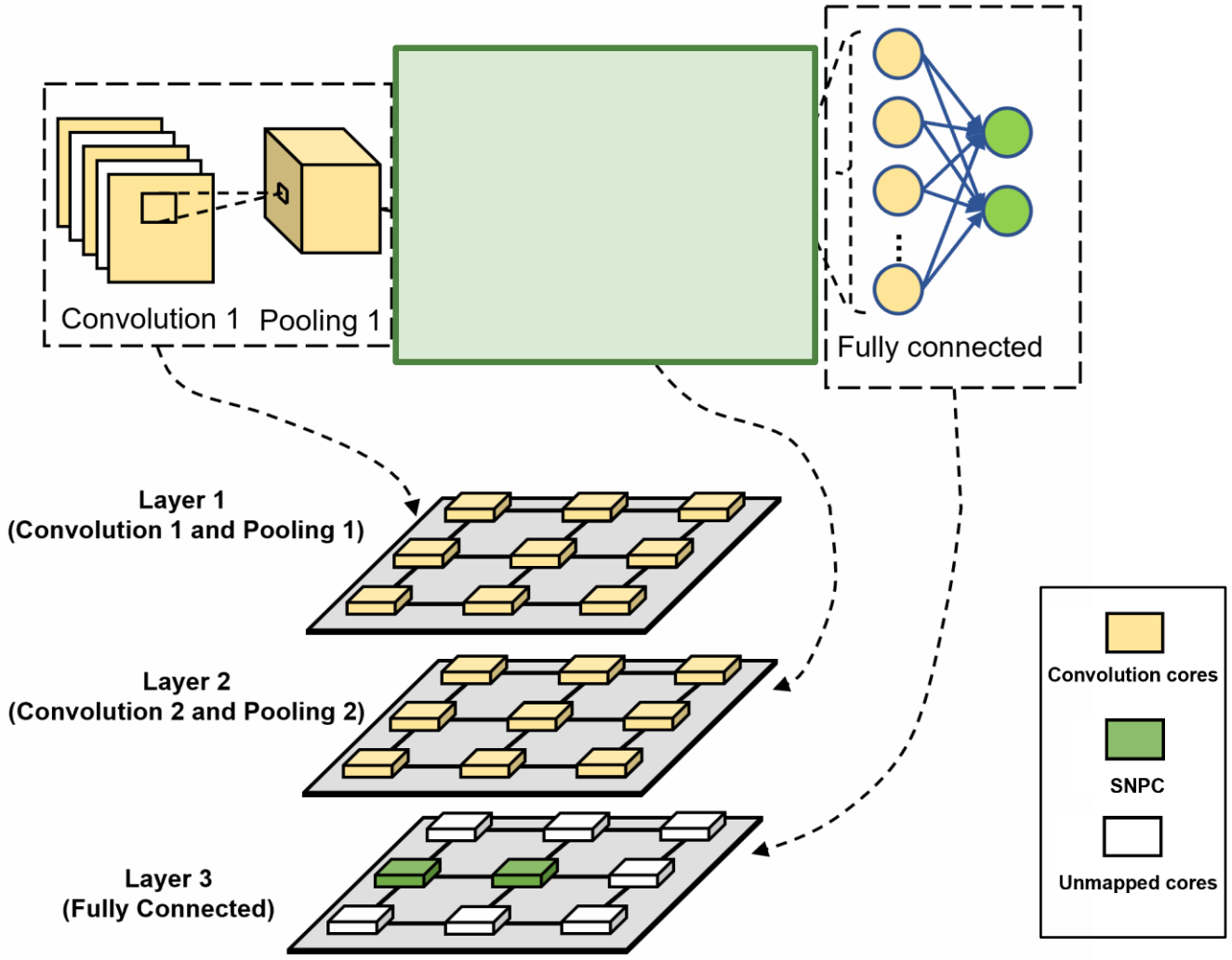

Figure 7.5. Layer-based mapping of SNN model on 3D-NoC-based neuromorphic system.

Related Journal Paper: Jiangkun Wang, Ogbodo Mark Ikechukwu, Khanh N. Dang, and Abderazek Ben Abdallah. 'Spike-Event X-ray Image Classification for 3D-NoC-Based Neuromorphic Pneumonia Detection', Electronics, vol. 11, no. 24, p. 4157, 2022. doi: 10.3390/electronics11244157.

Mapping of SNN model on 3D-NoC-based neuromorphic system

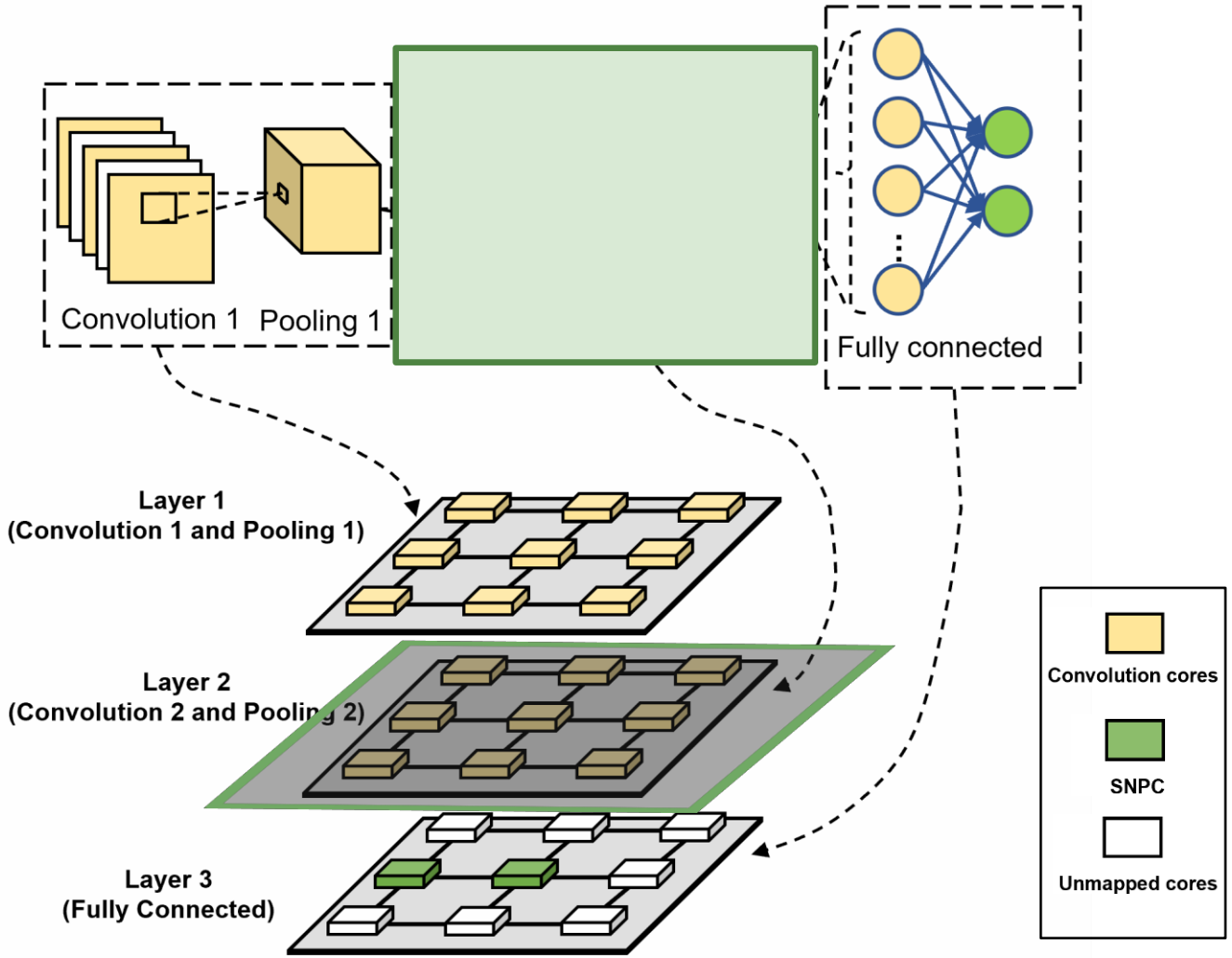

Figure 7.5. Layer-based mapping of SNN model on 3D-NoC-based neuromorphic system.

Related Journal Paper: Jiangkun Wang, Ogbodo Mark Ikechukwu, Khanh N. Dang, and Abderazek Ben Abdallah. 'Spike-Event X-ray Image Classification for 3D-NoC-Based Neuromorphic Pneumonia Detection', Electronics, vol. 11, no. 24, p. 4157, 2022. doi: 10.3390/electronics11244157.

Mapping of SNN model on 3D-NoC-based neuromorphic system

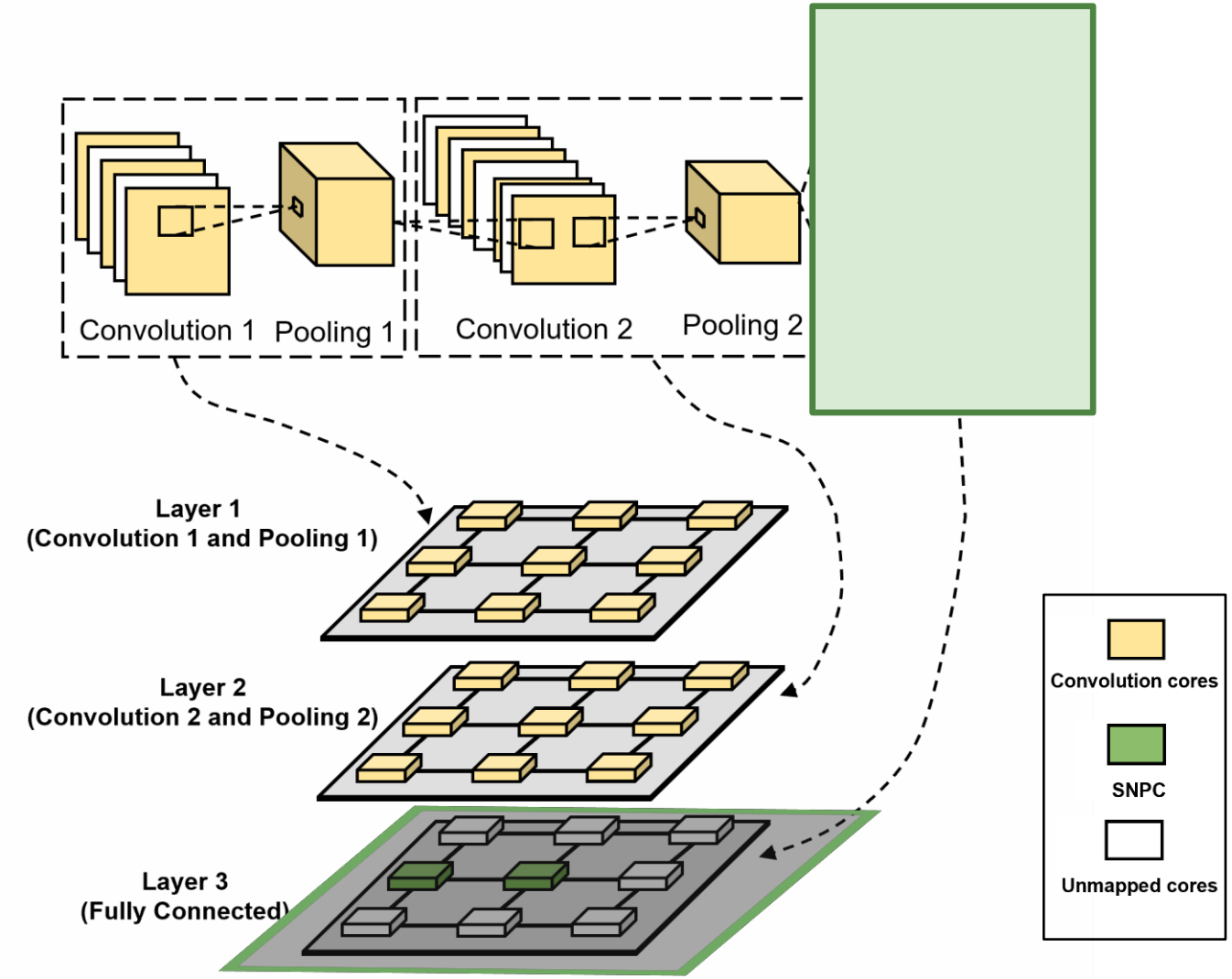

Figure 7.5. Layer-based mapping of SNN model on 3D-NoC-based neuromorphic system.

Related Journal Paper: Jiangkun Wang, Ogbodo Mark Ikechukwu, Khanh N. Dang, and Abderazek Ben Abdallah. 'Spike-Event X-ray Image Classification for 3D-NoC-Based Neuromorphic Pneumonia Detection', Electronics, vol. 11, no. 24, p. 4157, 2022. doi: 10.3390/electronics11244157.

Evaluation Result

Table 7.2. Dataset description.

Label	Class	Train	Test
COVID	COVID	2870	700
	COVID(Augmented)	14,349	-
Non-COVID	Normal	9791	400
	Lung_Opacity	5762	250
	Viral_Pneumonia	1288	50
Sum		34,060	1400

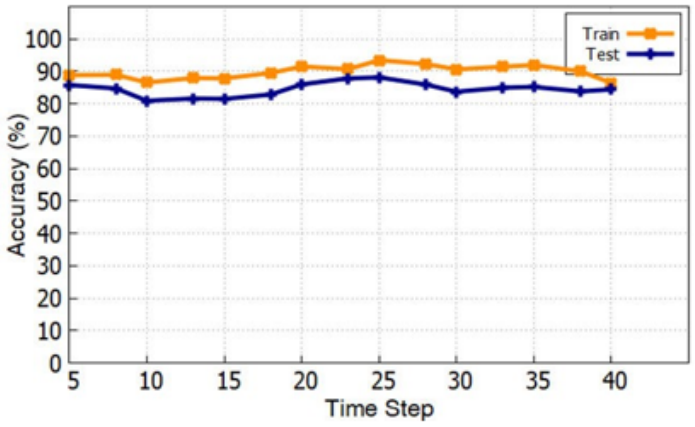

(a) Detection accuracy over various time-steps.

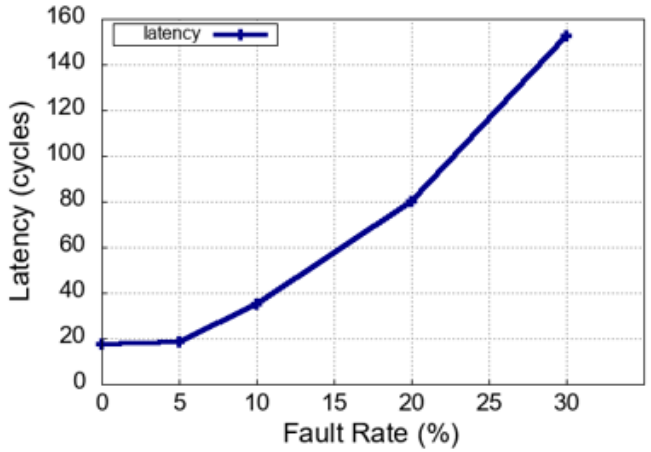

(b) Detection Latency over various fault-rate.

Accuracy and fault-rate evaluation result.

Core/Parameter	Area (mm²)		Power (mW)	
Convolution core	SNN	ANN	SNN	ANN
	0.0748	0.0755	0.007	0.011

Result comparison with existing works.

Works	Model	Platform	Dataset	Image Size	Accuracy
[fukuchi2022efficient]	SNN	Software	X-ray	64 × 64	80.7%
[kamal2021explainable]	SNN	Software	X-ray	256 × 256	78%
[che2020covid]	ANN	Software	X-ray	224 × 224	71.9%
[wang2022efficient]	ANN	FPGA	X-ray	256 × 256	94.4%
This work	SNN	FPGA	X-ray	64 × 64	88.43%

Real-World Deployment 3: Distributed Anthropomorphic Robots Enabling Human-Centered Intelligent Machines

Distributed Anthropomorphic Robots Enabling Human-Centered Intelligent Machines

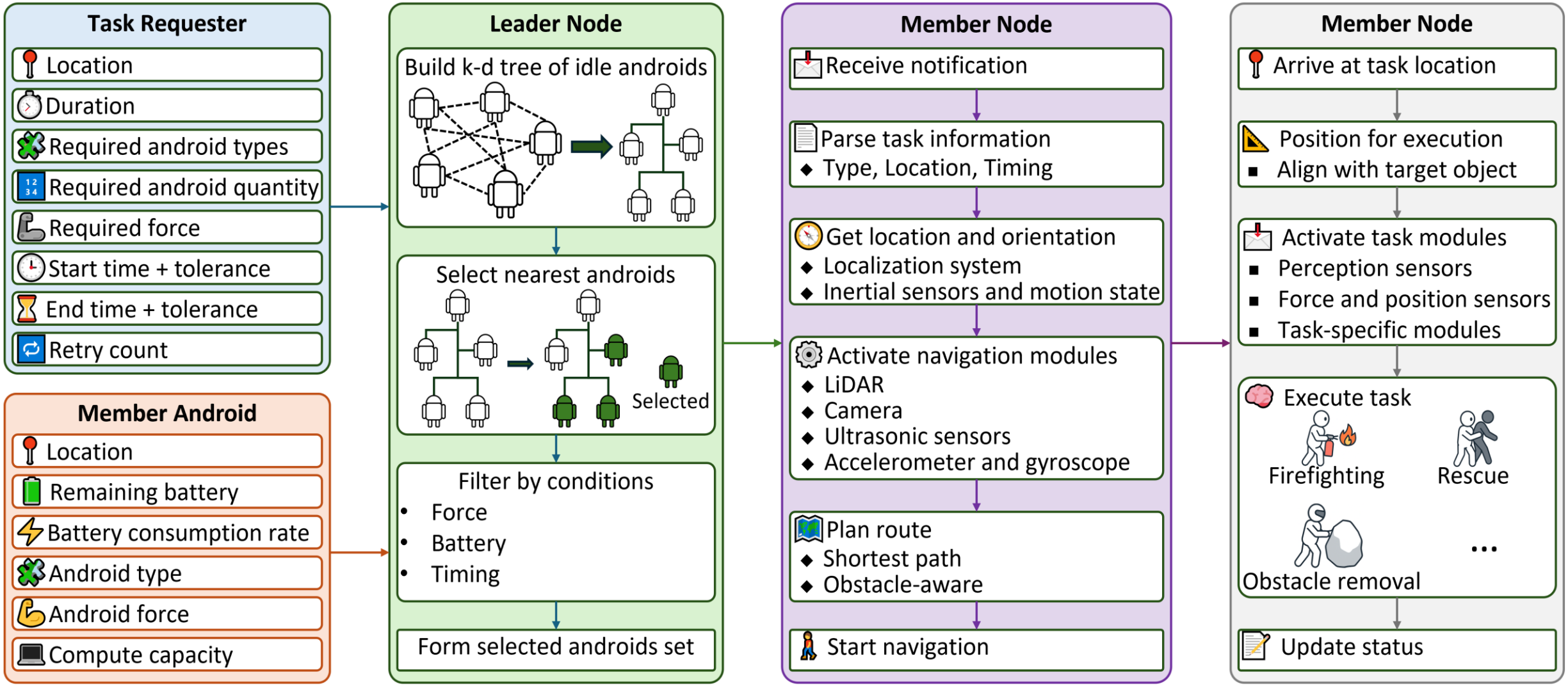

Fig. 1: Overview of the proposed distributed android coordination framework for critical missions.

Distributed Anthropomorphic Robots Enabling Human-Centered Intelligent Machines

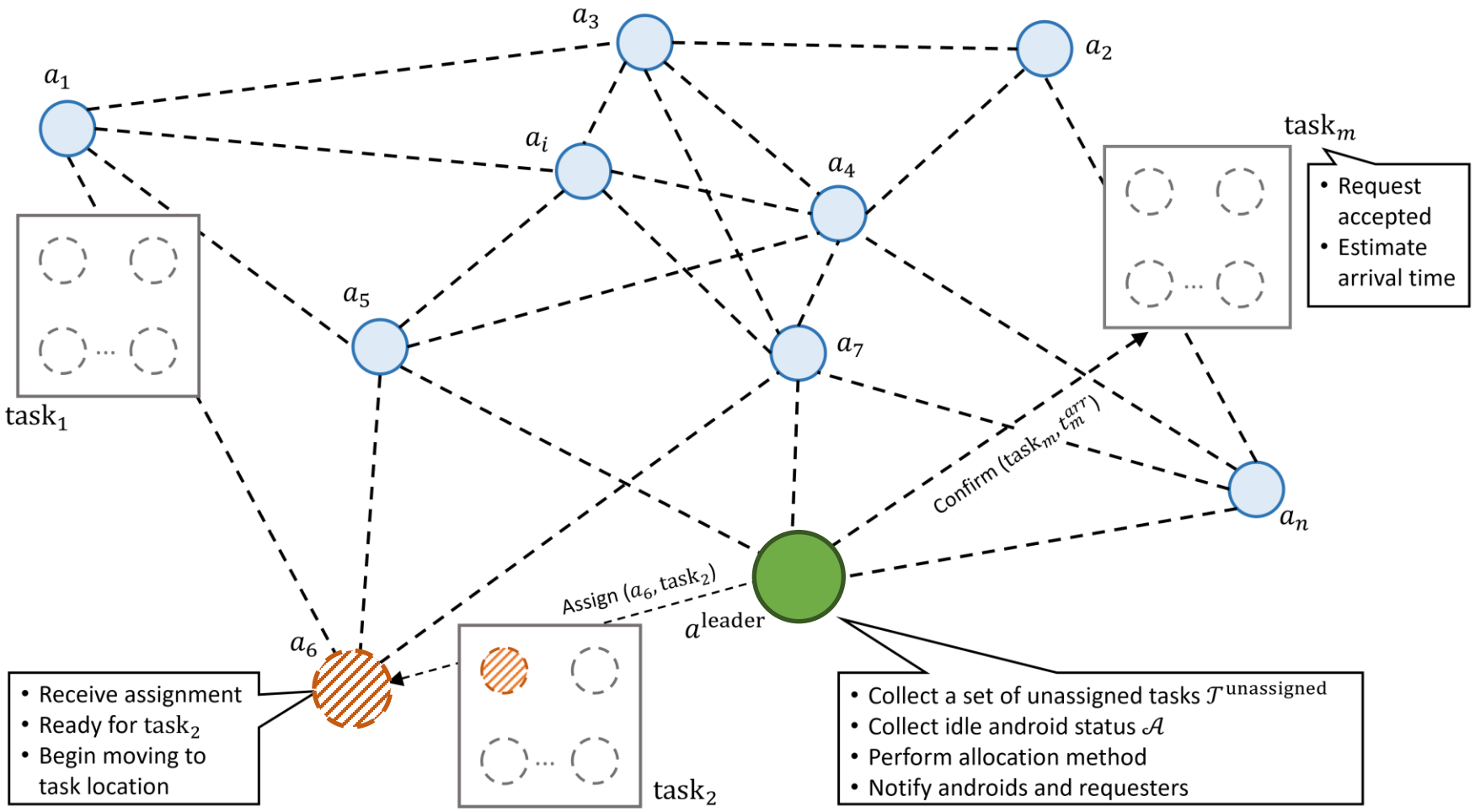

Fig. 2: Overview of the leader-based task assignment method for a distributed autonomous android system.

Distributed Anthropomorphic Robots Enabling Human-Centered Intelligent Machines

Preliminary Evaluation

- Implementation
  - Python 3.12
  - Bambu Lab P1S Combo 3D printer
- Benchmarks
  - IRoT
    - Type-based + Force-based + Battery-based
    - Without time-feasibility
  - COHERENT
    - Type-only based
- Evaluation metric:

  Task fulfillment success rate:

  Ratio of tasks successfully assigned to androids to the total number of tasks

Table I. Configuration of Task Parameters Based on Spatiotemporal and Physical Requirements

Parameter	Notation	Description	Value / Range
TaskID	j	Unique ID per task	1 to number of tasks
Location	l_j	Task 2D coordinates	(0, 0) to (99, 99)
Duration	w_j	Required task execution time	10-60 min
StartTime	t_j^{start}	Start time constraint	50% of tasks: 1st to 360th minute
StartTimeTolerance	$t_j^{\text{start\_tol}}$	Tolerance for delayed start	5-30 min
FinishTime	t_j^{finish}	End time constraint	50% of tasks: 11th to 420th
FinishTimeTolerance	$t_j^{\text{finish\_tol}}$	Tolerance for delayed finish	5-30 min
RetryCount	r_j	Max retry attempts for task	1
RequiredType	γ	Required android type	[‘A’, ‘B’, ‘C’]
RequiredNum	$n_{j,\gamma}^{\text{req}}$	Androids required for this type	1-3
MinForcePerAndroid	$f_{j,\gamma}^{\min}$	Min required force	1-10 N

Table II. Configuration of Android Parameters Based on Type, Force, and Battery Characteristics

Parameter	Notation	Description	Value / Range
AndroidID	i	Unique ID per android	1 to number of androids
Location	p_i	Android 2D coordinates	(0, 0) to (99, 99)
Type	$\gamma_i \in \Gamma$	Android type / capability	[‘A’, ‘B’, ‘C’]
Force	$f_{i,\gamma}$	Physical strength	1-10 N
RemainingBattery	b_i	Initial battery status	10-120 min
TaslConsumptionRate	β_i	Battery consumption rate to perform task	0.8 for A, 1.0 for B, 1.2 for C
StepConsumptionRate	β_i^{move}	Battery consumption per step	5% of full capacity

Configuration of task and android parameters

Distributed Anthropomorphic Robots Enabling Human-Centered Intelligent Machines

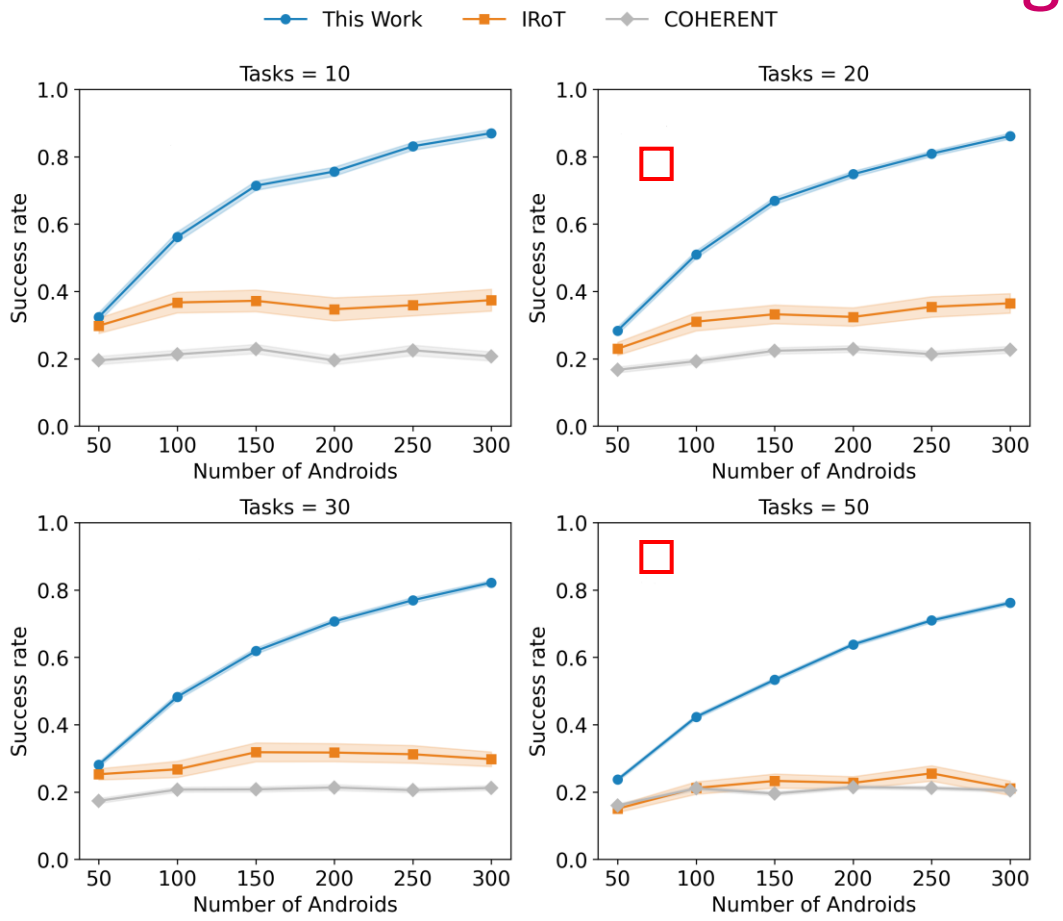

Fig. 4: Evaluation of the proposed method in terms of task fulfillment rate (with increasing number of androids)

(a) The developed android prototype. The prototype consists of articulated limb structures assembled from 3D-printed parts using modular joints. A wooden frame is temporarily used as the torso base to support initial mechanical integration and future component embedding.

(b) AlzuHand: AlzuHand is a 3D-printed, low-cost prosthetic hand designed for EMG-based control with real-time feedback, a neuromorphic prosthetic hand with sensory-motor

https://web-ext.u-aizu.ac.jp/misc/neuro-eng/aizuhand.html

Achieved a success rate about 2.0× higher than existing approaches with 30 tasks and 100 androids and more than 3.5× higher with 50 tasks and 300 androids.

Research Challenges & Opportunities

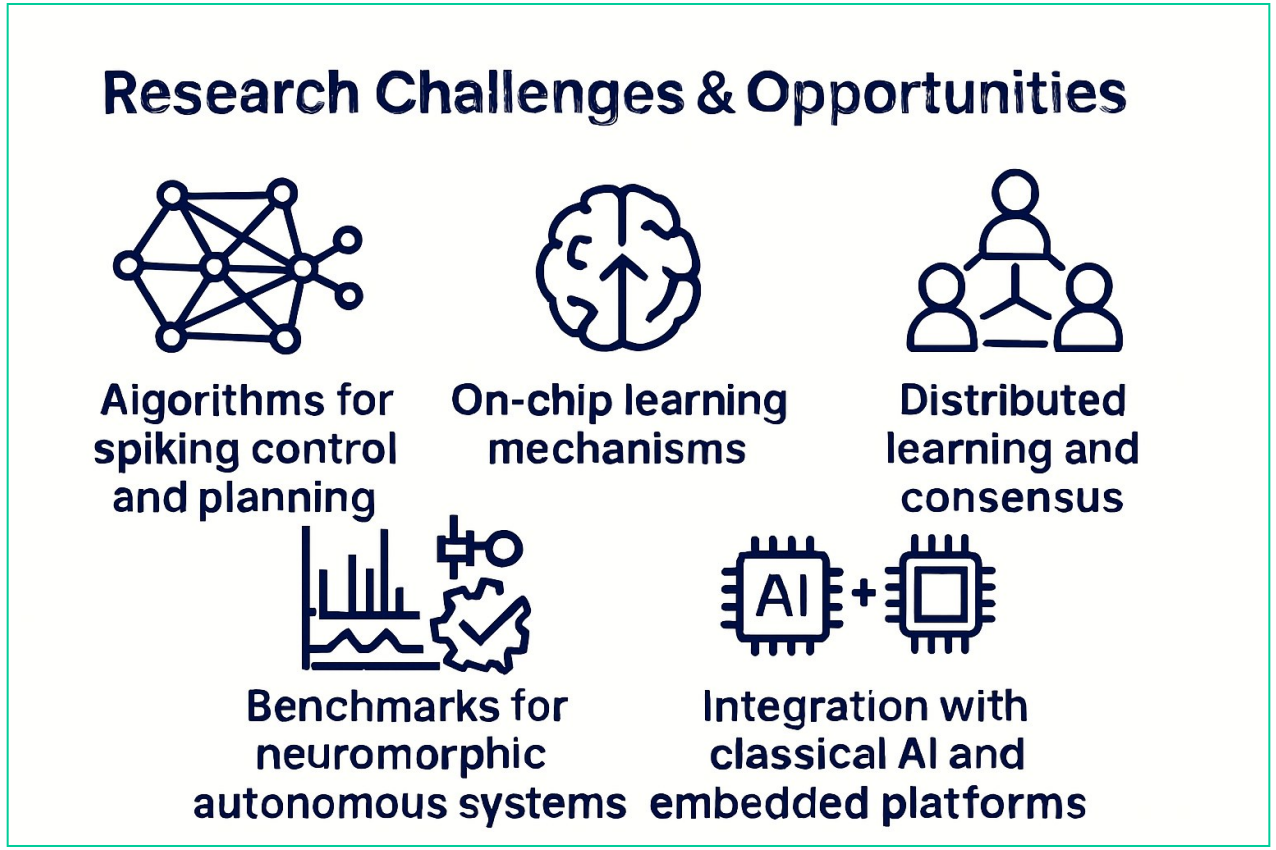

- Algorithms for spiking control and planning
- On-chip learning mechanisms
- Distributed learning and consensus
- Benchmarks for neuromorphic autonomous systems
- Integration with classical AI and embedded platforms

Agenda

- The Evolution of Autonomy
- Distributed Autonomous (DA) Systems
- Neuromorphic Computing
- DA + Neuromorphic Intelligence
- Applications and Case Studies
- Research Challenges
- Vision & Outlook

benab@u-aizu.ac.jp

Vising & Outlook

- **Cognitive Ecosystems**
  - ✓Intelligent agents, sensors, and environments working together with context-aware decisions, real-time adaptation, collaborative learning

- **Self-Organizing • Adaptive • Resilient**
  - ✓Systems that restructure, learn from sparse data, operate under uncertainty, and recover from failures

- **Neuromorphic Autonomy: The Next Decade**
  - ✓Convergence of neuromorphic computing + edge AI + embedded platforms enabling ultra-low-power, real-time autonomy for exploration, disaster response, smart infrastructure, defense

benab@u-aizu.ac.jp

Summary of Key Takeaways

- ✓ Autonomy is shifting from centralized to distributed architectures
- ✓ Neuromorphic computing brings efficiency and real-time responsiveness at the edge
- ✓ Their convergence enables scalable, adaptive, and resilient intelligent systems
- ✓ Demonstrated deployments: off-grid energy storage, V2G energy trading, anthropomorphic robots
- ✓ Neuromorphic-enabled distributed autonomy is no longer theoretical — it is already happening !

benab@u-aizu.ac.jp

Thank you for your attention!

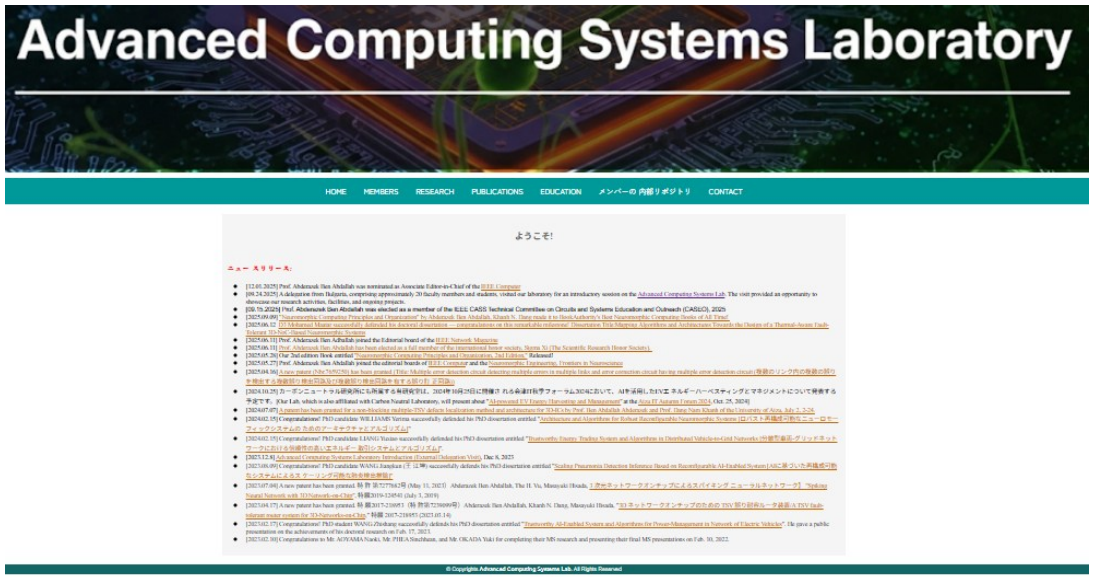

www.u-aizu.ac.jp/misc/neuro-eng/

Explore Our Books and Visit Our Lab Website!

Acknowledgement:
Thank you to Dr. Dang, Dr. Z. Wang, and former lab members Dr. Mark, Dr. J. Wang, Dr. Vu, and all other lab members for their contributions to the research presented here.

benab@u-aizu.ac.jp